

Strange-Meson Spectroscopy with COMPASS

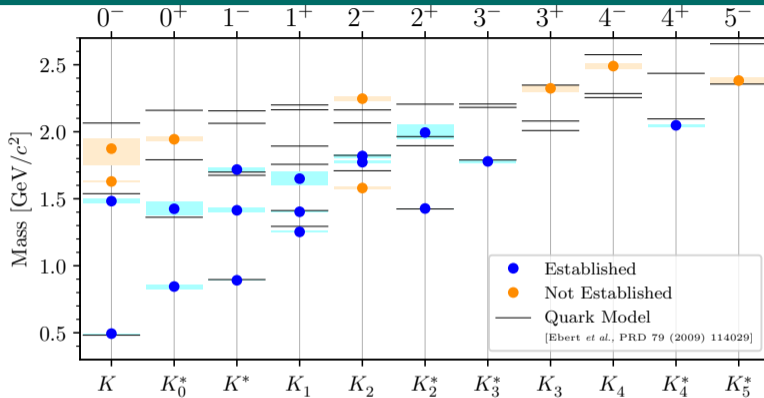
Stefan Wallner
(swallner@mpp.mpg.de)

Max Planck Institute for Physics

PWA13/ATHOS8
May 28, 2024



MAX PLANCK INSTITUTE
FOR PHYSICS



PDG lists 25 strange mesons

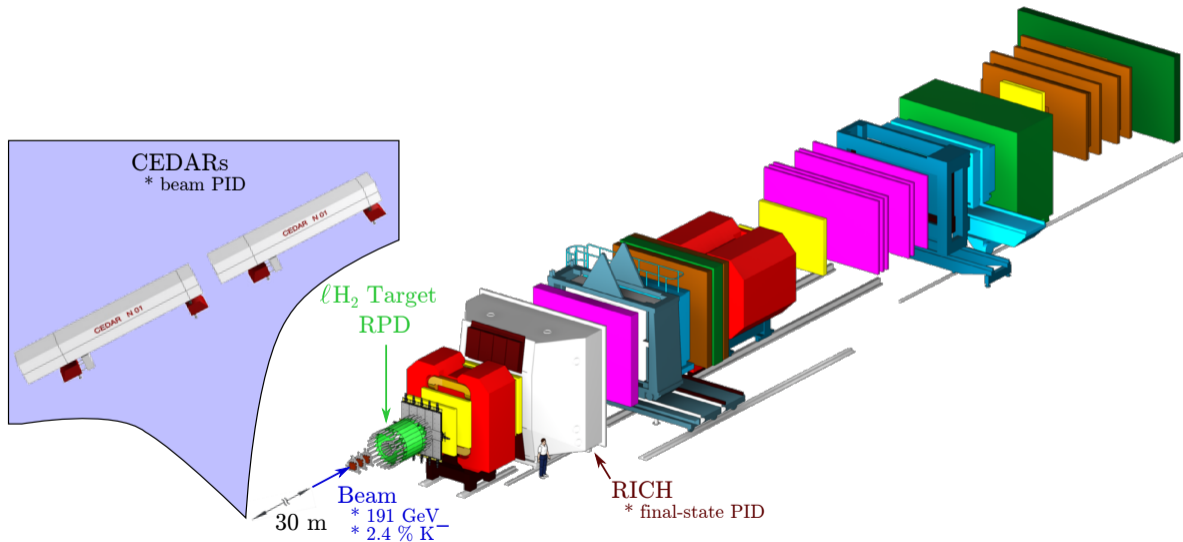
(2022)

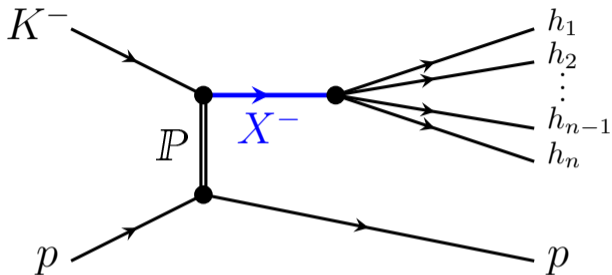
- ▶ 16 established states, 9 need further confirmation
- ▶ Missing states with respect to quark-model predictions
- ▶ Many measurements performed more than 30 years ago

Strange-Meson Spectroscopy with COMPASS

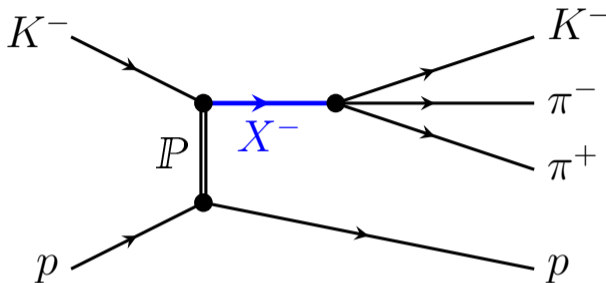
COMPASS Setup for Hadron Beams

[COMPASS, Nucl. Instrum. Methods 779 (2015) 69]





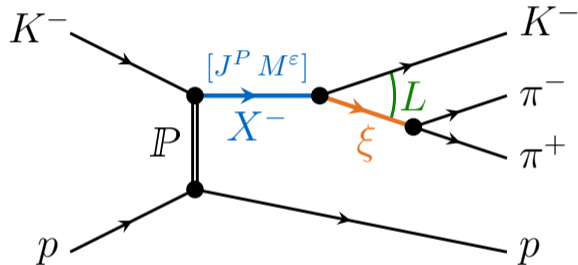
- ▶ Diffractive scattering of high-energy kaon beam
- ▶ Strange mesons appear as **intermediate resonances** X^-
- ▶ Decay to multi-body hadronic final states
- ▶ $K^- \pi^- \pi^+$ final state
 - ▶ Study in principle all strange mesons
 - ▶ Study a wide mass range
 - ▶ COMPASS measured world's largest data set of about 720 k events



- ▶ Diffractive scattering of high-energy kaon beam
- ▶ Strange mesons appear as **intermediate resonances** X^-
- ▶ Decay to multi-body hadronic final states
- ▶ **$K^- \pi^- \pi^+$ final state**
 - ▶ Study in principle **all strange mesons**
 - ▶ Study a **wide mass range**
 - ▶ COMPASS measured **world's largest data set** of about 720 k events

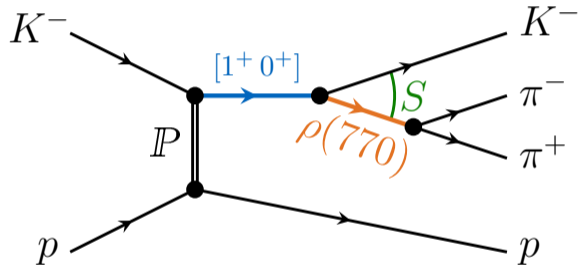
Partial wave: $J^P M^\epsilon \xi b^- L$

- ▶ J^P spin and parity
- ▶ M^ϵ spin projection
- ▶ ξ isobar resonance
- ▶ b^- bachelor particle
- ▶ L orbital angular momentum



Partial wave: $J^P M^{\xi} b^- L$

- ▶ J^P spin and parity
- ▶ M^{ξ} spin projection
- ▶ ξ isobar resonance
- ▶ b^- bachelor particle
- ▶ L orbital angular momentum



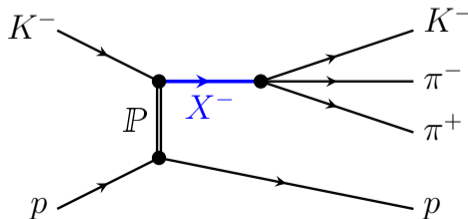
Data: 720 k diffractively produced $K^-\pi^-\pi^+$ candidates

Data: 720 k diffractively produced $K^-\pi^-\pi^+$ candidates

(I) Partial-Wave Decomposition

Performed independently in narrow $(m_{K\pi\pi}, t')$ cells
No assumption about $K\pi\pi$ resonances

Partial waves: Intensities and relative phases as a function of $(m_{K\pi\pi}, t')$



Data: 720 k diffractively produced $K^-\pi^-\pi^+$ candidates

(I) Partial-Wave Decomposition

Performed independently in narrow $(m_{K\pi\pi}, t')$ cells
No assumption about $K\pi\pi$ resonances

Partial waves: Intensities and relative phases as a function of $(m_{K\pi\pi}, t')$

(II) Resonance-Model Fit

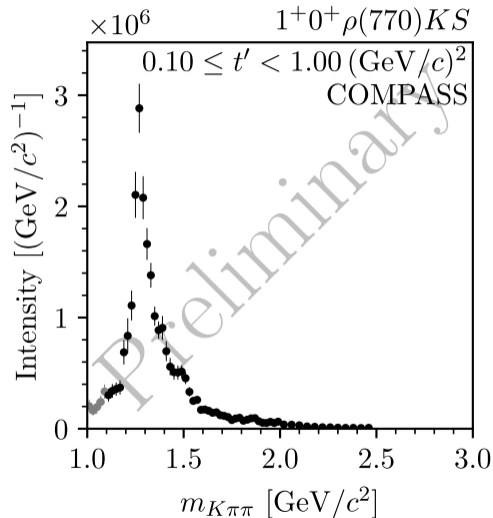
Model $m_{K\pi\pi}$ dependence of partial waves
 $K\pi\pi$ resonances and background

Resonance parameters: Masses and widths of the strange-meson resonances

Partial-Wave Decomposition

$$\mathcal{I}(\tau, m_{K\pi\pi}, t') = \sum_{a,b \in \mathbb{W}_z(m_{K\pi\pi}, t')} \Psi_a(\tau) \rho_{ab}(m_{K\pi\pi}, t') [\Psi_b(\tau)]^*$$

- ▶ Measure spin-density matrix $\rho_{ab}(m_{K\pi\pi}, t')$ in independently ($m_{K\pi\pi}, t'$) cells
 - ▶ No assumption about $K^-\pi^-\pi^+$ resonances
- ▶ Wave set $\mathbb{W}_z(m_{K\pi\pi}, t')$ inferred from data using regularization-based model-selection techniques
- ▶ Bootstrap resampling to improve uncertainty estimates
 - ▶ Performed about 20 M fits
- ▶ Detailed Monte Carlo input-output studies

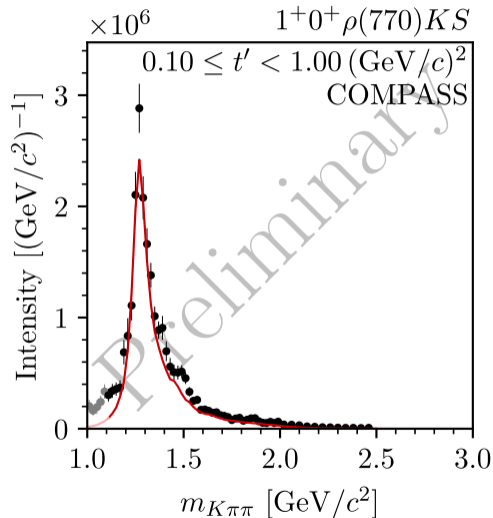


Resonance-Model Fit

$$\hat{\rho}_{ab}^{K\pi\pi}(m_{K\pi\pi}, t') = \hat{\mathcal{T}}_a(m_{K\pi\pi}, t') \left[\hat{\mathcal{T}}_b(m_{K\pi\pi}, t') \right]^*$$

$$\hat{\mathcal{T}}_a(m_{K\pi\pi}, t') = \sum_{k \in \mathbb{S}_a} K(m_{K\pi\pi}, t')^k \mathcal{C}_a(t') \mathcal{D}_k(m_{K\pi\pi}; \zeta_k)$$

- ▶ Model $m_{K\pi\pi}$ dependence of **partial-wave amplitudes**
- ▶ Breit-Wigner amplitudes for $K^-\pi^-\pi^+$ resonance components
- ▶ **Coherent non-resonant component** parameterizing other $K^-\pi^-\pi^+$ production mechanisms

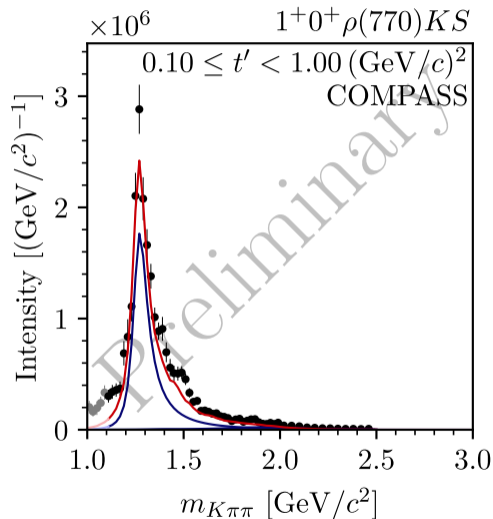


Resonance-Model Fit

$$\hat{\rho}_{ab}^{K\pi\pi}(m_{K\pi\pi}, t') = \hat{\mathcal{T}}_a(m_{K\pi\pi}, t') \left[\hat{\mathcal{T}}_b(m_{K\pi\pi}, t') \right]^*$$

$$\hat{\mathcal{T}}_a(m_{K\pi\pi}, t') = \sum_{k \in \mathbb{S}_a} K(m_{K\pi\pi}, t')^k \mathcal{C}_a(t') \mathcal{D}_k(m_{K\pi\pi}; \zeta_k)$$

- ▶ Model $m_{K\pi\pi}$ dependence of **partial-wave amplitudes**
- ▶ Breit-Wigner amplitudes for $K^-\pi^-\pi^+$ **resonance components**
- ▶ **Coherent non-resonant component** parameterizing other $K^-\pi^-\pi^+$ production mechanisms

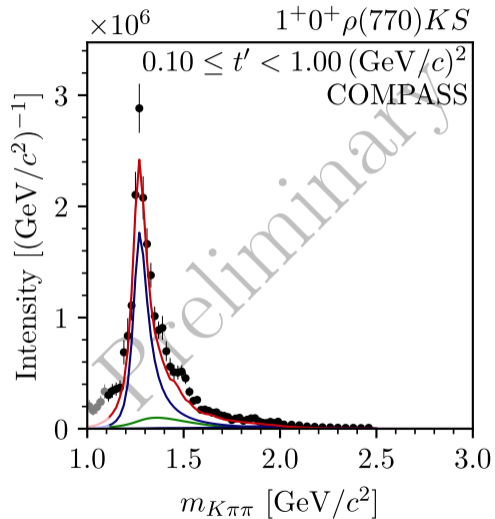


Resonance-Model Fit

$$\hat{\rho}_{ab}^{K\pi\pi}(m_{K\pi\pi}, t') = \hat{\mathcal{T}}_a(m_{K\pi\pi}, t') \left[\hat{\mathcal{T}}_b(m_{K\pi\pi}, t') \right]^*$$

$$\hat{\mathcal{T}}_a(m_{K\pi\pi}, t') = \sum_{k \in \mathbb{S}_a} K(m_{K\pi\pi}, t')^k \mathcal{C}_a(t') \mathcal{D}_k(m_{K\pi\pi}; \zeta_k)$$

- ▶ Model $m_{K\pi\pi}$ dependence of **partial-wave amplitudes**
- ▶ Breit-Wigner amplitudes for $K^-\pi^-\pi^+$ **resonance components**
- ▶ **Coherent non-resonant component** parameterizing other $K^-\pi^-\pi^+$ production mechanisms

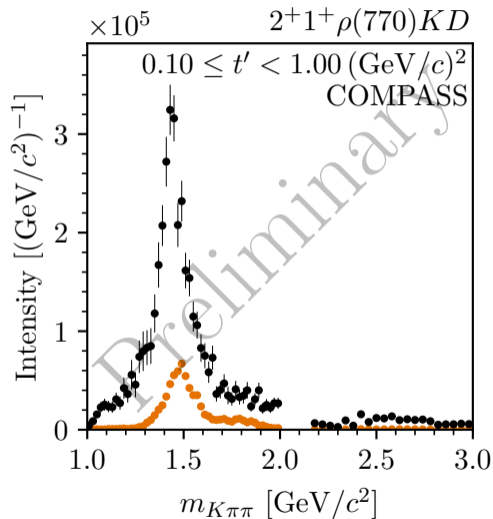


Incoherent Backgrounds

- ▶ **Incoherent background** from π^- diffraction to $\pi^-\pi^-\pi^+$ and other reactions (in total about 10%)
- ▶ **Very good model for dominant $\pi^-\pi^-\pi^+$ background** from COMPASS $\pi^-\pi^-\pi^+$ analysis
 - ▶ Study background in partial waves by
 - ▶ Generate pseudodata from $\pi^-\pi^-\pi^+$ model
 - ▶ Apply $K^-\pi^-\pi^+$ reconstruction event selection
 - ▶ Project into $K^-\pi^-\pi^+$ partial waves
 - ▶ Large in some waves, e.g. with $\rho(770)$ isobar
 - ▶ Small in other waves, e.g. with $K^*(892)$ isobar

Incoherent Backgrounds

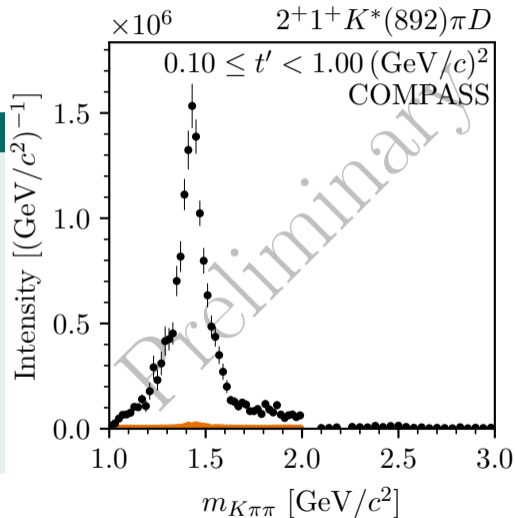
- ▶ **Incoherent background** from π^- diffraction to $\pi^-\pi^-\pi^+$ and other reactions (in total about 10%)
- ▶ **Very good model for dominant $\pi^-\pi^-\pi^+$ background** from COMPASS $\pi^-\pi^-\pi^+$ analysis
 - ▶ Study background in partial waves by
 - ▶ Generate pseudodata from $\pi^-\pi^-\pi^+$ model
 - ▶ Apply $K^-\pi^-\pi^+$ reconstruction event selection
 - ▶ **Project into $K^-\pi^-\pi^+$ partial waves**
 - ▶ Large in some waves, e.g. with $\rho(770)$ isobar
 - ▶ Small in other waves, e.g. with $K^*(892)$ isobar



$K^-\pi^-\pi^+$ data, $\pi^-\pi^-\pi^+$ pseudo data

Incoherent Backgrounds

- ▶ **Incoherent background** from π^- diffraction to $\pi^-\pi^-\pi^+$ and other reactions (in total about 10%)
- ▶ **Very good model for dominant $\pi^-\pi^-\pi^+$ background** from COMPASS $\pi^-\pi^-\pi^+$ analysis
 - ▶ Study background in partial waves by
 - ▶ Generate pseudodata from $\pi^-\pi^-\pi^+$ model
 - ▶ Apply $K^-\pi^-\pi^+$ reconstruction event selection
 - ▶ **Project into $K^-\pi^-\pi^+$ partial waves**
 - ▶ Large in some waves, e.g. with $\rho(770)$ isobar
 - ▶ Small in other waves, e.g. with $K^*(892)$ isobar



$K^-\pi^-\pi^+$ data, $\pi^-\pi^-\pi^+$ pseudo data

Handling of Incoherent Backgrounds

- ▶ Challenging to explicitly treat in partial-wave decomposition

➔ Effectively taken into account

$$\rho_{ab} = \sum_z \mathcal{T}_a^z [\mathcal{T}_b^z]^*$$

➔ Measured ρ_{ab} include background

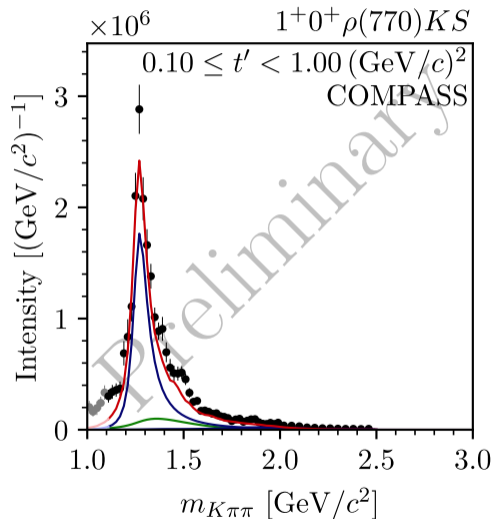
- ▶ Explicitly model them in resonance-model fit

$$\hat{\rho}_{ab}(m_{K\pi\pi}, t') = \hat{\rho}_{ab}^{K\pi\pi}(m_{K\pi\pi}, t')$$

- ▶ $\pi^-\pi^-\pi^+$ background modeled by partial-wave projection of $\pi^-\pi^-\pi^+$ pseudodata

▶ Yield is only free parameter

- ▶ Incoherent effective background component for other background processes



Handling of Incoherent Backgrounds

- ▶ Challenging to explicitly treat in partial-wave decomposition

➔ Effectively taken into account

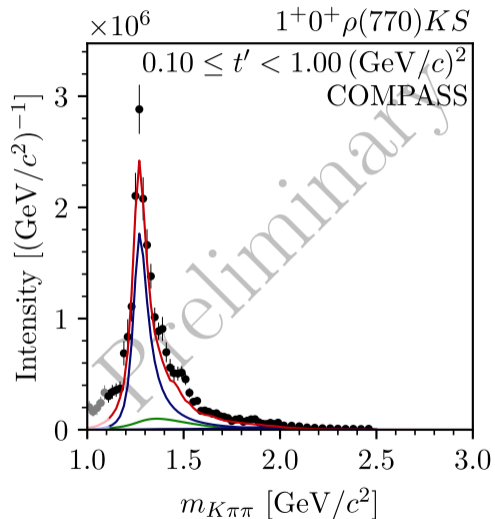
$$\rho_{ab} = \sum_z \mathcal{T}_a^z [\mathcal{T}_b^z]^*$$

➔ Measured ρ_{ab} include background

- ▶ Explicitly model them in resonance-model fit

$$\hat{\rho}_{ab}(m_{K\pi\pi}, t') = \hat{\rho}_{ab}^{K\pi\pi}(m_{K\pi\pi}, t')$$

- ▶ $\pi^-\pi^-\pi^+$ background modeled by partial-wave projection of $\pi^-\pi^-\pi^+$ pseudodata
 - ▶ Yield is only free parameter
- ▶ Incoherent effective background component for other background processes



Handling of Incoherent Backgrounds

- ▶ Challenging to explicitly treat in partial-wave decomposition

➔ Effectively taken into account

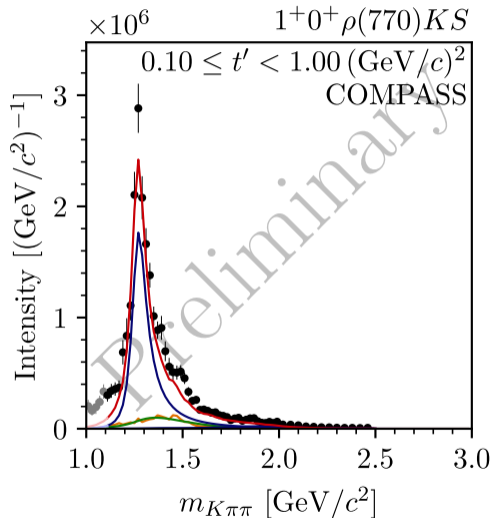
$$\rho_{ab} = \sum_z \mathcal{T}_a^z [\mathcal{T}_b^z]^*$$

➔ Measured ρ_{ab} include background

- ▶ Explicitly model them in resonance-model fit

$$\hat{\rho}_{ab}(m_{K\pi\pi}, t') = \hat{\rho}_{ab}^{K\pi\pi}(m_{K\pi\pi}, t') + \hat{\rho}_{ab}^{3\pi}(m_{K\pi\pi}, t')$$

- ▶ $\pi^-\pi^-\pi^+$ background modeled by partial-wave projection of $\pi^-\pi^-\pi^+$ pseudodata
 - ▶ Yield is only free parameter
- ▶ Incoherent effective background component for other background processes



Handling of Incoherent Backgrounds

- ▶ Challenging to explicitly treat in partial-wave decomposition

➔ Effectively taken into account

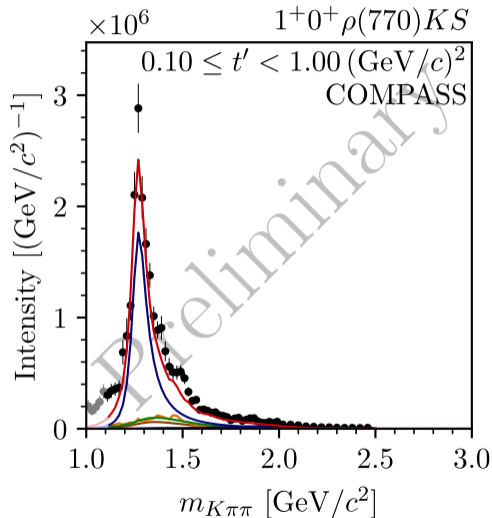
$$\rho_{ab} = \sum_z \mathcal{T}_a^z [\mathcal{T}_b^z]^*$$

➔ Measured ρ_{ab} include background

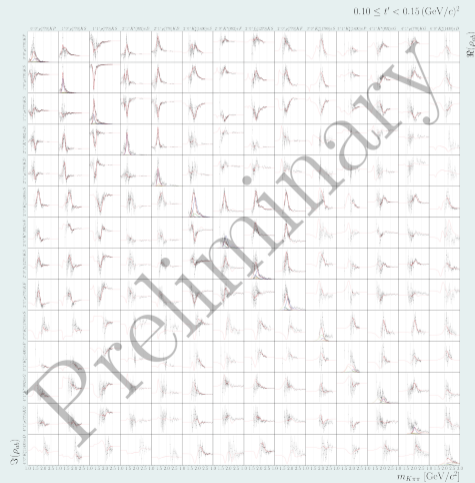
- ▶ Explicitly model them in resonance-model fit

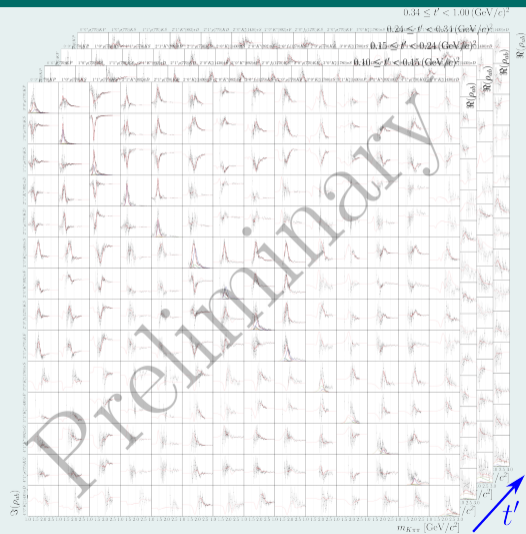
$$\hat{\rho}_{ab}(m_{K\pi\pi}, t') = \hat{\rho}_{ab}^{K\pi\pi}(m_{K\pi\pi}, t') + \hat{\rho}_{ab}^{3\pi}(m_{K\pi\pi}, t') + \hat{\rho}_{ab}^{\text{Bkg}}(m_{K\pi\pi}, t')$$

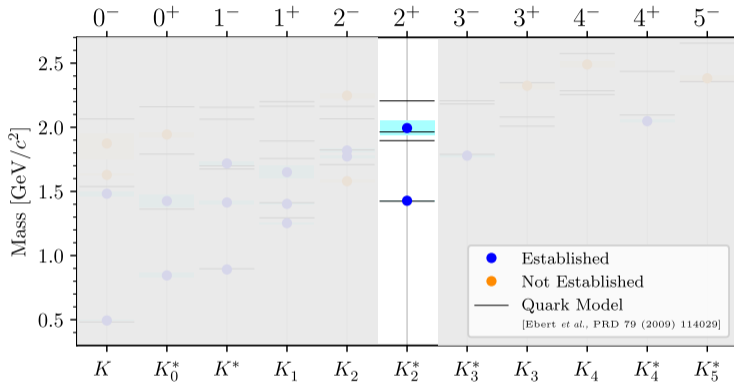
- ▶ $\pi^-\pi^-\pi^+$ background modeled by partial-wave projection of $\pi^-\pi^-\pi^+$ pseudodata
 - ▶ Yield is only free parameter
- ▶ Incoherent effective background component for other background processes



- ▶ Simultaneously included 14 partial waves in resonance-model fit
- ▶ Modeled by 13 strange-meson resonance components
- ▶ Using measured intensities and interference terms (relative phases)



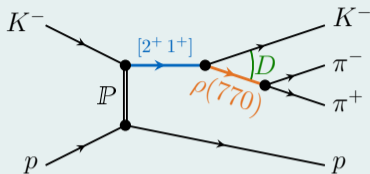




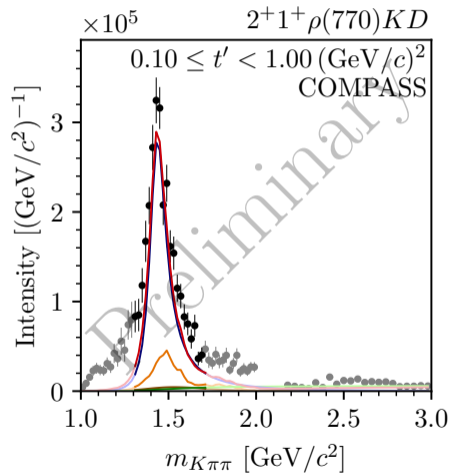
PDG

(2022)

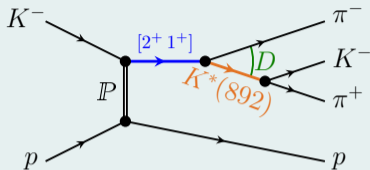
► $K_2^*(1430)$ well known resonance



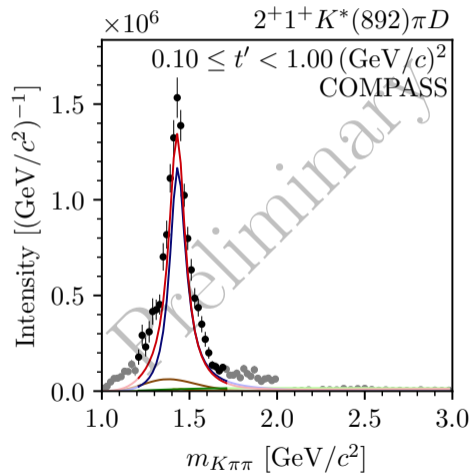
- ▶ $K_2^*(1430)$ signal
 - ▶ $m_0 = (1430.9 \pm 1.4^{+3.1}_{-1.5}) \text{ MeV}/c^2$
 - ▶ $\Gamma_0 = (111 \pm 3^{+4}_{-16}) \text{ MeV}/c^2$
- ▶ In different decays
 - ▶ $\rho(770) K D$
 - ▶ $K^*(892) \pi D$
- ▶ In agreement with previous measurements
- ▶ Cleaner signal in COMPASS data
- ▶ Fitted yield of $\pi^-\pi^-\pi^+$ background consistent with expectation



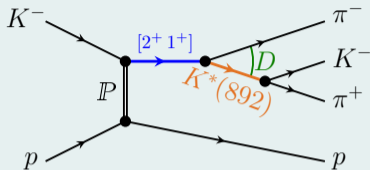
total resonance model,
resonances, non-resonant, $\pi\pi\pi$ background, effective background



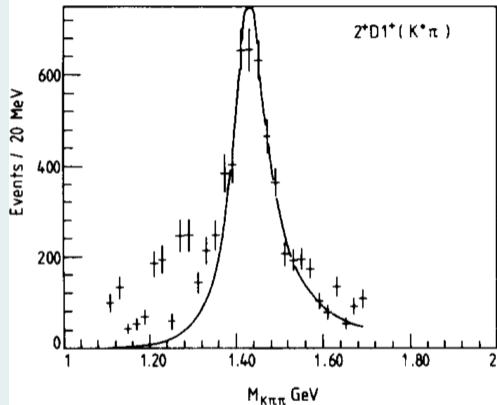
- ▶ $K_2^*(1430)$ signal
 - ▶ $m_0 = (1430.9 \pm 1.4^{+3.1}_{-1.5}) \text{ MeV}/c^2$
 - ▶ $\Gamma_0 = (111 \pm 3^{+4}_{-16}) \text{ MeV}/c^2$
- ▶ In different decays
 - ▶ $\rho(770) K D$
 - ▶ $K^*(892) \pi D$
- ▶ In agreement with previous measurements
- ▶ Cleaner signal in COMPASS data
- ▶ Fitted yield of $\pi^-\pi^-\pi^+$ background consistent with expectation

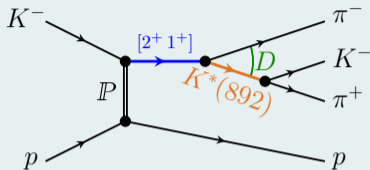


total resonance model,
resonances, non-resonant, $\pi\pi\pi$ background, effective background

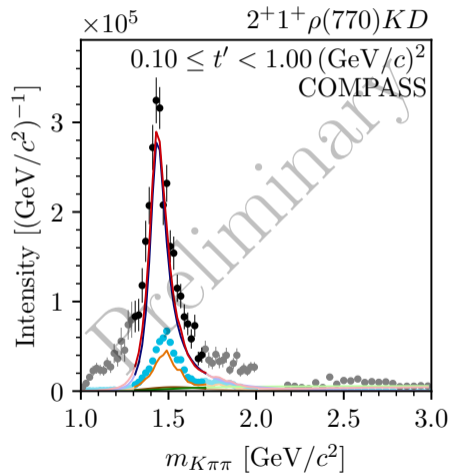


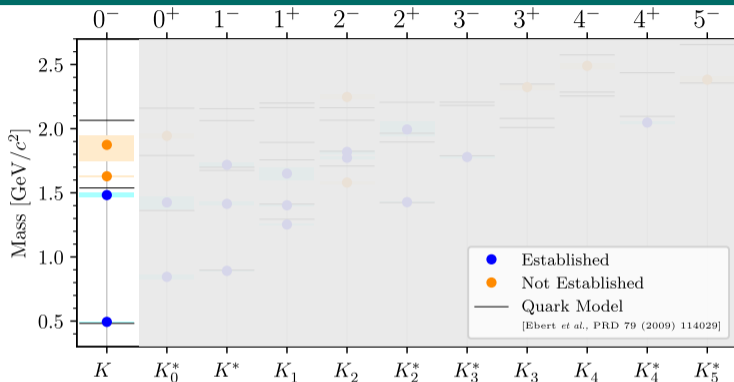
- ▶ $K_2^*(1430)$ signal
 - ▶ $m_0 = (1430.9 \pm 1.4^{+3.1}_{-1.5}) \text{ MeV}/c^2$
 - ▶ $\Gamma_0 = (111 \pm 3^{+4}_{-16}) \text{ MeV}/c^2$
- ▶ In different decays
 - ▶ $\rho(770) K D$
 - ▶ $K^*(892) \pi D$
- ▶ In agreement with previous measurements
- ▶ Cleaner signal in COMPASS data
- ▶ Fitted yield of $\pi^-\pi^-\pi^+$ background consistent with expectation



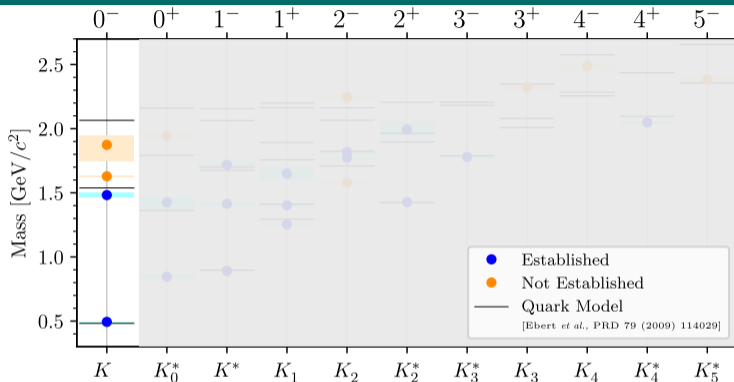


- ▶ $K_2^*(1430)$ signal
 - ▶ $m_0 = (1430.9 \pm 1.4^{+3.1}_{-1.5}) \text{ MeV}/c^2$
 - ▶ $\Gamma_0 = (111 \pm 3^{+4}_{-16}) \text{ MeV}/c^2$
- ▶ In **different decays**
 - ▶ $\rho(770) K D$
 - ▶ $K^*(892) \pi D$
- ▶ In agreement with previous measurements
- ▶ Cleaner signal in COMPASS data
- ▶ Fitted yield of $\pi^-\pi^-\pi^+$ background consistent with expectation





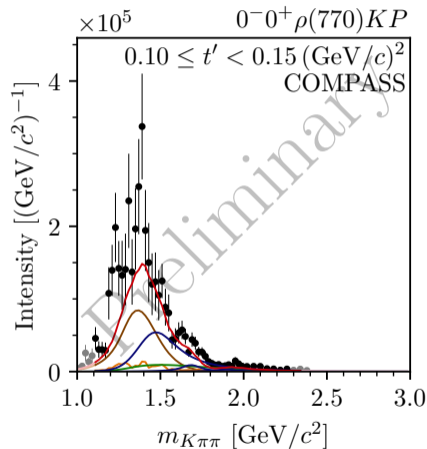
- ▶ $K(1460)$ and $K(1830)$
- ▶ $K(1630)$
 - ▶ Unexpectedly small width of only $16 \text{ MeV}/c^2$
 - ▶ J^P of $K(1630)$ unclear



- ▶ $K(1460)$ and $K(1830)$
- ▶ $K(1630)$
 - ▶ Unexpectedly small width of only $16 \text{ MeV}/c^2$
 - ▶ J^P of $K(1630)$ unclear

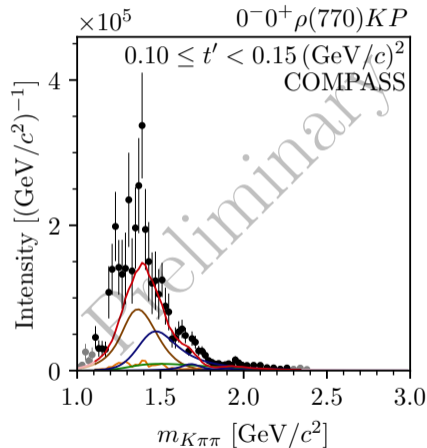
COMPASS $K^-\pi^-\pi^+$ data

- ▶ Peak at about $1.4 \text{ GeV}/c^2$
 - ▶ Established $K(1460)$
 - ▶ But, $m_{K\pi\pi} \lesssim 1.5 \text{ GeV}/c^2$ region weakly affected by known analysis artifacts
- ▶ Second peak at about $1.7 \text{ GeV}/c^2$
 - ▶ $K(1630)$ signal with 8.3σ statistical significance
 - ▶ Accompanied by rising phase
- ▶ Weak signal at about $2.0 \text{ GeV}/c^2$
 - ▶ $K(1830)$ signal with 5.4σ statistical significance



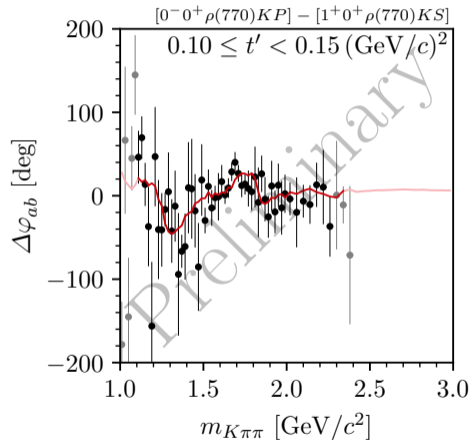
COMPASS $K^-\pi^-\pi^+$ data

- ▶ Peak at about $1.4 \text{ GeV}/c^2$
 - ▶ Established $K(1460)$
 - ▶ But, $m_{K\pi\pi} \lesssim 1.5 \text{ GeV}/c^2$ region weakly affected by known analysis artifacts
- ▶ Second peak at about $1.7 \text{ GeV}/c^2$
 - ▶ $K(1630)$ signal with 8.3σ statistical significance
 - ▶ Accompanied by rising phase
- ▶ Weak signal at about $2.0 \text{ GeV}/c^2$
 - ▶ $K(1830)$ signal with 5.4σ statistical significance



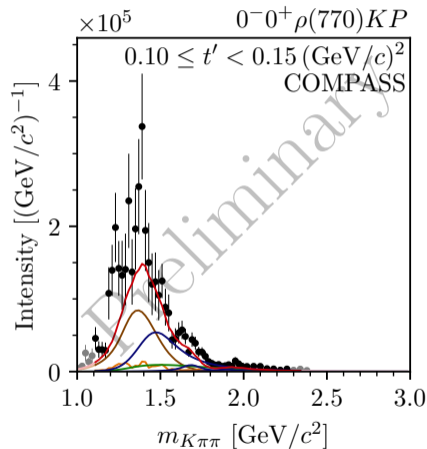
COMPASS $K^-\pi^-\pi^+$ data

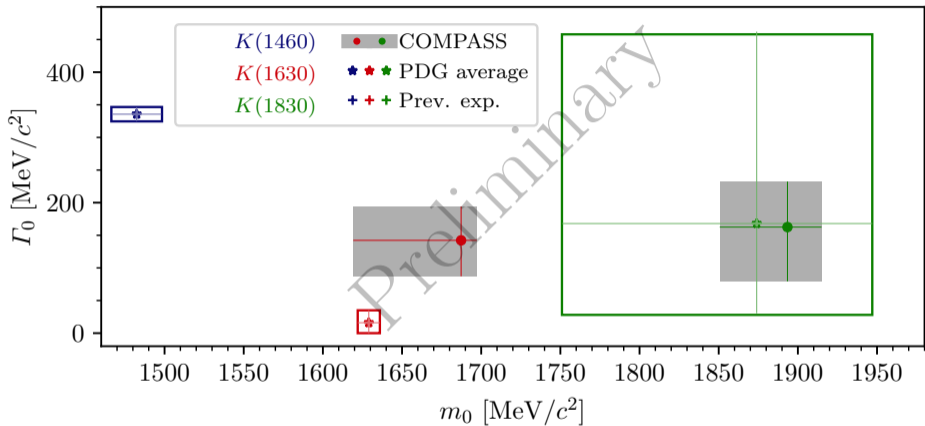
- ▶ Peak at about $1.4 \text{ GeV}/c^2$
 - ▶ Established $K(1460)$
 - ▶ But, $m_{K\pi\pi} \lesssim 1.5 \text{ GeV}/c^2$ region weakly affected by known analysis artifacts
- ▶ Second peak at about $1.7 \text{ GeV}/c^2$
 - ▶ $K(1630)$ signal with 8.3σ statistical significance
 - ▶ Accompanied by rising phase
- ▶ Weak signal at about $2.0 \text{ GeV}/c^2$
 - ▶ $K(1830)$ signal with 5.4σ statistical significance



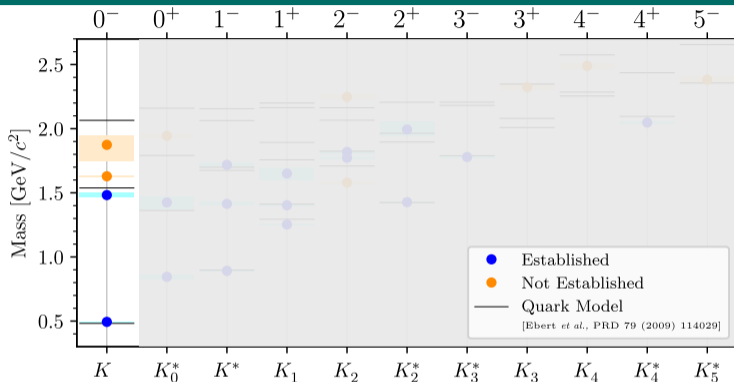
COMPASS $K^-\pi^-\pi^+$ data

- ▶ Peak at about $1.4 \text{ GeV}/c^2$
 - ▶ Established $K(1460)$
 - ▶ But, $m_{K\pi\pi} \lesssim 1.5 \text{ GeV}/c^2$ region weakly affected by known analysis artifacts
- ▶ Second peak at about $1.7 \text{ GeV}/c^2$
 - ▶ $K(1630)$ signal with 8.3σ statistical significance
 - ▶ Accompanied by rising phase
- ▶ Weak signal at about $2.0 \text{ GeV}/c^2$
 - ▶ $K(1830)$ signal with 5.4σ statistical significance

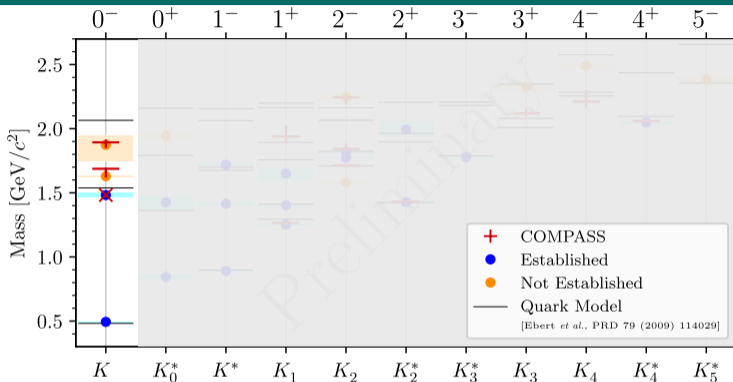




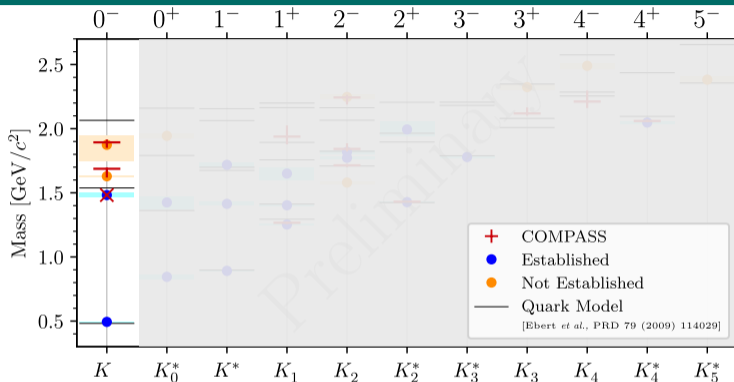
- ▶ $K(1830)$ parameters in good agreement with LChb measurement [PRL 118 (2017) 022003]
- ▶ Expected $K(1630)$ width of about 140 MeV/c²



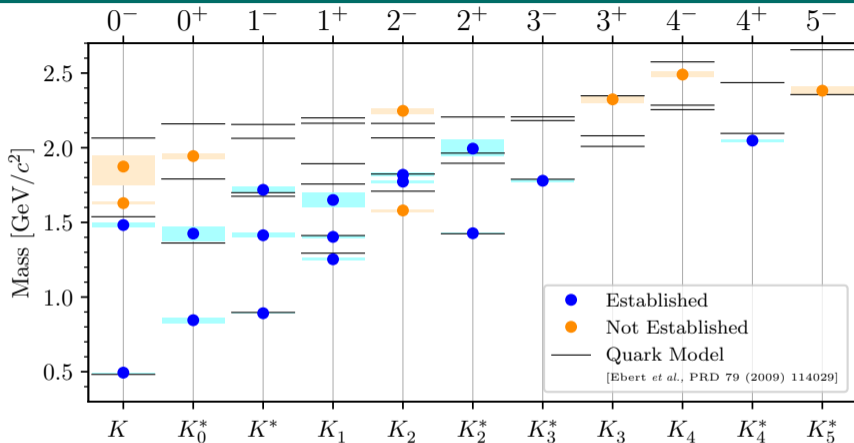
- ▶ Indications for 3 excited K from a single analysis
- ▶ Quark-model predicts only two excited states: potentially $K(1460)$ and $K(1830)$
 - $K(1630)$ supernumerary signal
 - Candidate for **exotic non- $q\bar{q}$ state**; other explanations possible ($K^*(892)$ ω threshold nearby)



- ▶ Indications for 3 excited K from a single analysis
- ▶ Quark-model predicts only two excited states: potentially $K(1460)$ and $K(1830)$
 - $K(1630)$ supernumerary signal
 - Candidate for exotic non- $q\bar{q}$ state; other explanations possible ($K^*(892)$ ω threshold nearby)

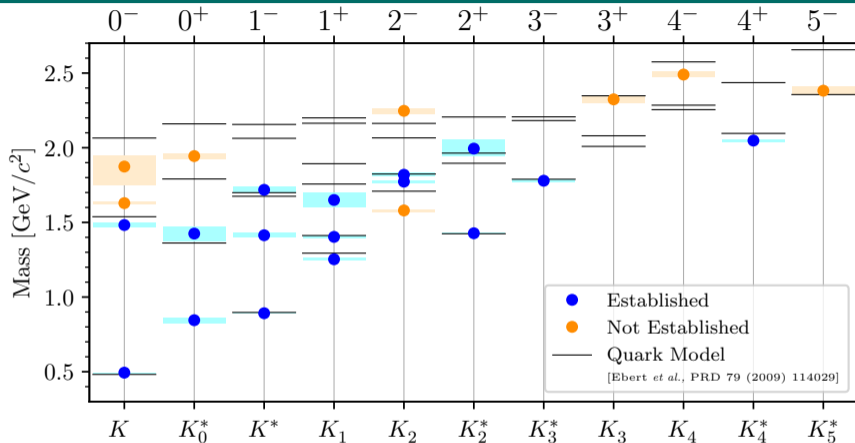


- ▶ Indications for 3 excited K from a single analysis
- ▶ Quark-model predicts only two excited states: potentially $K(1460)$ and $K(1830)$
 - ➡ $K(1630)$ supernumerary signal
 - ➡ Candidate for **exotic non- $q\bar{q}$ state**; other explanations possible ($K^*(892)$ ω threshold nearby)



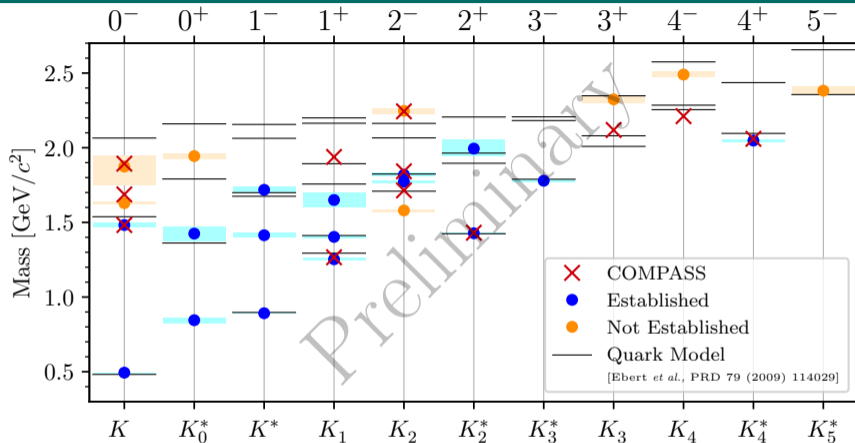
The Strange-Meson Spectrum

- ▶ Many strange mesons require further confirmation
- ▶ Search for strange partners of exotic non-strange light mesons



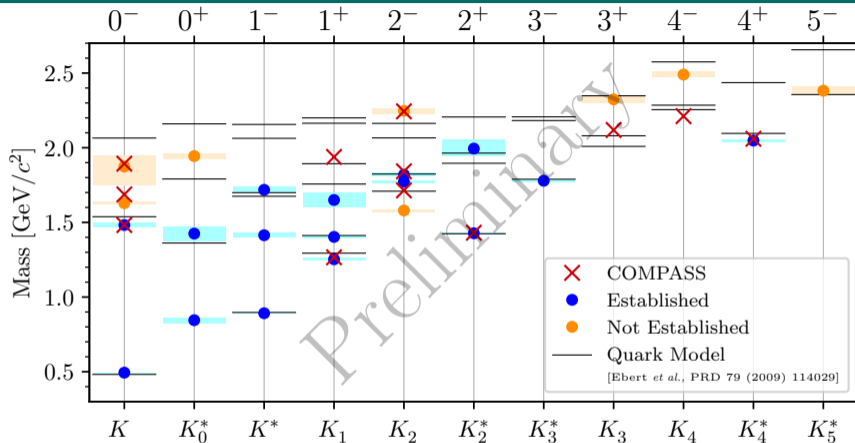
COMPASS

- ▶ World's largest data sample on $K^- \pi^- \pi^+$ \Rightarrow Most detailed and comprehensive analysis
- ▶ Candidate for exotic strange-meson signal with $J^P = 0^-$



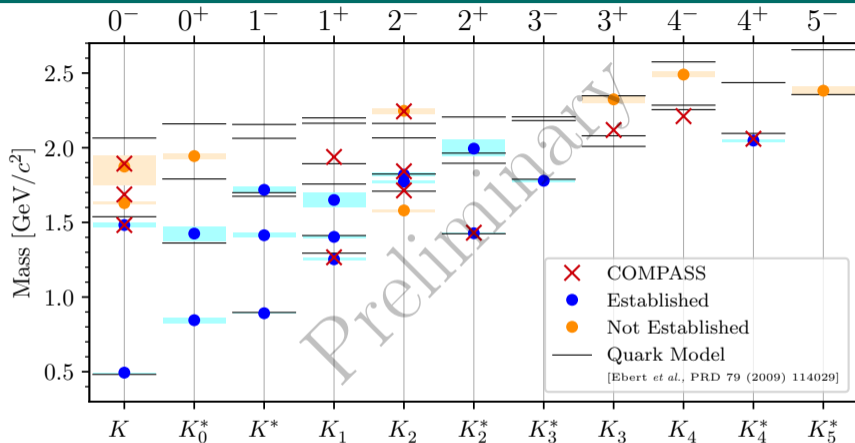
COMPASS

- ▶ World's largest data sample on $K^- \pi^- \pi^+$ \Rightarrow Most detailed and comprehensive analysis
- ▶ Candidate for exotic strange-meson signal with $J^P = 0^-$



AMBER: Proposal for High-Precision Strange-Meson Spectroscopy

- ▶ Goal: Collect $10 - 20 \times 10^6$ $K^- \pi^- \pi^+$ events using high-energy kaon beam
- ▶ AMBER is open for interested collaborators to join



COMPASS

- ▶ World's largest data sample on $K^- \pi^- \pi^+$ \Rightarrow Most detailed and comprehensive analysis
- ▶ Candidate for exotic strange-meson signal with $J^P = 0^-$

Backup

7 Partial-Wave Decomposition

- Treating the $\pi^-\pi^-\pi^+$ and Other Backgrounds

8 Resonance-Model Fit

- Modeling the $K^-\pi^-\pi^+$ Signal
- Modeling the $\pi^-\pi^-\pi^+$ Background
- Modeling the Effective Background
- χ^2 Fit Procedure

9 Wave-Set Selection

- Regularization: LASSO
- Regularization: Generalized Pareto
- Regularization: Cauchy
- For the $K^-\pi^-\pi^+$ Final State

10 14-Wave Resonance-Model Fit

- Searching for Exotic Strange Mesons with $J^P = 0^-$
- Partial Waves with $J^P = 2^+$
- Partial Waves with $J^P = 2^-$
- Partial Waves with $J^P = 4^+$

11 Kinematic Distribution of $K^-\pi^-\pi^+$ Events

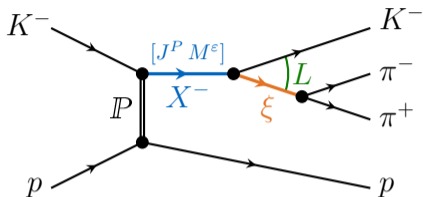
- Subsystem
- $m_{K^-\pi^-}$
- t' Spectrum
- Exclusivity

12 Systematic Studies of the Partial-Wave Decomposition

- 14 Waves
- Leakage Waves

13 Leakage Effect

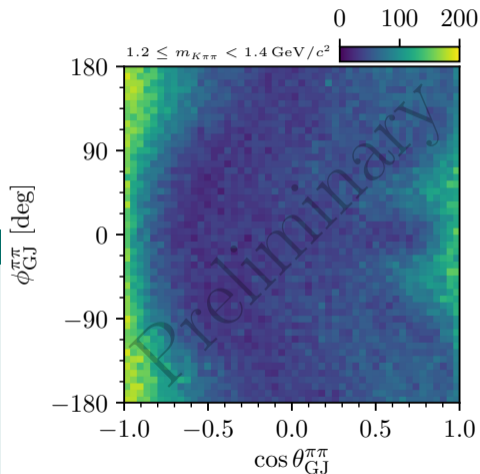
14 Incoherent $\pi^-\pi^-\pi^+$ Background



Partial wave

$$J^P M^E \xi b L$$

- ▶ $J^P M^E$: Spin, parity, and spin projection of X^-
- ▶ ξ : Isobar
- ▶ b : Bachelor particle. Here: Spectator K^-
- ▶ L : Angular momentum between bachelor and isobar



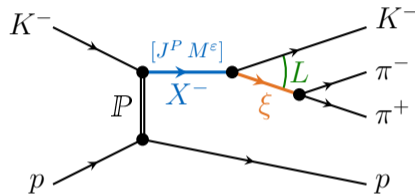
Model intensity

$$\mathcal{I}(\tau, m_{K\pi\pi}, t') = \sum_z \left| \sum_{a \in \mathbb{W}_z(m_{K\pi\pi}, t')} \mathcal{T}_a^z(m_{K\pi\pi}, t') \Psi_a^z(\tau; m_{K\pi\pi}) \right|^2$$

► Model intensity distribution

- in 5D $K^- \pi^- \pi^+$ phase-space
- for a given $(m_{K\pi\pi}, t')$ cell
- as **incoherent sum** over **coherent sectors** z
 - “Rank” of the partial-wave model = number of coherent sectors

- Ψ_a^z known, assuming the isobar model
- Wave set $\mathbb{W}_z(m_{K\pi\pi}, t')$ inferred from data using regularization-based model-selection techniques
- \mathcal{T}_a^z extracted in maximum-likelihood fit, independently for each $(m_{K\pi\pi}, t')$ cell



Spin-Density Matrix

$$\rho_{ab} = \sum_z \mathcal{T}_a^z [\mathcal{T}_b^z]^*$$

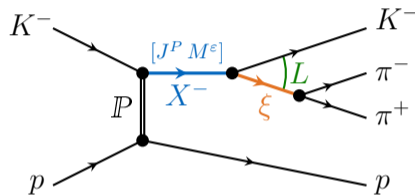
Model intensity

$$\mathcal{I}(\tau, m_{K\pi\pi}, t') = \sum_z \left| \sum_{a \in \mathbb{W}_z(m_{K\pi\pi}, t')} \mathcal{T}_a^z(m_{K\pi\pi}, t') \Psi_a^z(\tau; m_{K\pi\pi}) \right|^2$$

► Model intensity distribution

- in 5D $K^- \pi^- \pi^+$ phase-space
- for a given $(m_{K\pi\pi}, t')$ cell
- as incoherent sum over coherent sectors z
 - “Rank” of the partial-wave model = number of coherent sectors

- Ψ_a^z known, assuming the isobar model
- Wave set $\mathbb{W}_z(m_{K\pi\pi}, t')$ inferred from data using regularization-based model-selection techniques
- \mathcal{T}_a^z extracted in maximum-likelihood fit, independently for each $(m_{K\pi\pi}, t')$ cell



Spin-Density Matrix

$$\rho_{ab} = \sum_z \mathcal{T}_a^z [\mathcal{T}_b^z]^*$$

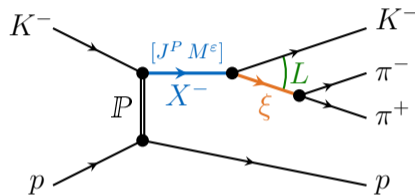
Model intensity

$$\mathcal{I}(\tau, m_{K\pi\pi}, t') = \sum_z \left| \sum_{a \in \mathbb{W}_z(m_{K\pi\pi}, t')} \mathcal{T}_a^z(m_{K\pi\pi}, t') \Psi_a^z(\tau; m_{K\pi\pi}) \right|^2$$

► Model intensity distribution

- in 5D $K^- \pi^- \pi^+$ phase-space
- for a given $(m_{K\pi\pi}, t')$ cell
- as incoherent sum over coherent sectors z
 - “Rank” of the partial-wave model = number of coherent sectors

- Ψ_a^z known, assuming the isobar model
- Wave set $\mathbb{W}_z(m_{K\pi\pi}, t')$ inferred from data using regularization-based model-selection techniques
- \mathcal{T}_a^z extracted in maximum-likelihood fit, independently for each $(m_{K\pi\pi}, t')$ cell



Spin-Density Matrix

$$\rho_{ab} = \sum_z \mathcal{T}_a^z [\mathcal{T}_b^z]^*$$

Approach

- ▶ Effectively take into account in partial-wave decomposition by **incoherently adding additional coherent sectors z**
(Model background by $K^- \pi^- \pi^+$ partial waves)
 - ➔ Increasing the rank of the spin-density matrix ρ_{ab}
 - ➔ Signal not separated from background in partial-wave decomposition
 - ➔ Partial-wave amplitudes include background
- ▶ Model signal and background contributions in resonance-model fit using more constrained signal model
 - ➔ Separate signal from background

$$\mathcal{I}(\tau, m_{K\pi\pi}, t') = \sum_z \left| \sum_{a \in \mathbb{W}_z(m_{K\pi\pi}, t')} \mathcal{T}_a^z(m_{K\pi\pi}, t') \Psi_a^z(\tau; m_{K\pi\pi}) \right|^2$$

$$\rho_{ab} = \sum_z \mathcal{T}_a^z [\mathcal{T}_b^z]^*$$

True physics intensity distribution

$$\mathcal{I}(\tau) = \left| \sum_a^{\text{waves}} \mathcal{T}_a \Psi_a(\tau) \right|^2$$

Experimentally measured intensity distribution

$$\mathcal{I}_{\text{measured}}(\tau) = \eta(\tau) \mathcal{I}(\tau)$$

- ▶ Take into account different processes \mathfrak{p}
 - ▶ Different model intensities $\mathcal{I}^{\mathfrak{p}}$
 - ▶ Different experimental acceptance $\eta^{\mathfrak{p}}$
 - ▶ Formulated in terms of different phase-space variables $\tau^{\mathfrak{p}}$
 - ▶ Jacobian terms $J(\tau^{K\pi\pi} \rightarrow \tau^{\mathfrak{p}})$ from variable transformation

True physics intensity distribution for process p

$$\mathcal{I}^p(\tau) = \left| \sum_a^{\text{waves}} \mathcal{T}_a^p \Psi_a^p(\tau) \right|^2$$

Experimentally measured intensity distribution

$$\mathcal{I}_{\text{measured}}(\tau) = \sum_p \eta^p(\tau) \mathcal{I}^p(\tau)$$

- ▶ Take into account different processes p
 - ▶ Different model intensities \mathcal{I}^p
 - ▶ Different experimental acceptance η^p
 - ▶ Formulated in terms of different phase-space variables τ^p
 - ▶ Jacobian terms $J(\tau^{K\pi\pi} \rightarrow \tau^p)$ from variable transformation

True physics intensity distribution for process \mathbf{p}

$$\mathcal{I}^{\mathbf{p}}(\tau^{\mathbf{p}}) = \left| \sum_a^{\text{waves}} \mathcal{T}_a^{\mathbf{p}} \Psi_a^{\mathbf{p}}(\tau^{\mathbf{p}}) \right|^2$$

Experimentally measured intensity distribution

$$\mathcal{I}_{\text{measured}}(\tau^{K\pi\pi}) = \sum_{\mathbf{p}} \eta^{\mathbf{p}}(\tau^{\mathbf{p}}) \mathcal{I}^{\mathbf{p}}(\tau^{\mathbf{p}}) J(\tau^{K\pi\pi} \rightarrow \tau^{\mathbf{p}})$$

- ▶ Take into account different processes \mathbf{p}
 - ▶ Different model intensities $\mathcal{I}^{\mathbf{p}}(\tau^{\mathbf{p}})$
 - ▶ Different experimental acceptance $\eta^{\mathbf{p}}(\tau^{\mathbf{p}})$
 - ▶ Formulated in terms of different phase-space variables $\tau^{\mathbf{p}}$
 - ▶ Jacobian terms $J(\tau^{K\pi\pi} \rightarrow \tau^{\mathbf{p}})$ from variable transformation

True physics intensity distribution for process p

$$\mathcal{I}^p(\tau^p) = \left| \sum_a^{\text{waves}} \mathcal{T}_a^p \Psi_a^p(\tau^p) \right|^2$$

- ▶ $\mathcal{I}^{\pi\pi\pi}$ known by COMPASS analysis
- ▶ $\eta^{\pi\pi\pi}$ from detector simulation

Experimentally measured intensity distribution

$$\mathcal{I}_{\text{measured}}(\tau^{K\pi\pi}) = \sum_p \eta^p(\tau^p) \mathcal{I}^p(\tau^p) J(\tau^{K\pi\pi} \rightarrow \tau^p)$$

- ▶ $\eta^{\pi\pi\pi}$ computationally expensive
- ▶ Different $m_{3\pi}$ bins enter one $m_{K\pi\pi}$ bin
- ▶ Other background channels: $K^-K^-K^+$, ...
 - ▶ \mathcal{I}^p unknown
 - ▶ Unknown background channels

True physics intensity distribution for process p

$$\mathcal{I}^p(\tau^p) = \left| \sum_a^{\text{waves}} \mathcal{T}_a^p \Psi_a^p(\tau^p) \right|^2$$

- ▶ $\mathcal{I}^{\pi\pi\pi}$ known by COMPASS analysis
- ▶ $\eta^{\pi\pi\pi}$ from detector simulation

Experimentally measured intensity distribution

$$\mathcal{I}_{\text{measured}}(\tau^{K\pi\pi}) = \sum_p \eta^p(\tau^p) \mathcal{I}^p(\tau^p) J(\tau^{K\pi\pi} \rightarrow \tau^p)$$

- ▶ $\eta^{\pi\pi\pi}$ computationally expensive
- ▶ Different $m_{3\pi}$ bins enter one $m_{K\pi\pi}$ bin
- ▶ Other background channels: $K^-K^-K^+$, ...
 - ▶ \mathcal{I}^p unknown
 - ▶ Unknown background channels

True physics intensity distribution for process p

$$\mathcal{I}^p(\tau^p) = \left| \sum_a^{\text{waves}} \mathcal{T}_a^p \Psi_a^p(\tau^p) \right|^2$$

- ▶ $\mathcal{I}^{\pi\pi\pi}$ known by COMPASS analysis
- ▶ $\eta^{\pi\pi\pi}$ from detector simulation

Experimentally measured intensity distribution

$$\mathcal{I}_{\text{measured}}(\tau^{K\pi\pi}) = \sum_p \eta^p(\tau^p) \mathcal{I}^p(\tau^p) J(\tau^{K\pi\pi} \rightarrow \tau^p)$$

- ▶ $\eta^{\pi\pi\pi}$ computationally expensive
- ▶ Different $m_{3\pi}$ bins enter one $m_{K\pi\pi}$ bin
- ▶ Other background channels: $K^-K^-K^+$, ...
 - ▶ \mathcal{I}^p unknown
 - ▶ Unknown background channels

Approximate model for process p by $K^-\pi^-\pi^+$ partial waves

$$\eta^p(\tau^p) \left| \sum_a^{\text{waves}} \mathcal{T}_a^p \Psi_a^p(\tau^p) \right|^2 \approx \eta^{K\pi\pi}(\tau^{K\pi\pi}) \left| \sum_a^{\text{waves}} \tilde{\mathcal{T}}_a^p \Psi_a^{K\pi\pi}(\tau^{K\pi\pi}) \right|^2$$

Total true physics intensity distribution

$$\mathcal{I}(\tau^{K\pi\pi}) = \sum_p \left| \sum_a^{\text{waves}} \mathcal{T}_a^p \Psi_a^{K\pi\pi}(\tau^{K\pi\pi}) \right|^2$$

Experimentally measured intensity distribution

$$\mathcal{I}_{\text{measured}}(\tau^{K\pi\pi}) = \eta^{K\pi\pi}(\tau^{K\pi\pi}) \mathcal{I}(\tau^{K\pi\pi})$$

- ▶ How well can $K^-\pi^-\pi^+$ partial waves approximate the distribution of process p
 - ▶ Is the set of $K^-\pi^-\pi^+$ partial waves sufficient?
 - ➔ Automatic wave-set selection using model-selection techniques

Approximate model for process p by $K^-\pi^-\pi^+$ partial waves

$$\eta^p(\tau^p) \left| \sum_a^{\text{waves}} \mathcal{T}_a^p \Psi_a^p(\tau^p) \right|^2 \approx \eta^{K\pi\pi}(\tau^{K\pi\pi}) \left| \sum_a^{\text{waves}} \tilde{\mathcal{T}}_a^p \Psi_a^{K\pi\pi}(\tau^{K\pi\pi}) \right|^2$$

Total true physics intensity distribution

$$\mathcal{I}(\tau^{K\pi\pi}) = \sum_p \left| \sum_a^{\text{waves}} \mathcal{T}_a^p \Psi_a^{K\pi\pi}(\tau^{K\pi\pi}) \right|^2$$

Experimentally measured intensity distribution

$$\mathcal{I}_{\text{measured}}(\tau^{K\pi\pi}) = \eta^{K\pi\pi}(\tau^{K\pi\pi}) \mathcal{I}(\tau^{K\pi\pi})$$

- ▶ How well can $K^-\pi^-\pi^+$ partial waves approximate the distribution of process p
 - ▶ Is the set of $K^-\pi^-\pi^+$ partial waves sufficient?
 - Automatic wave-set selection using model-selection techniques

Approximate model for process p by $K^-\pi^-\pi^+$ partial waves

$$\eta^p(\tau^p) \left| \sum_a^{\text{waves}} \mathcal{T}_a^p \Psi_a^p(\tau^p) \right|^2 \approx \eta^{K\pi\pi}(\tau^{K\pi\pi}) \left| \sum_a^{\text{waves}} \tilde{\mathcal{T}}_a^p \Psi_a^{K\pi\pi}(\tau^{K\pi\pi}) \right|^2$$

Total true physics intensity distribution

$$\mathcal{I}(\tau^{K\pi\pi}) = \sum_{a,b}^{\text{waves}} \Psi_a^{K\pi\pi}(\tau^{K\pi\pi}) \rho_{a,b} [\Psi_b^{K\pi\pi}(\tau^{K\pi\pi})]^*$$

Spin-density matrix with rank $N_r > 1$

$$\rho_{a,b} = \sum_p \mathcal{T}_a^p [\mathcal{T}_b^p]^*$$

- ▶ How well can $K^-\pi^-\pi^+$ partial waves approximate the distribution of process p
 - ▶ Is the set of $K^-\pi^-\pi^+$ partial waves sufficient?
 - ➔ Automatic wave-set selection using model-selection techniques

Approximate model for process p by $K^-\pi^-\pi^+$ partial waves

$$\eta^p(\tau^p) \left| \sum_a^{\text{waves}} \mathcal{T}_a^p \Psi_a^p(\tau^p) \right|^2 \approx \eta^{K\pi\pi}(\tau^{K\pi\pi}) \left| \sum_a^{\text{waves}} \tilde{\mathcal{T}}_a^p \Psi_a^{K\pi\pi}(\tau^{K\pi\pi}) \right|^2$$

Total true physics intensity distribution

$$\mathcal{I}(\tau^{K\pi\pi}) = \sum_{a,b}^{\text{waves}} \Psi_a^{K\pi\pi}(\tau^{K\pi\pi}) \rho_{a,b} [\Psi_b^{K\pi\pi}(\tau^{K\pi\pi})]^*$$

Spin-density matrix with rank $N_r > 1$

$$\rho_{a,b} = \sum_p^{N_r} \mathcal{T}_a^p [\mathcal{T}_b^p]^*$$

- ▶ How well can $K^-\pi^-\pi^+$ partial waves approximate the distribution of process p
 - ▶ Is the set of $K^-\pi^-\pi^+$ partial waves sufficient?
 - ➔ Automatic wave-set selection using model-selection techniques

Approximate model for process p by $K^-\pi^-\pi^+$ partial waves

$$\eta^p(\tau^p) \left| \sum_a^{\text{waves}} \mathcal{T}_a^p \Psi_a^p(\tau^p) \right|^2 \approx \eta^{K\pi\pi}(\tau^{K\pi\pi}) \left| \sum_a^{\text{waves}} \tilde{\mathcal{T}}_a^p \Psi_a^{K\pi\pi}(\tau^{K\pi\pi}) \right|^2$$

Total true physics intensity distribution

$$\mathcal{I}(\tau^{K\pi\pi}) = \sum_{a,b}^{\text{waves}} \Psi_a^{K\pi\pi}(\tau^{K\pi\pi}) \rho_{a,b} [\Psi_b^{K\pi\pi}(\tau^{K\pi\pi})]^*$$

Spin-density matrix with rank $N_r > 1$

$$\rho_{a,b} = \sum_r^{N_r} \mathcal{T}_a^r [T_b^r]^*$$

▶ Experimentally measurable quantities are spin-density matrix elements

- ➡ Transition amplitudes \mathcal{T}_a^p are only effective parameters
- ➡ Cannot determine \mathcal{T}_a^p of individual processes
- ➡ Cannot separate different processes

Approximate model for process p by $K^-\pi^-\pi^+$ partial waves

$$\eta^p(\tau^p) \left| \sum_a^{\text{waves}} \mathcal{T}_a^p \Psi_a^p(\tau^p) \right|^2 \approx \eta^{K\pi\pi}(\tau^{K\pi\pi}) \left| \sum_a^{\text{waves}} \tilde{\mathcal{T}}_a^p \Psi_a^{K\pi\pi}(\tau^{K\pi\pi}) \right|^2$$

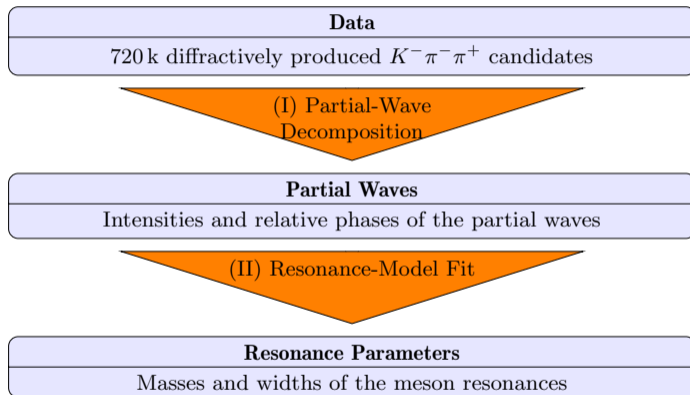
Total true physics intensity distribution

$$\mathcal{I}(\tau^{K\pi\pi}) = \sum_{a,b}^{\text{waves}} \Psi_a^{K\pi\pi}(\tau^{K\pi\pi}) \rho_{a,b} [\Psi_b^{K\pi\pi}(\tau^{K\pi\pi})]^*$$

Spin-density matrix with rank $N_r > 1$

$$\rho_{a,b} = \sum_r^{N_r} \mathcal{T}_a^r [T_b^r]^*$$

- ▶ Large number of fit parameters: $N_{\text{para}} = N_r(2N_{\text{waves}} - N_r)$
- ▶ Sufficient rank of spin-density matrix must be determined
 - ▶ Rank two needed to describe pure $\pi^-\pi^-\pi^+$ Monte Carlo sample using $K^-\pi^-\pi^+$ partial waves
 - ▶ Used rank three to model $K^-\pi^-\pi^+$ sample



- ▶ Spin-density matrix $\rho_{ab}(m_{K\pi\pi}, t')$ measured in partial-wave decomposition
- ▶ Model spin-density matrix in resonance-model fit

$$\hat{\rho}_{ab}(m_{K\pi\pi}, t') = \hat{\rho}_{ab}^{K\pi\pi}(m_{K\pi\pi}, t') + \hat{\rho}_{ab}^{3\pi}(m_{K\pi\pi}, t') + \hat{\rho}_{ab}^{\text{Bkg}}(m_{K\pi\pi}, t')$$

Model transition amplitudes as coherent sum over various components

$$\hat{T}_a^z(m_{K\pi\pi}, t') = \sum_{k \in \mathbb{S}_a} K(m_{K\pi\pi}, t')^k C_a^{K\pi\pi}(t') \mathcal{D}_k(m_{K\pi\pi}; \zeta_k)$$

- ▶ Dynamic functions $\mathcal{D}_k(m_{K\pi\pi}; \zeta_k)$
 - ▶ For resonances: rel. Breit-Wigner
 - ▶ For non-resonant terms: $\mathcal{D}_k^{\text{NR}}(m_{K\pi\pi}; a_k, c_k) = (m_{K\pi\pi} - m_{\text{thr}})^{a_k} e^{-b(c_k) \tilde{q}_k^2(m_{K\pi\pi})}$
- ▶ “Coupling amplitudes”: ${}^k C_a^z(t')$
 - ▶ Independent coupling amplitude for each t' bin
- ▶ Kinematic factor $K(m_{K\pi\pi}, t')$
- ▶ **Coherently summed** over all assumed model components

Model transition amplitudes as coherent sum over various components

$$\hat{T}_a^z(m_{K\pi\pi}, t') = \sum_{k \in \mathbb{S}_a} K(m_{K\pi\pi}, t')^k \mathcal{C}_a^{K\pi\pi}(t') \mathcal{D}_k(m_{K\pi\pi}; \zeta_k)$$

- ▶ Dynamic functions $\mathcal{D}_k(m_{K\pi\pi}; \zeta_k)$
 - ▶ For resonances: rel. Breit-Wigner
 - ▶ For non-resonant terms: $\mathcal{D}_k^{\text{NR}}(m_{K\pi\pi}; a_k, c_k) = (m_{K\pi\pi} - m_{\text{thr}})^{a_k} e^{-b(c_k) \tilde{q}_k^2(m_{K\pi\pi})}$
- ▶ “Coupling amplitudes”: ${}^k \mathcal{C}_a^z(t')$
 - ▶ Independent coupling amplitude for each t' bin
- ▶ Kinematic factor $K(m_{K\pi\pi}, t')$
- ▶ Coherently summed over all assumed model components

Model transition amplitudes as coherent sum over various components

$$\hat{T}_a^z(m_{K\pi\pi}, t') = \sum_{k \in \mathbb{S}_a} K(m_{K\pi\pi}, t')^k C_a^{K\pi\pi}(t') \mathcal{D}_k(m_{K\pi\pi}; \zeta_k)$$

- ▶ Dynamic functions $\mathcal{D}_k(m_{K\pi\pi}; \zeta_k)$
 - ▶ For resonances: rel. Breit-Wigner
 - ▶ For non-resonant terms: $\mathcal{D}_k^{\text{NR}}(m_{K\pi\pi}; a_k, c_k) = (m_{K\pi\pi} - m_{\text{thr}})^{a_k} e^{-b(c_k) \tilde{q}_k^2(m_{K\pi\pi})}$
- ▶ “Coupling amplitudes”: ${}^k C_a^z(t')$
 - ▶ Independent coupling amplitude for each t' bin
- ▶ Kinematic factor $K(m_{K\pi\pi}, t')$
- ▶ Coherently summed over all assumed model components

Model transition amplitudes as coherent sum over various components

$$\hat{T}_a^z(m_{K\pi\pi}, t') = \sum_{k \in \mathbb{S}_a} K(m_{K\pi\pi}, t')^k C_a^{K\pi\pi}(t') \mathcal{D}_k(m_{K\pi\pi}; \zeta_k)$$

- ▶ Dynamic functions $\mathcal{D}_k(m_{K\pi\pi}; \zeta_k)$
 - ▶ For resonances: rel. Breit-Wigner
 - ▶ For non-resonant terms: $\mathcal{D}_k^{\text{NR}}(m_{K\pi\pi}; a_k, c_k) = (m_{K\pi\pi} - m_{\text{thr}})^{a_k} e^{-b(c_k) \tilde{q}_k^2(m_{K\pi\pi})}$
- ▶ “Coupling amplitudes”: ${}^k C_a^z(t')$
 - ▶ Independent coupling amplitude for each t' bin
- ▶ Kinematic factor $K(m_{K\pi\pi}, t')$
- ▶ **Coherently summed** over all assumed model components

3π spin-density matrix

$$\hat{\rho}_{ab}^{\pi\pi\pi}(m_{K\pi\pi}, t') = \left| C^{\pi\pi\pi} \right|^2 \rho_{ab}^{\pi\pi\pi}(m_{K\pi\pi}, t')$$

- ▶ $\rho_{ab}^{\pi\pi\pi}(m_{K\pi\pi}, t')$ obtained from PWD of $\pi^- \pi^- \pi^+$ pseudodata sample
 - ▶ $m_{K\pi\pi}$ dependence fixed
 - ▶ t' dependence fixed
 - ▶ Rel. strength between partial waves fixed (freed in a study)
- ▶ One global real-valued yield parameter $\left| C^{\pi\pi\pi} \right|^2$

Background spin-density matrix

- ▶ Additional incoherent contribution from other processes: $K^- K^- K^+$, ...
- ▶ Transition amplitudes modeled by non-resonant parameterizations for each partial wave

$$\hat{\mathcal{T}}_a^{\text{eBKG}}(m_{K\pi\pi}, t') = K(m_{K\pi\pi}, t') \mathcal{C}_a^{\text{eBKG}}(t') \mathcal{D}_{k_a}^{\text{eBKG}}(m_{K\pi\pi}; a_{k_a}, c_{k_a})$$

- ▶ χ^2 fit of the real and imaginary parts of the spin-density matrix
 - ▶ Taking into account correlations between spin-density matrix elements
 - ▶ Shape parameters (m_0, Γ_0, \dots) and coupling amplitudes are free parameters
- ▶ For the main fit, we performed 2000 fit attempts with random start-parameter values for the shape parameters, e.g. mass and width parameters, and the coupling and branching amplitudes.
- ▶ Start-parameter ranges for the shape parameters are chosen according to previous measurements (see note)
- ▶ The best result is the one which yielded the smallest χ^2 value

- ▶ χ^2 fit of the real and imaginary parts of the spin-density matrix
 - ▶ Taking into account correlations between spin-density matrix elements
 - ▶ Shape parameters (m_0, Γ_0, \dots) and coupling amplitudes are free parameters
- ▶ For the main fit, we performed 2000 fit attempts with random start-parameter values for the shape parameters, e.g. mass and width parameters, and the coupling and branching amplitudes.
- ▶ Start-parameter ranges for the shape parameters are chosen according to previous measurements (see note)
- ▶ The best result is the one which yielded the smallest χ^2 value

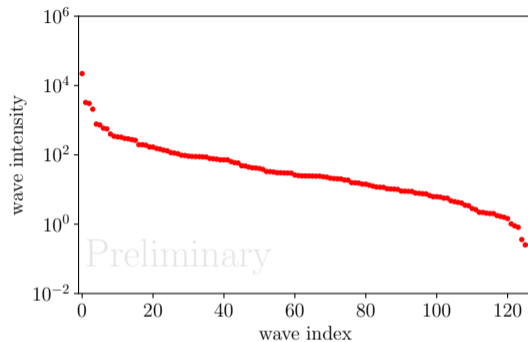
$$\mathcal{I}(\tau, m_{K\pi\pi}, t') = \left| \sum_{a \in \mathbb{W}(m_{K\pi\pi}, t')} \mathcal{T}_a(m_{K\pi\pi}, t') \Psi_a(\tau; m_{K\pi\pi}) \right|^2$$

Challenge: Find the “best” set of waves that describes the data

- ▶ If the wave set is too large
 - ↳ Starting to describe statistical fluctuations
- ▶ If waves that contribute to the data are missing
 - ↳ Intensity can be wrongly attributed to other waves
 - ↳ Model leakage

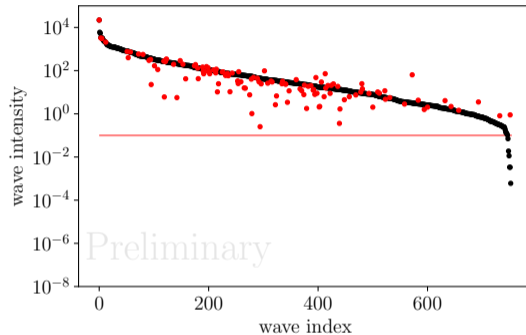
Infer wave set from data

- ▶ **Systematically construct** large set of allowed partial waves
 - ↳ “Wave pool”
- ▶ Fit wave pool to data
 - ▶ Impose penalty on $|\mathcal{T}_a|^2 \Rightarrow$ **regularization**
 - ▶ Suppress insignificant waves
- ▶ **Select waves** that significantly contribute to data
 - ↳ “Best” subset of waves that describe the data



- ▶ $\pi^- \pi^- \pi^+$ Monte Carlo mock data set with 126 partial waves
- ▶ Fitting wave pool of 753 waves
 - ▶ Massive overfitting
 - ▶ Almost all waves pick up intensity

Courtesy F. Kaspar, TUM



- ▶ $\pi^- \pi^- \pi^+$ Monte Carlo mock data set with 126 partial waves
- ▶ Fitting wave pool of 753 waves
 - Massive overfitting
 - Almost all waves pick up intensity

Courtesy F. Kaspar, TUM

$$\ln \mathcal{L}_{\text{fit}} = \ln \mathcal{L}_{\text{extended}} + \sum_a^{\text{waves}} \ln \mathcal{L}_{\text{reg}}(|\mathcal{T}_a|; \{c_{\text{para}}\})$$

LASSO/L1 regularization¹

$$\ln \mathcal{L}_{\text{reg}}(|\mathcal{T}_a|; \lambda) = -\lambda |\mathcal{T}_a|$$

- ▶ Maximum at $|\mathcal{T}_a| = 0$
- ▶ Well established²
- ▶ “Smoothing” at $|\mathcal{T}_a| = 0$

$$|\mathcal{T}_a| \rightarrow \sqrt{|\mathcal{T}_a|^2 + \varepsilon}$$

¹ Robert Tibshirani. “Regression Shrinkage and Selection via the Lasso”. In: Journal of the Royal Statistical Society. Series B 58.1 (1996)

² Baptiste Guegan et al. “Model selection for amplitude analysis”. In: JINST 10.09 (2015), P09002

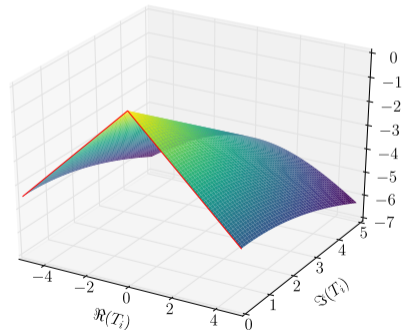
$$\ln \mathcal{L}_{\text{fit}} = \ln \mathcal{L}_{\text{extended}} + \sum_a^{\text{waves}} \ln \mathcal{L}_{\text{reg}}(|\mathcal{T}_a|; \{c_{\text{para}}\})$$

LASSO/L1 regularization¹

$$\ln \mathcal{L}_{\text{reg}}(|\mathcal{T}_a|; \lambda) = -\lambda |\mathcal{T}_a|$$

- ▶ Maximum at $|\mathcal{T}_a| = 0$
- ▶ Well established²
- ▶ “Smoothing” at $|\mathcal{T}_a| = 0$

$$|\mathcal{T}_a| \rightarrow \sqrt{|\mathcal{T}_a|^2 + \varepsilon}$$



¹ Robert Tibshirani. “Regression Shrinkage and Selection via the Lasso”. In: Journal of the Royal Statistical Society. Series B 58.1 (1996)

² Baptiste Guegan et al. “Model selection for amplitude analysis”. In: JINST 10.09 (2015), P09002

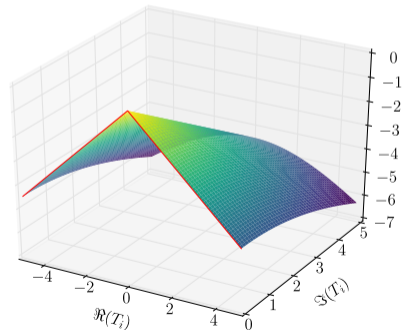
$$\ln \mathcal{L}_{\text{fit}} = \ln \mathcal{L}_{\text{extended}} + \sum_a^{\text{waves}} \ln \mathcal{L}_{\text{reg}}(|\mathcal{T}_a|; \{c_{\text{para}}\})$$

LASSO/L1 regularization¹

$$\ln \mathcal{L}_{\text{reg}}(|\mathcal{T}_a|; \lambda) = -\lambda |\mathcal{T}_a|$$

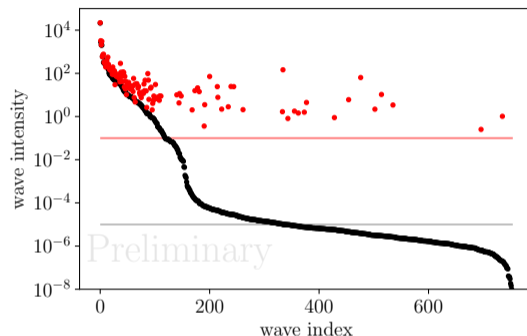
- ▶ Maximum at $|\mathcal{T}_a| = 0$
- ▶ Well established²
- ▶ “Smoothing” at $|\mathcal{T}_a| = 0$

$$|\mathcal{T}_a| \rightarrow \sqrt{|\mathcal{T}_a|^2 + \varepsilon}$$



¹ Robert Tibshirani. “Regression Shrinkage and Selection via the Lasso”. In: Journal of the Royal Statistical Society. Series B 58.1 (1996)

² Baptiste Guegan et al. “Model selection for amplitude analysis”. In: JINST 10.09 (2015), P09002



$$\lambda = 0.3$$

$$\varepsilon = 10^{-5}$$

- ▶ Bias also on large transition amplitudes
- ▶ Some additional waves
- ▶ Some waves missing

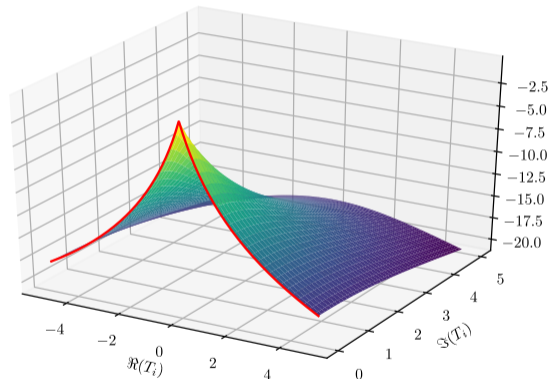
Courtesy F. Kaspar, TUM

Generalized Pareto¹

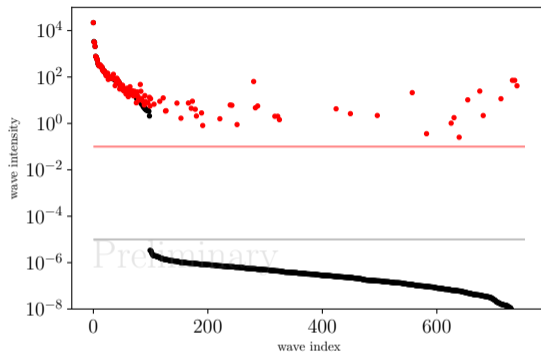
$$\ln \mathcal{L}_{\text{reg}}(|\mathcal{T}_a|; \Gamma, \zeta) = -\frac{1}{\zeta} \ln \left[1 + \zeta \frac{|\mathcal{T}_a|}{\Gamma} \right]$$

- ▶ Wave **intensities** spread over **orders of magnitudes**
- ▶ Use **logarithmic prior**
 - ➔ Heavy-tailed
 - ➔ Less bias on large waves
- ▶ LASSO-like for $|\mathcal{T}_a| \rightarrow 0$
- ▶ “Smoothing” at $|\mathcal{T}_a| = 0$

$$|\mathcal{T}_a| \rightarrow \sqrt{|\mathcal{T}_a|^2 + \varepsilon}$$



¹ Artin Armagan, David B. Dunson, and Jaeyong Lee. “Generalized double Pareto shrinkage”. In: *Statistica Sinica* (2013). doi: 10.5705/ss.2011.048.



$$\zeta = 0.5$$

$$\Gamma = 0.1$$

$$\varepsilon = 10^{-5}$$

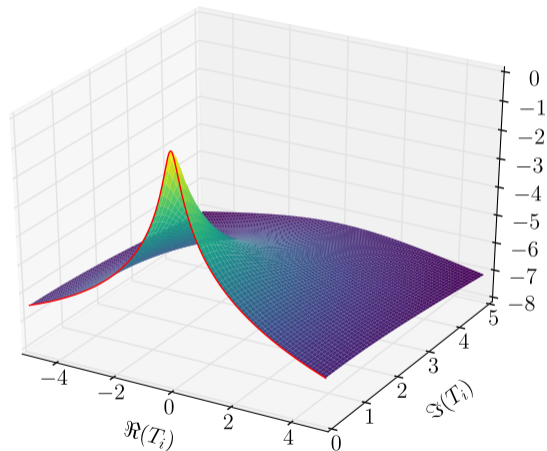
- ▶ Less bias on large transition amplitudes
- ▶ Clear **kink** in intensity distribution to smoothing scale \Rightarrow Selection
- ▶ Less additional waves
- ▶ Some small waves missing

Courtesy F. Kaspar, TUM

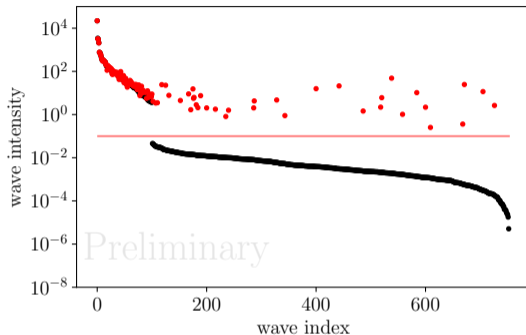
“Cauchy”

$$\ln \mathcal{L}_{\text{reg}}(|\mathcal{T}_a|; \Gamma) = -\ln \left[1 + \frac{|\mathcal{T}_a|^2}{\Gamma_a^2} \right]$$

- ▶ Logarithmic prior
- ▶ L2-like for $|\mathcal{T}_a| \rightarrow 0$



$$\Gamma = 0.2$$



- ▶ Less bias on large transition amplitudes
- ▶ Clear kink in intensity distribution
- ▶ Few additional waves
- ▶ Few small waves missing

Courtesy F. Kaspar, TUM

Wave pool

- ▶ Spin $J \leq 7$
 - ▶ Angular momentum $L \leq 7$
 - ▶ Positive naturality of exchange particle
 - ▶ 12 isobars
 - ▶ $[K\pi]_S^{K\pi}$, $[K\pi]_S^{K\eta}$, $K^*(892)$, $K^*(1680)$, $K_2^*(1430)$, $K_3^*(1780)$
 - ▶ $[\pi\pi]_S$, $f_0(980)$, $f_0(1500)$, $\rho(770)$, $f_2(1270)$, $\rho_3(1690)$
- ⇒ “Wave pool” of 596 waves

“only” 720 k events

Wave pool

- ▶ Spin $J \leq 7$
 - ▶ Angular momentum $L \leq 7$
 - ▶ Positive naturality of exchange particle
 - ▶ 12 isobars
 - ▶ $[K\pi]_S^{K\pi}$, $[K\pi]_S^{K\eta}$, $K^*(892)$, $K^*(1680)$, $K_2^*(1430)$, $K_3^*(1780)$
 - ▶ $[\pi\pi]_S$, $f_0(980)$, $f_0(1500)$, $\rho(770)$, $f_2(1270)$, $\rho_3(1690)$
- ⇒ “Wave pool” of 596 waves

“only” 720 k events

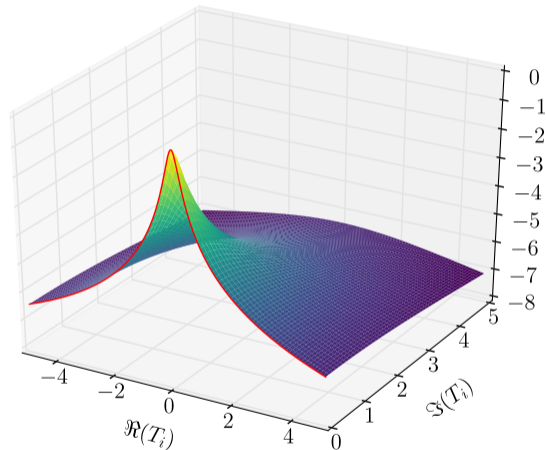
Regularization

$$\ln \mathcal{L}_{\text{reg}}(|\mathcal{T}_a|; \Gamma) = -\ln \left[1 + \frac{|\mathcal{T}_a|^2}{\Gamma_a^2} \right]$$

- ▶ Use Cauchy regularization
- ▶ Scale of $|\mathcal{T}_a|$ depends on experimental acceptance
 - ▶ Apply penalty on expected number \bar{N}_a of observed events

$$\Gamma_a = \frac{\Gamma}{\sqrt{\bar{n}_a}} \Rightarrow \frac{|\mathcal{T}_a|^2}{\Gamma_a^2} = \frac{\bar{N}_a}{\Gamma^2}$$

- ▶ Γ is a universal parameter



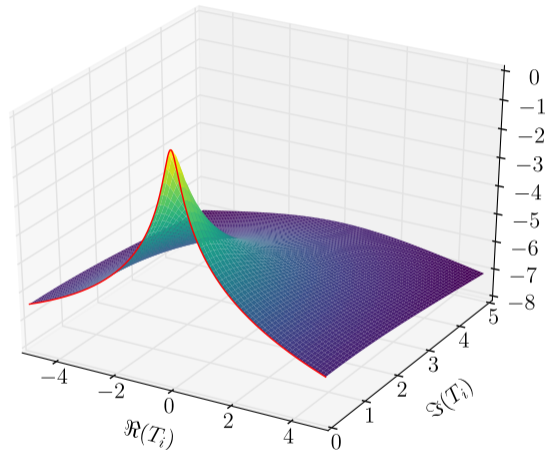
Regularization

$$\ln \mathcal{L}_{\text{reg}}(|\mathcal{T}_a|; \Gamma) = -\ln \left[1 + \frac{|\mathcal{T}_a|^2}{\Gamma_a^2} \right]$$

- ▶ Use Cauchy regularization
- ▶ Scale of $|\mathcal{T}_a|$ depends on experimental acceptance
 - ▶ Apply penalty on expected number \bar{N}_a of observed events

$$\Gamma_a = \frac{\Gamma}{\sqrt{\bar{\eta}_a}} \Rightarrow \frac{|\mathcal{T}_a|^2}{\Gamma_a^2} = \frac{\bar{N}_a}{\Gamma^2}$$

- ▶ Γ is a universal parameter



Regularization

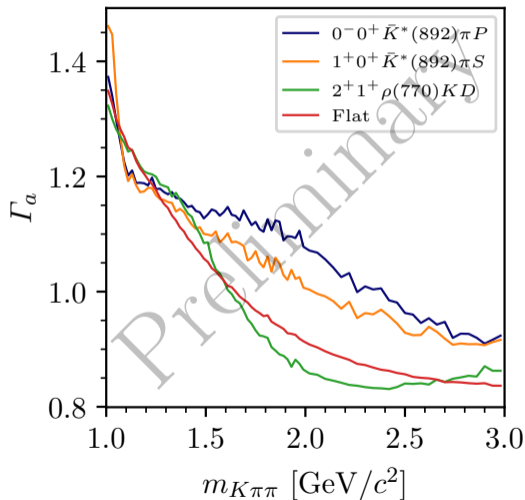
$$\ln \mathcal{L}_{\text{reg}}(|\mathcal{T}_a|; \Gamma) = -\ln \left[1 + \frac{|\mathcal{T}_a|^2}{\Gamma_a^2} \right]$$

- ▶ Use Cauchy regularization
- ▶ Scale of $|\mathcal{T}_a|$ depends on experimental acceptance
 - ▶ Apply penalty on expected number \bar{N}_a of observed events

$$\Gamma_a = \frac{\Gamma}{\sqrt{\bar{\eta}_a}} \Rightarrow \frac{|\mathcal{T}_a|^2}{\Gamma_a^2} = \frac{\bar{N}_a}{\Gamma^2}$$

- ▶ Γ is a universal parameter

COMPASS



Regularization

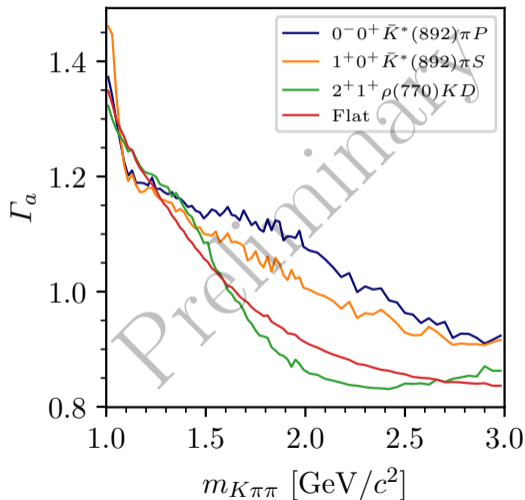
$$\ln \mathcal{L}_{\text{reg}}(|\mathcal{T}_a|; \Gamma) = -\ln \left[1 + \frac{|\mathcal{T}_a|^2}{\Gamma_a^2} \right]$$

- ▶ Use Cauchy regularization
- ▶ Scale of $|\mathcal{T}_a|$ depends on experimental acceptance
 - ▶ Apply penalty on expected number \bar{N}_a of observed events

$$\Gamma_a = \frac{\Gamma}{\sqrt{\bar{\eta}_a}} \Rightarrow \frac{|\mathcal{T}_a|^2}{\Gamma_a^2} = \frac{\bar{N}_a}{\Gamma^2}$$

- ▶ Γ is a universal parameter

COMPASS



Imposing continuity of the wave set

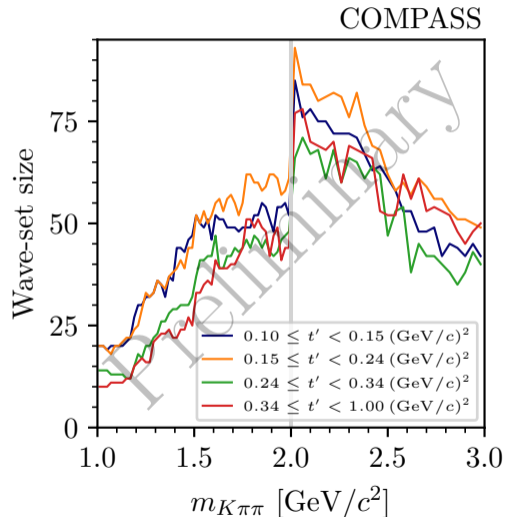
- ▶ Wave-set inferred independently for each $(m_{K\pi\pi}, t')$ cell
- ▶ Impose continuity of the wave set in $m_{K\pi\pi}$ by adding additional regularization term

$$\ln \mathcal{L}_{\text{cont}}(\{\mathcal{T}_a(m_{K\pi\pi}, t')\}; \lambda) = \sum_{j=i-3}^{j=i+3} \lambda \left| \mathcal{T}_a(m_{K\pi\pi}, t')(m_{K\pi\pi}^{j+1}) - \mathcal{T}_a(m_{K\pi\pi}, t')(m_{K\pi\pi}^j) \right|^2,$$

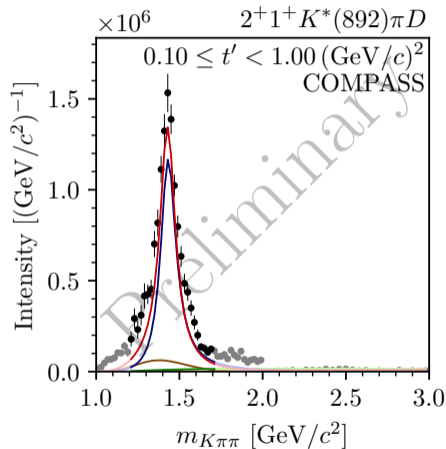
which suppresses fluctuations among neighboring $m_{K\pi\pi}$ bins

Wave-set size

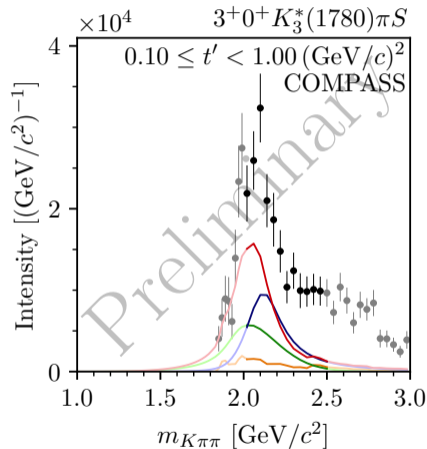
- ▶ 5 to 90 waves per $(m_{K\pi\pi}, t')$ cell
- ▶ Larger wave set for larger binning in $m_{K\pi\pi}$
- ▶ Larger wave set in t' bins with more events



- ▶ Selection of large signals
- ▶ as well as of signals at per-mil level

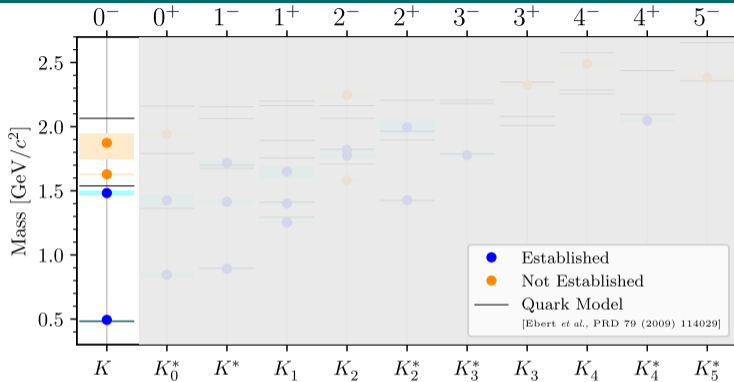


- ▶ Selection of large signals
- ▶ as well as of signals at per-mil level



14-Wave Resonance-Model Fit

Searching for Exotic Strange Mesons with $J^P = 0^-$



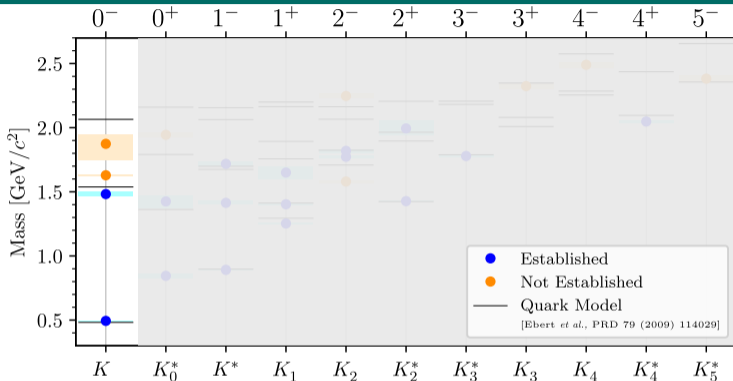
PDG

(2022)

- ▶ $K(1460)$ and $K(1830)$
- ▶ $K(1630)$
 - ▶ Unexpectedly small width of only $16 \text{ MeV}/c^2$
 - ▶ J^P of $K(1630)$ unclear

14-Wave Resonance-Model Fit

Searching for Exotic Strange Mesons with $J^P = 0^-$



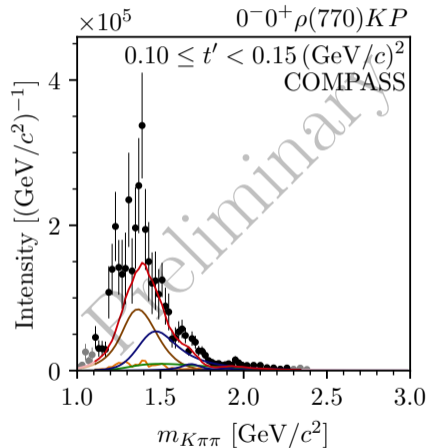
PDG

(2022)

- ▶ $K(1460)$ and $K(1830)$
- ▶ $K(1630)$
 - ▶ Unexpectedly small width of only $16 \text{ MeV}/c^2$
 - ▶ J^P of $K(1630)$ unclear

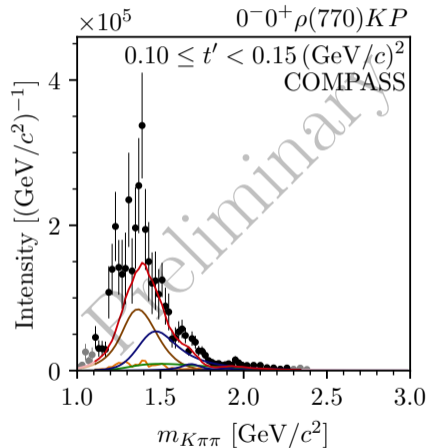
COMPASS $K^-\pi^-\pi^+$ data

- ▶ Peak at about $1.4 \text{ GeV}/c^2$
 - ▶ Potentially from established $K(1460)$
 - ▶ But, $m_{K\pi\pi} \lesssim 1.5 \text{ GeV}/c^2$ region affected by analysis artifacts
- ▶ Second peak at about $1.7 \text{ GeV}/c^2$
 - ▶ $K(1630)$ signal with 8.3σ statistical significance
 - ▶ Accompanied by rising phase
- ▶ Weak signal at about $2.0 \text{ GeV}/c^2$
 - ▶ $K(1830)$ signal with 5.4σ statistical significance



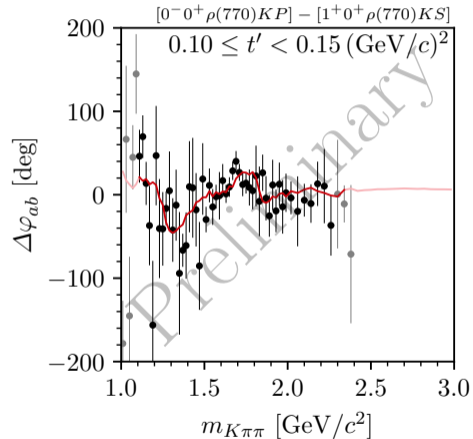
COMPASS $K^-\pi^-\pi^+$ data

- ▶ Peak at about $1.4 \text{ GeV}/c^2$
 - ▶ Potentially from established $K(1460)$
 - ▶ But, $m_{K\pi\pi} \lesssim 1.5 \text{ GeV}/c^2$ region affected by analysis artifacts
- ▶ Second peak at about $1.7 \text{ GeV}/c^2$
 - ▶ $K(1630)$ signal with 8.3σ statistical significance
 - ▶ Accompanied by rising phase
- ▶ Weak signal at about $2.0 \text{ GeV}/c^2$
 - ▶ $K(1830)$ signal with 5.4σ statistical significance



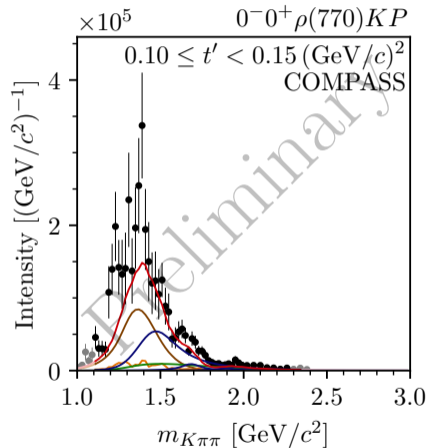
COMPASS $K^- \pi^- \pi^+$ data

- ▶ Peak at about $1.4 \text{ GeV}/c^2$
 - ▶ Potentially from established $K(1460)$
 - ▶ But, $m_{K\pi\pi} \lesssim 1.5 \text{ GeV}/c^2$ region affected by analysis artifacts
- ▶ Second peak at about $1.7 \text{ GeV}/c^2$
 - ▶ $K(1630)$ signal with 8.3σ statistical significance
 - ▶ Accompanied by rising phase
- ▶ Weak signal at about $2.0 \text{ GeV}/c^2$
 - ▶ $K(1830)$ signal with 5.4σ statistical significance



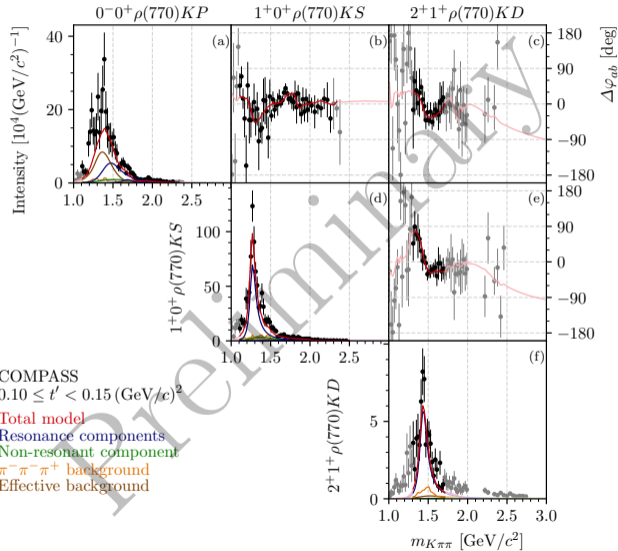
COMPASS $K^-\pi^-\pi^+$ data

- ▶ Peak at about $1.4 \text{ GeV}/c^2$
 - ▶ Potentially from established $K(1460)$
 - ▶ But, $m_{K\pi\pi} \lesssim 1.5 \text{ GeV}/c^2$ region affected by analysis artifacts
- ▶ Second peak at about $1.7 \text{ GeV}/c^2$
 - ▶ $K(1630)$ signal with 8.3σ statistical significance
 - ▶ Accompanied by rising phase
- ▶ Weak signal at about $2.0 \text{ GeV}/c^2$
 - ▶ $K(1830)$ signal with 5.4σ statistical significance



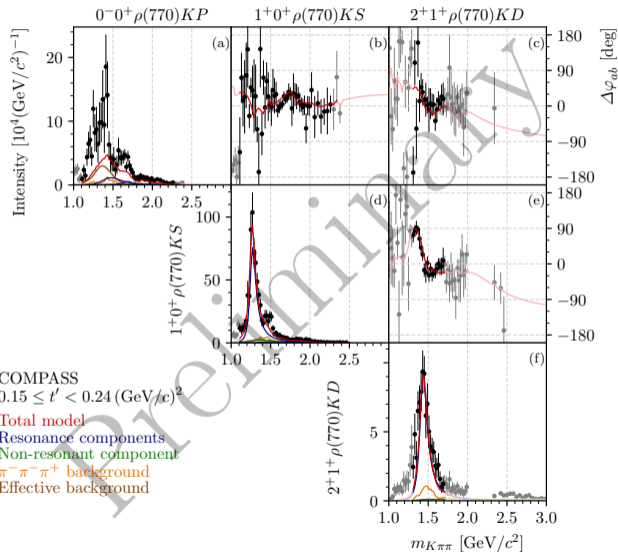
14-Wave Resonance-Model Fit

Searching for Exotic Strange Mesons with $J^P = 0^-$



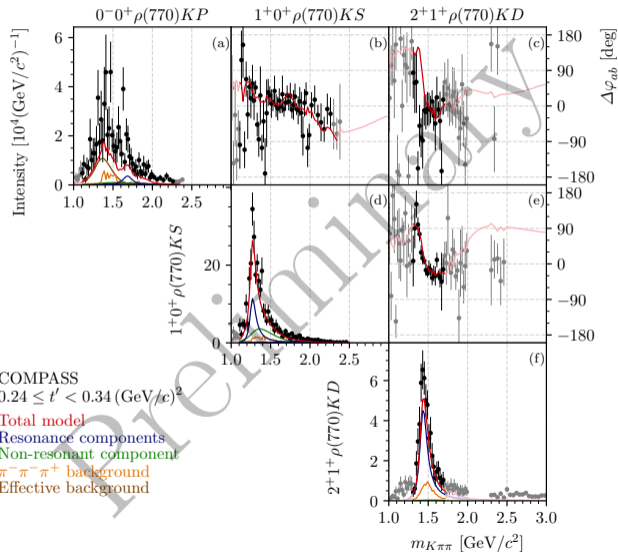
14-Wave Resonance-Model Fit

Searching for Exotic Strange Mesons with $J^P = 0^-$



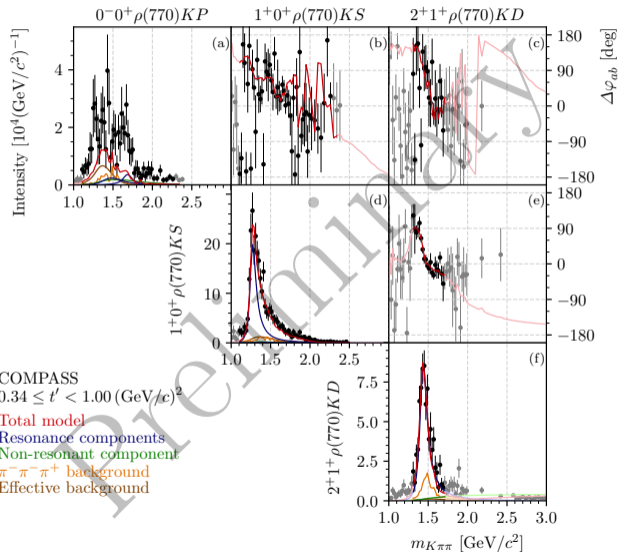
14-Wave Resonance-Model Fit

Searching for Exotic Strange Mesons with $J^P = 0^-$



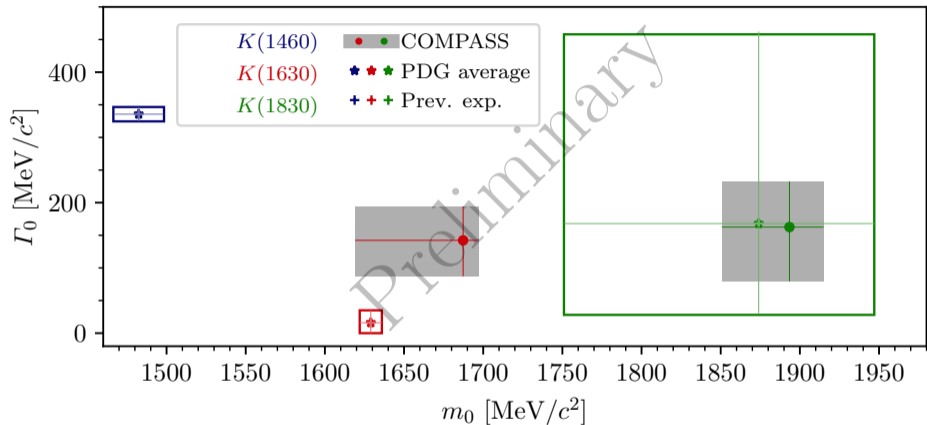
14-Wave Resonance-Model Fit

Searching for Exotic Strange Mesons with $J^P = 0^-$



14-Wave Resonance-Model Fit

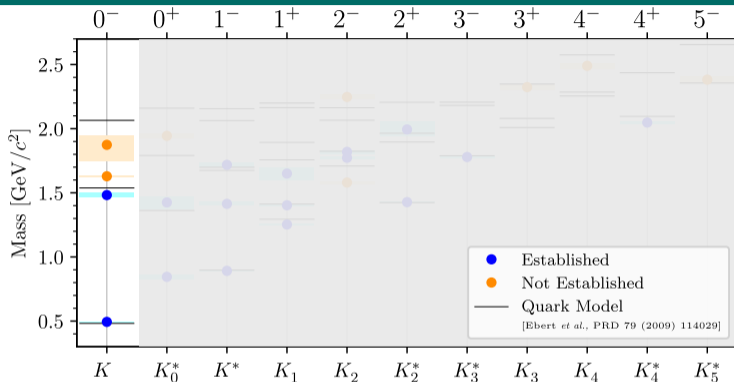
Searching for Exotic Strange Mesons with $J^P = 0^-$



- ▶ $K(1830)$ parameters in good agreement with LCHb measurement [PRL 118 (2017) 022003]
- ▶ Realistic $K(1630)$ width of about $140 \text{ MeV}/c^2$

14-Wave Resonance-Model Fit

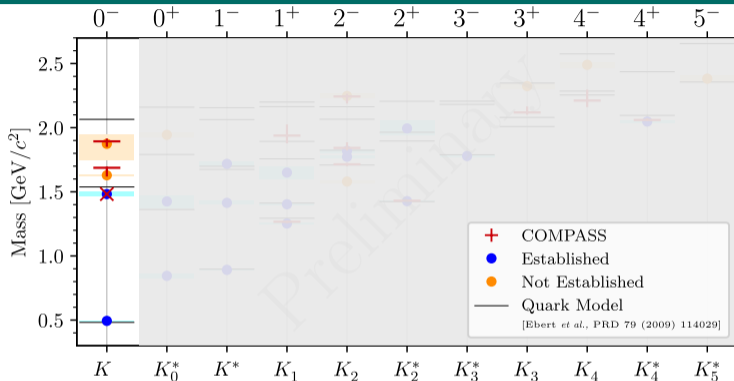
Searching for Exotic Strange Mesons with $J^P = 0^-$



- ▶ Indications for 3 excited K from a single analysis
- ▶ Quark-model predicts only two excited states: potentially $K(1460)$ and $K(1830)$
 - $K(1630)$ supernumerary signal
 - Candidate for **exotic non- $q\bar{q}$ state**; other explanations possible ($K^*(892)$ ω threshold nearby)

14-Wave Resonance-Model Fit

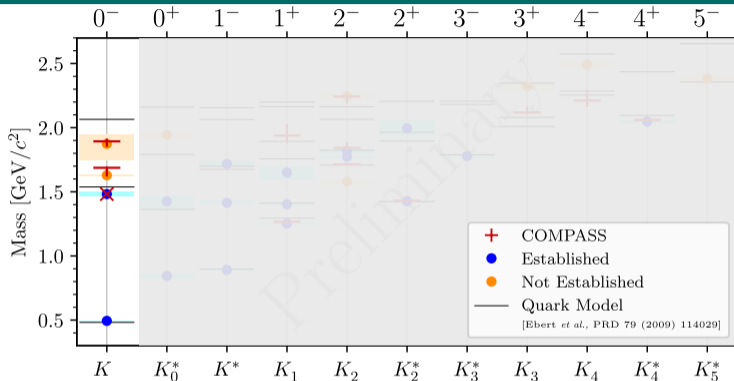
Searching for Exotic Strange Mesons with $J^P = 0^-$



- ▶ Indications for 3 excited K from a single analysis
- ▶ Quark-model predicts only two excited states: potentially $K(1460)$ and $K(1830)$
 - $K(1630)$ supernumerary signal
 - Candidate for exotic non- $q\bar{q}$ state; other explanations possible ($K^*(892)$ ω threshold nearby)

14-Wave Resonance-Model Fit

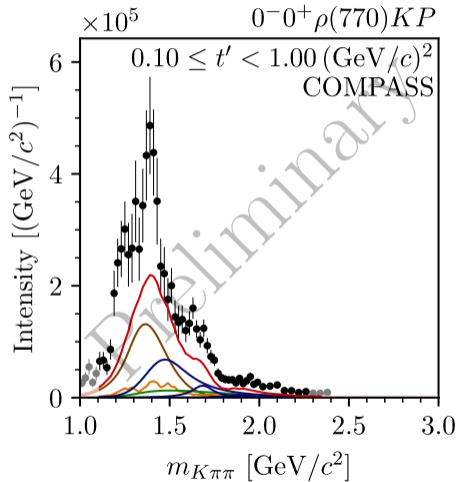
Searching for Exotic Strange Mesons with $J^P = 0^-$



- ▶ Indications for 3 excited K from a single analysis
- ▶ Quark-model predicts only two excited states: potentially $K(1460)$ and $K(1830)$
 - ➔ $K(1630)$ supernumerary signal
 - ➔ Candidate for **exotic non- $q\bar{q}$ state**; other explanations possible ($K^*(892)$ ω threshold nearby)

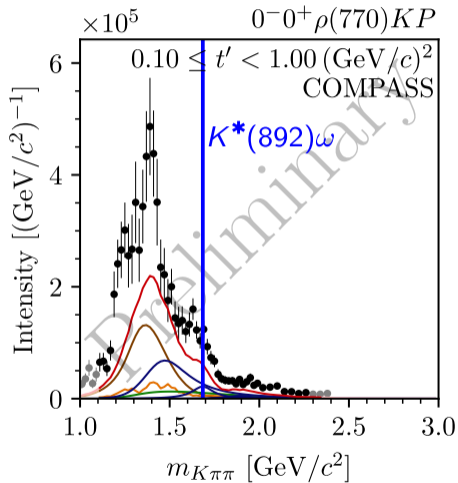
14-Wave Resonance-Model Fit

Searching for Exotic Strange Mesons with $J^P = 0^-$



14-Wave Resonance-Model Fit

Searching for Exotic Strange Mesons with $J^P = 0^-$

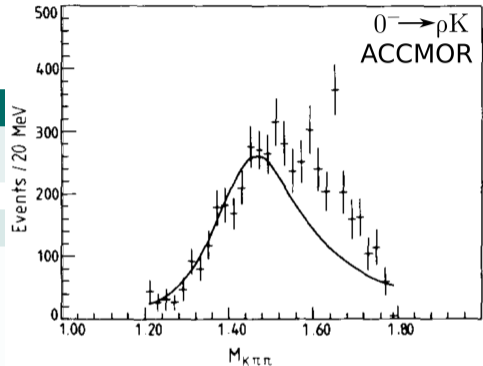


$K^- \pi^- \pi^+$ from ACCMOR

- ▶ Potential $K(1630)$ signal already in ACCMOR analysis

$K^- \pi^- \pi^+$ from LHCb

- ▶ Measurement of $D^0 \rightarrow K^\mp \pi^\pm \pi^\pm \pi^\mp$ at LHCb
 - ▶ Study strange mesons in $K\pi\pi$ subsystem
 - ▶ MIPWA of $J^P = 0^-$ amplitude
 - ▶ Potential signal above $1.6 \text{ GeV}/c^2$
 - ▶ Limited by kinematic range

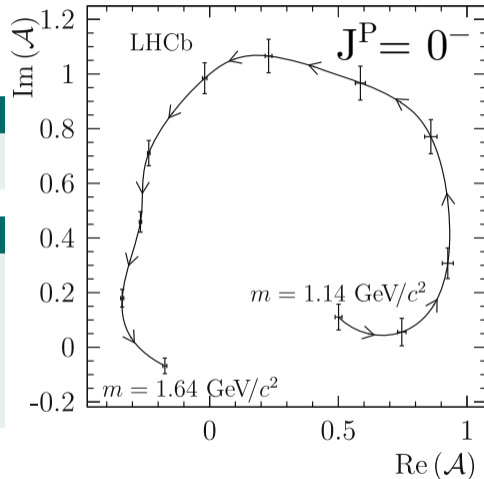


$K^- \pi^- \pi^+$ from ACCMOR

- ▶ Potential $K(1630)$ signal already in ACCMOR analysis

$K^- \pi^- \pi^+$ from LHCb

- ▶ Measurement of $D^0 \rightarrow K^\mp \pi^\pm \pi^\pm \pi^\mp$ at LHCb
 - ▶ Study strange mesons in $K\pi\pi$ subsystem
 - ▶ MIPWA of $J^P = 0^-$ amplitude
 - ▶ Potential signal above $1.6 \text{ GeV}/c^2$
 - ▶ Limited by kinematic range

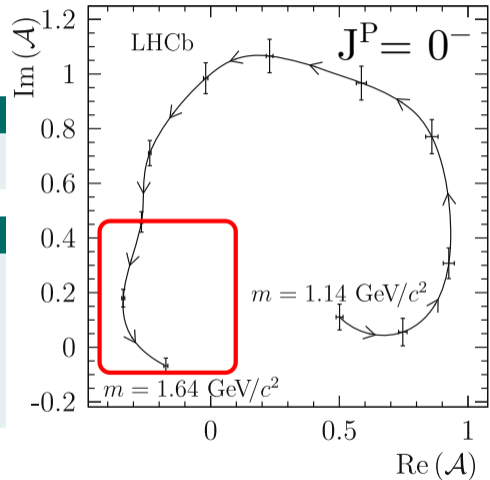


$K^- \pi^- \pi^+$ from ACCMOR

- ▶ Potential $K(1630)$ signal already in ACCMOR analysis

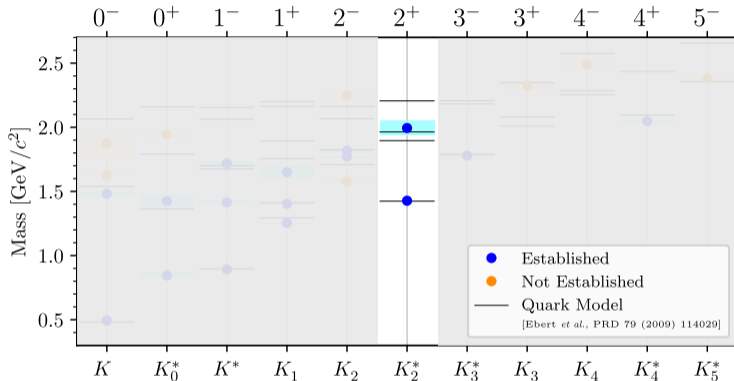
$K^- \pi^- \pi^+$ from LHCb

- ▶ Measurement of $D^0 \rightarrow K^\mp \pi^\pm \pi^\pm \pi^\mp$ at LHCb
 - ▶ Study strange mesons in $K\pi\pi$ subsystem
 - ▶ MIPWA of $J^P = 0^-$ amplitude
 - ▶ Potential signal above $1.6 \text{ GeV}/c^2$
 - ▶ Limited by kinematic range



14-Wave Resonance-Model Fit

Partial Waves with $J^P = 2^+$



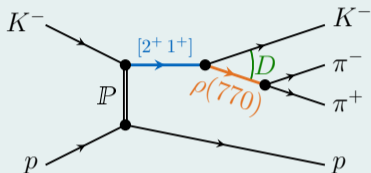
PDG

(2022)

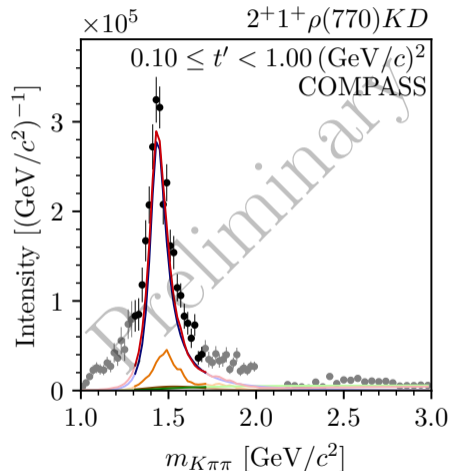
► $K_2^*(1430)$ well known resonance

14-Wave Resonance-Model Fit

Partial Waves with $J^P = 2^+$



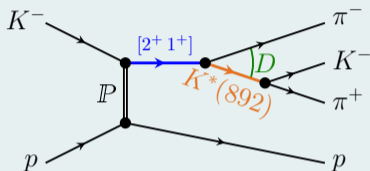
- ▶ Signal in $K_2^*(1430)$ mass region
- ▶ In **different decays**
 - ▶ $\rho(770) K D$
 - ▶ $K^*(892) \pi D$
- ▶ In agreement with previous measurements
- ▶ **Cleaner** signal in **COMPASS** data



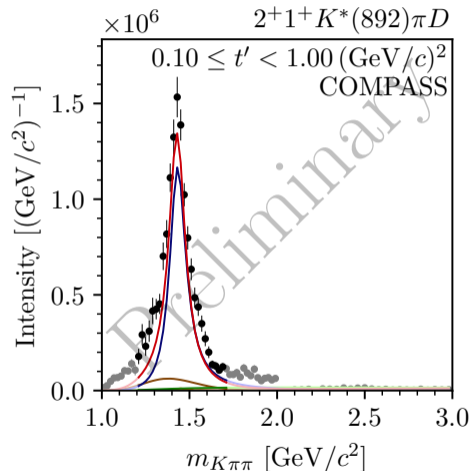
total resonance model, resonances, non-resonant, $\pi\pi\pi$ background, effective background

14-Wave Resonance-Model Fit

Partial Waves with $J^P = 2^+$



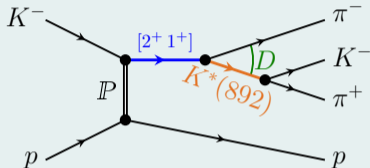
- ▶ Signal in $K_2^*(1430)$ mass region
- ▶ In **different decays**
 - ▶ $\rho(770) K D$
 - ▶ $K^*(892) \pi D$
- ▶ In agreement with previous measurements
- ▶ **Cleaner** signal in **COMPASS** data



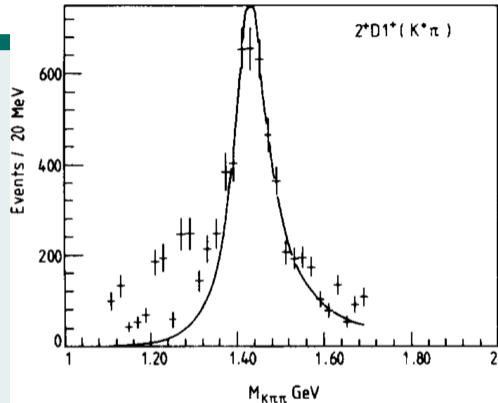
total resonance model, resonances, non-resonant, $\pi\pi\pi$ background, effective background

14-Wave Resonance-Model Fit

Partial Waves with $J^P = 2^+$

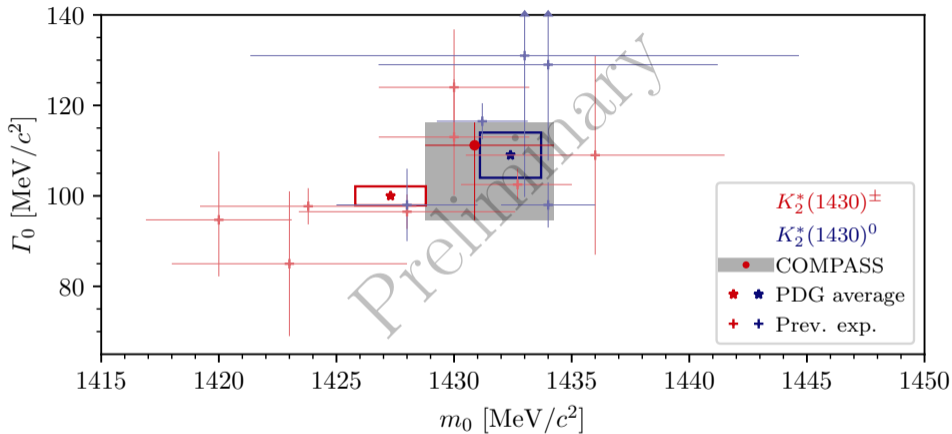


- ▶ Signal in $K_2^*(1430)$ mass region
- ▶ In **different decays**
 - ▶ $\rho(770) K D$
 - ▶ $K^*(892) \pi D$
- ▶ In agreement with previous measurements
- ▶ **Cleaner** signal in **COMPASS** data



14-Wave Resonance-Model Fit

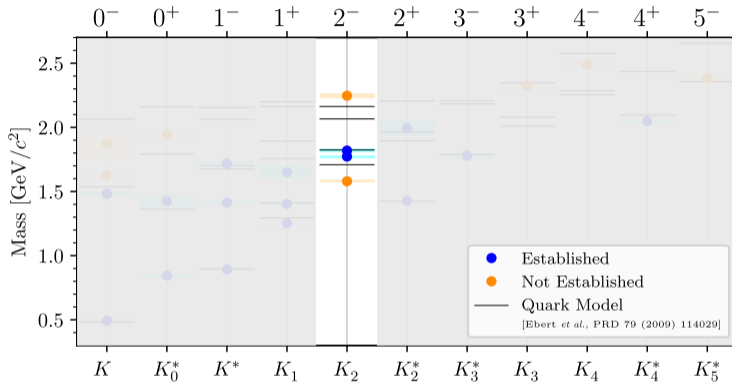
Partial Waves with $J^P = 2^+$



- ▶ $K_2^*(1430)$ parameters consistent with previous observations
- ▶ Better agreement with PDG average values for neutral $K_2^*(1430)$

14-Wave Resonance-Model Fit

Partial Waves with $J^P = 2^-$



PDG

(2022)

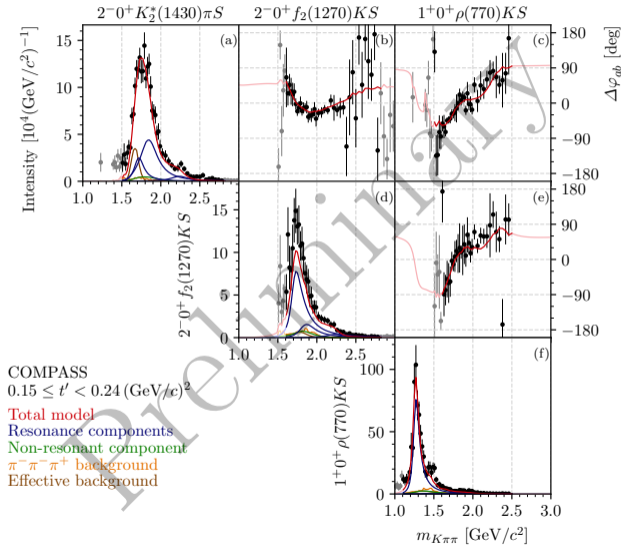
- ▶ Established $K_2(1770)$ and $K_2(1820)$
- ▶ $K_2(2250)$ need further confirmation

14-Wave Resonance-Model Fit

Partial Waves with $J^P = 2^-$



- ▶ Simultaneously fit 4 waves with $J^P = 2^-$
- ▶ 1.8 GeV/c² peak modeled by $K_2(1770)$, $K_2(1820)$
- ▶ High-mass shoulder modeled by $K_2(2250)$
- ▶ Different intensity spectra and large phase motions among 2^- waves

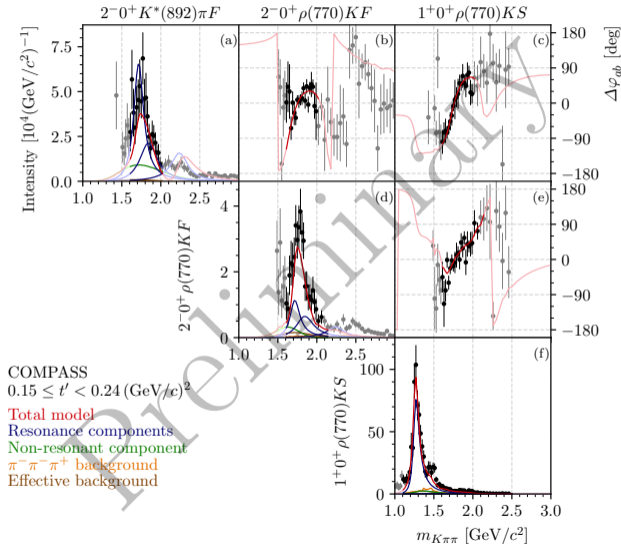


14-Wave Resonance-Model Fit

Partial Waves with $J^P = 2^-$

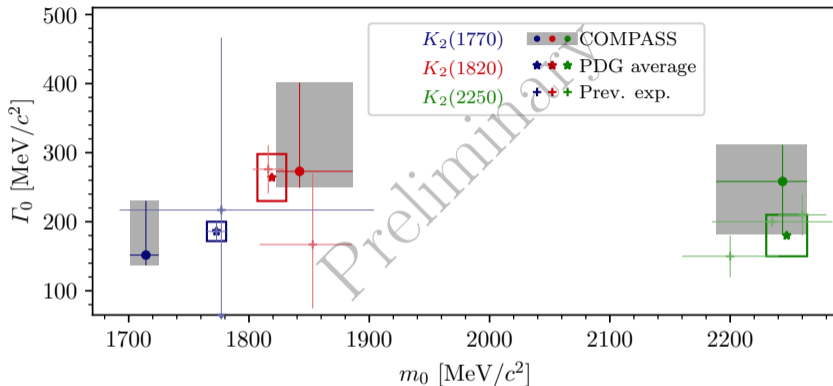


- ▶ Simultaneously fit 4 waves with $J^P = 2^-$
- ▶ $1.8 \text{ GeV}/c^2$ peak modeled by $K_2(1770)$, $K_2(1820)$
- ▶ High-mass shoulder modeled by $K_2(2250)$
- ▶ Different intensity spectra and large phase motions among 2^- waves



14-Wave Resonance-Model Fit

Partial Waves with $J^P = 2^-$

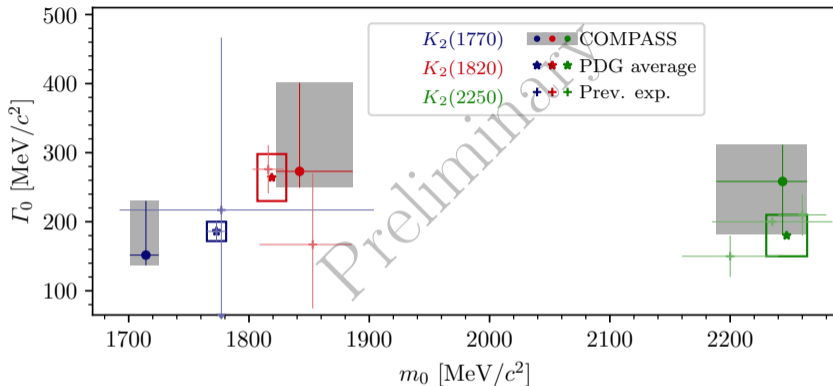


$K_2(1770)$ and $K_2(1820)$

- ▶ Two states were considered by only three measurements ACCMOR, LASS, LHCb
- ▶ Only LHCb measurement could confirm two states (3σ statistical significance)
- ▶ We observe two states with 11σ statistical significance

14-Wave Resonance-Model Fit

Partial Waves with $J^P = 2^-$

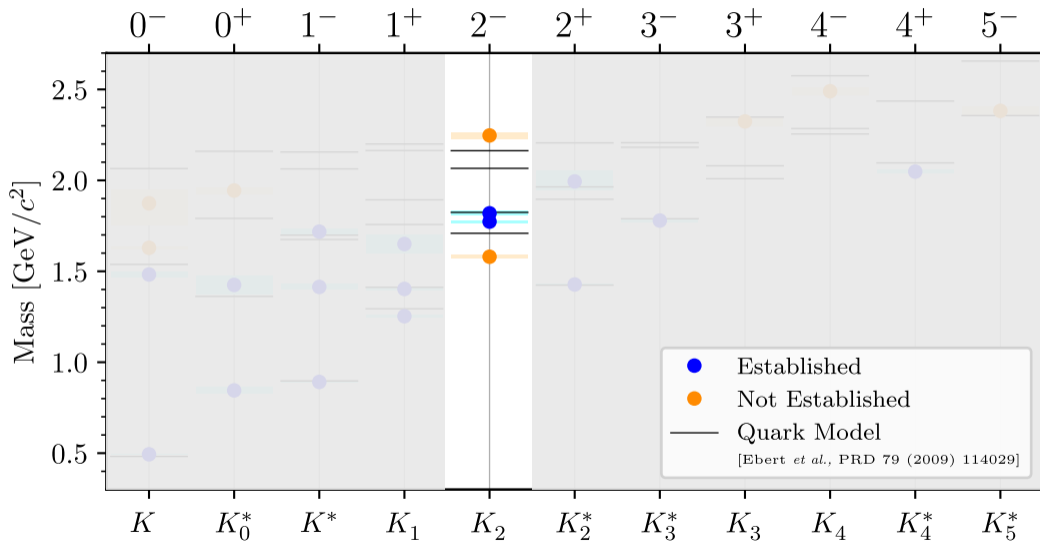


$K_2(2250)$

- ▶ Studied so far mainly in $\bar{\Lambda}(\bar{p})$ final states
- ▶ First simultaneous measurement of $K_2(1770)$, $K_2(1820)$, and $K_2(2250)$
- ▶ Resonance parameters consistent with previous observations

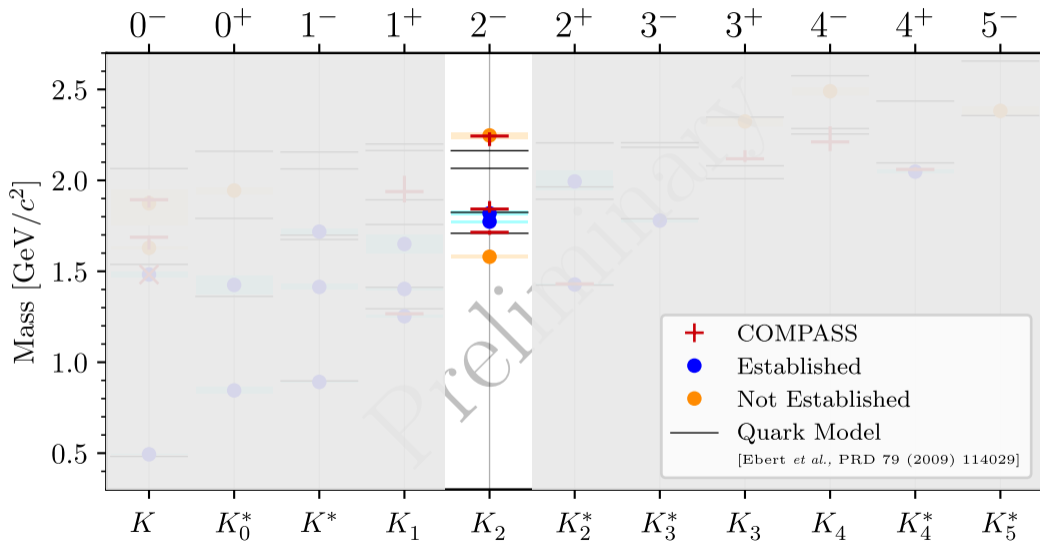
14-Wave Resonance-Model Fit

Partial Waves with $J^P = 2^-$



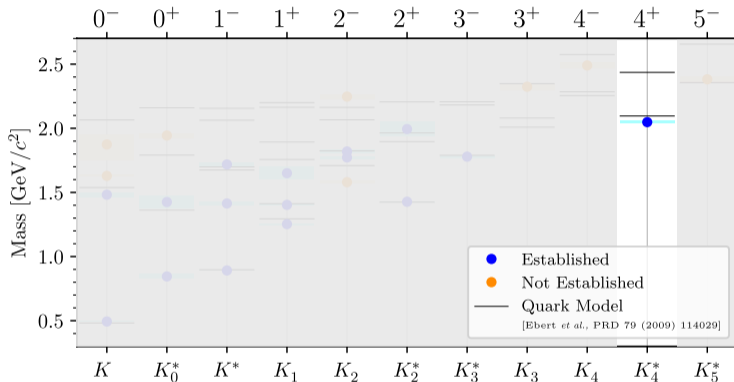
14-Wave Resonance-Model Fit

Partial Waves with $J^P = 2^-$



14-Wave Resonance-Model Fit

Partial Waves with $J^P = 4^+$



PDG

(2022)

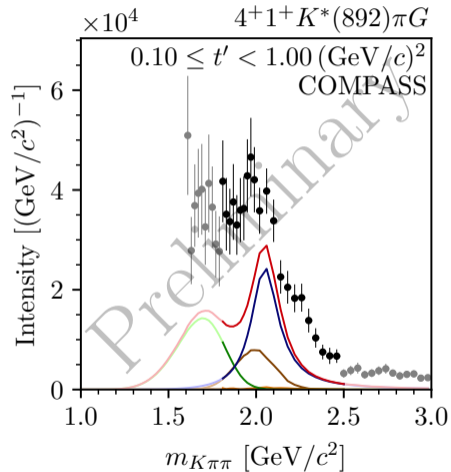
► $K_4^*(2045)$ known resonance

14-Wave Resonance-Model Fit

Partial Waves with $J^P = 4^+$



- ▶ Signal $K_4^*(2045)$ signal in $K^*(892) \pi$ and $\rho(770) K$ decays



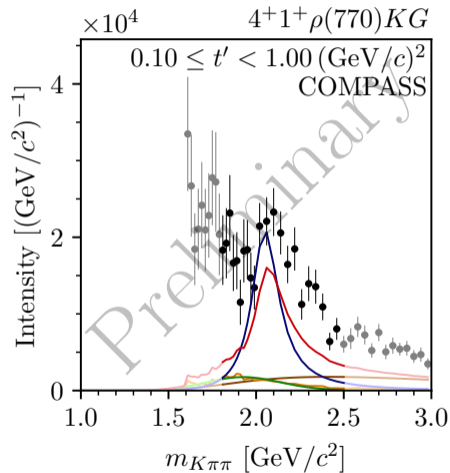
total resonance model, resonances, non-resonant, $\pi\pi\pi$ background, effective background

14-Wave Resonance-Model Fit

Partial Waves with $J^P = 4^+$



- Signal $K_4^*(2045)$ signal in $K^*(892) \pi$ and $\rho(770) K$ decays



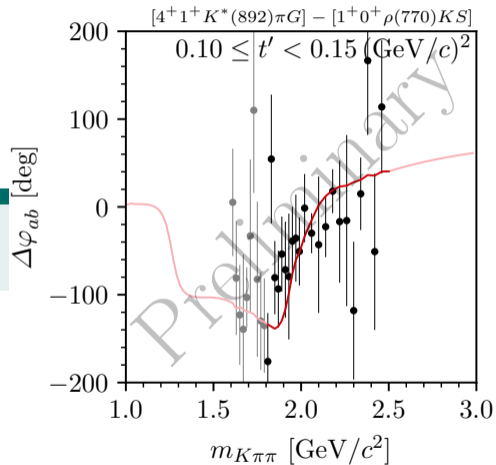
total resonance model, resonances, non-resonant, $\pi\pi\pi$ background, effective background

14-Wave Resonance-Model Fit

Partial Waves with $J^P = 4^+$



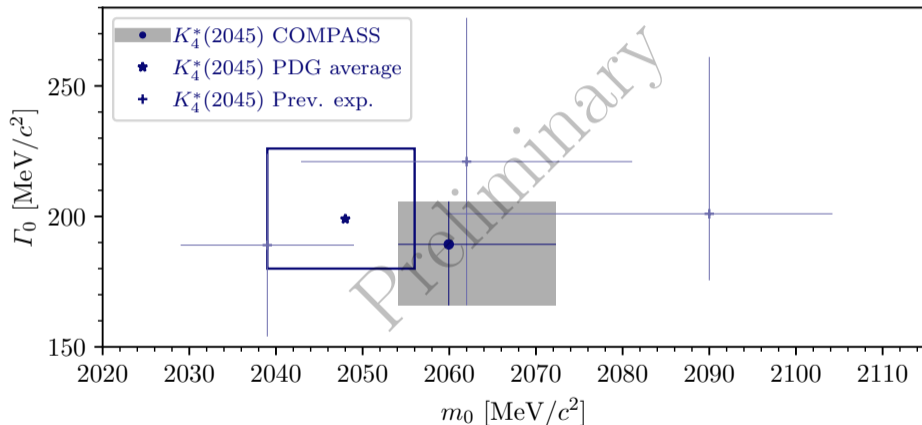
- ▶ Signal $K_4^*(2045)$ signal in $K^*(892) \pi$ and $\rho(770) K$ decays



total resonance model, resonances, non-resonant, $\pi\pi\pi$ background, effective background

14-Wave Resonance-Model Fit

Partial Waves with $J^P = 4^+$



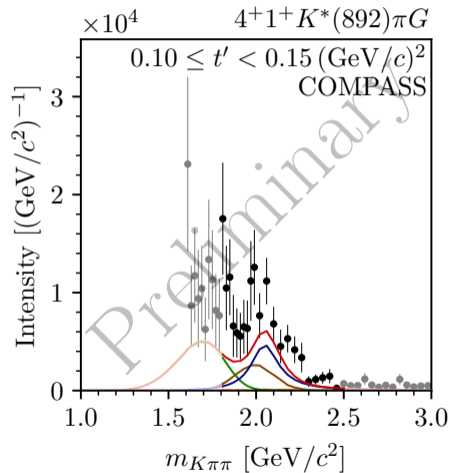
14-Wave Resonance-Model Fit

Partial Waves with $J^P = 4^+$



- ▶ Imperfect description of magnitude of intensity,
- ▶ Also, real and imaginary parts of **interference terms described well, including their magnitude**
- ▶ Intensities and real and imaginary parts of interference terms not directly related as $\text{Rank}[\rho_{ab}] > 1$
 $|\rho_{ab}| \neq \sqrt{|\rho_{aa}| |\rho_{bb}|}$
 - ▶ Analysis artifacts in intensities of small waves, which are the least constrained by data

- ▶ Results validated by Monte Carlo input-output and systematic studies
- ▶ Imperfections considered in systematic uncertainties
- ▶ Results in agreement with previous experiments



total resonance model, resonances, non-resonant, $\pi\pi\pi$ background, effective background

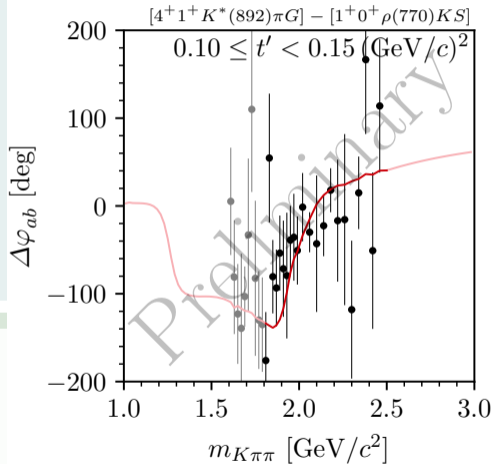
14-Wave Resonance-Model Fit

Partial Waves with $J^P = 4^+$



- ▶ Imperfect description of magnitude of intensity, , while relative phase described well
- ▶ Also, real and imaginary parts of **interference terms described well, including their magnitude**
- ▶ Intensities and real and imaginary parts of interference terms not directly related as $\text{Rank}[\rho_{ab}] > 1$
 $|\rho_{ab}| \neq \sqrt{|\rho_{aa}| |\rho_{bb}|}$
 - ▶ Analysis artifacts in intensities of small waves, which are the least constrained by data

- ▶ Results validated by Monte Carlo input-output and systematic studies
- ▶ Imperfections considered in systematic uncertainties
- ▶ Results in agreement with previous experiments



total resonance model, resonances, non-resonant, $\pi\pi\pi$ background, effective background

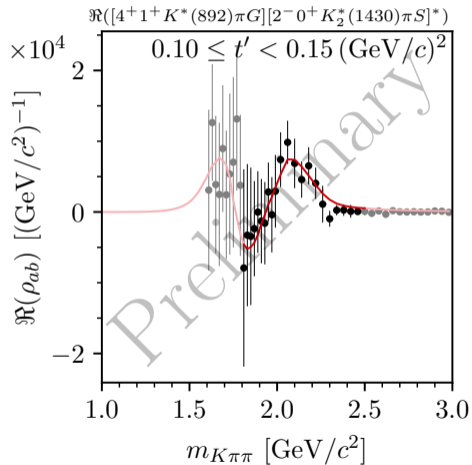
14-Wave Resonance-Model Fit

Partial Waves with $J^P = 4^+$



- ▶ Imperfect description of magnitude of intensity, , while relative phase described well
- ▶ Also, real and imaginary parts of **interference terms described well, including their magnitude**
- ▶ Intensities and real and imaginary parts of interference terms not directly related as $\text{Rank}[\rho_{ab}] > 1$
 $|\rho_{ab}| \neq \sqrt{|\rho_{aa}| |\rho_{bb}|}$
 - ▶ Analysis artifacts in intensities of small waves, which are the least constrained by data

- ▶ Results validated by Monte Carlo input-output and systematic studies
- ▶ Imperfections considered in systematic uncertainties
- ▶ Results in agreement with previous experiments



total resonance model, resonances, non-resonant, $\pi\pi\pi$ background, effective background

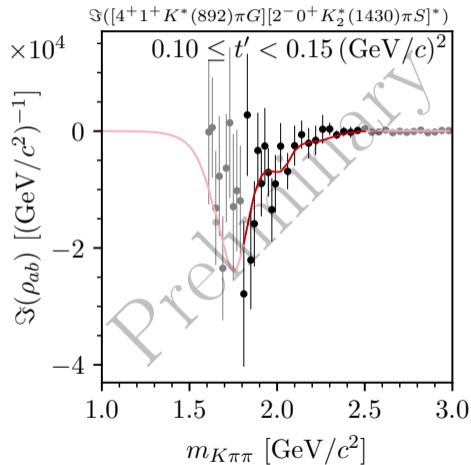
14-Wave Resonance-Model Fit

Partial Waves with $J^P = 4^+$



- ▶ Imperfect description of magnitude of intensity, , while relative phase described well
- ▶ Also, real and imaginary parts of **interference terms described well, including their magnitude**
- ▶ Intensities and real and imaginary parts of interference terms not directly related as $\text{Rank}[\rho_{ab}] > 1$
 $|\rho_{ab}| \neq \sqrt{|\rho_{aa}| |\rho_{bb}|}$
 - ▶ Analysis artifacts in intensities of small waves, which are the least constrained by data

- ▶ Results validated by Monte Carlo input-output and systematic studies
- ▶ Imperfections considered in systematic uncertainties
- ▶ Results in agreement with previous experiments



total resonance model, resonances, non-resonant, $\pi\pi\pi$ background, effective background

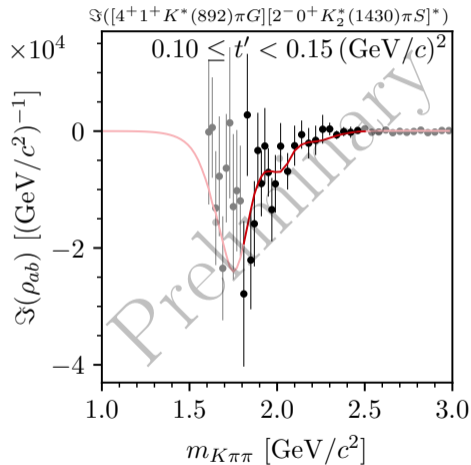
14-Wave Resonance-Model Fit

Partial Waves with $J^P = 4^+$



- ▶ Imperfect description of magnitude of intensity, , while relative phase described well
- ▶ Also, real and imaginary parts of **interference terms described well, including their magnitude**
- ▶ Intensities and real and imaginary parts of interference terms not directly related as $\text{Rank}[\rho_{ab}] > 1$
 $|\rho_{ab}| \neq \sqrt{|\rho_{aa}| |\rho_{bb}|}$
 - ▶ Analysis artifacts in **intensities of small waves, which are the least constrained by data**

- ▶ Results validated by Monte Carlo input-output and systematic studies
- ▶ Imperfections considered in systematic uncertainties
- ▶ Results in agreement with previous experiments



total resonance model, resonances, non-resonant, $\pi\pi\pi$ background, effective background

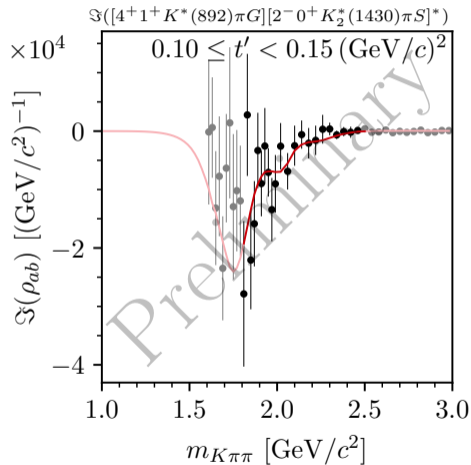
14-Wave Resonance-Model Fit

Partial Waves with $J^P = 4^+$



- ▶ Imperfect description of magnitude of intensity, , while relative phase described well
- ▶ Also, real and imaginary parts of **interference terms described well, including their magnitude**
- ▶ Intensities and real and imaginary parts of interference terms not directly related as $\text{Rank}[\rho_{ab}] > 1$
 $|\rho_{ab}| \neq \sqrt{|\rho_{aa}| |\rho_{bb}|}$
 - ▶ Analysis artifacts in **intensities of small waves, which are the least constrained by data**

- ▶ Results validated by Monte Carlo input-output and systematic studies
- ▶ Imperfections considered in systematic uncertainties
- ▶ Results in agreement with previous experiments



total resonance model, resonances, non-resonant, $\pi\pi\pi$ background, effective background

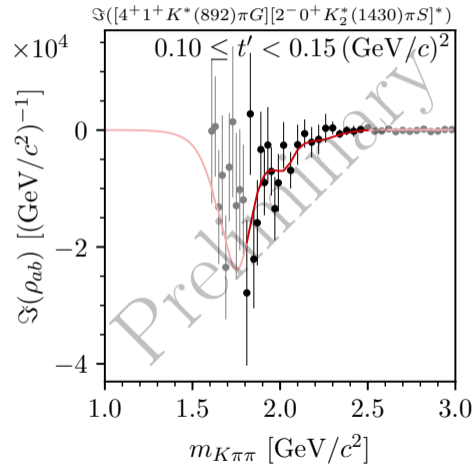
14-Wave Resonance-Model Fit

Partial Waves with $J^P = 4^+$

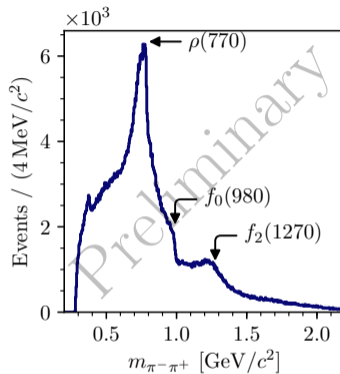
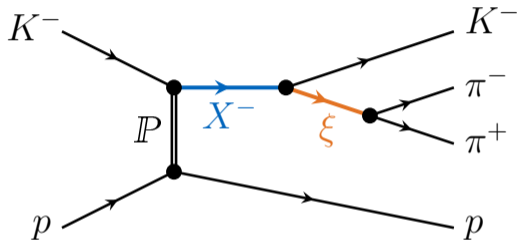


- ▶ Imperfect description of magnitude of intensity, , while relative phase described well
- ▶ Also, real and imaginary parts of **interference terms described well, including their magnitude**
- ▶ Intensities and real and imaginary parts of interference terms not directly related as $\text{Rank}[\rho_{ab}] > 1$
 $|\rho_{ab}| \neq \sqrt{|\rho_{aa}| |\rho_{bb}|}$
 - ▶ Analysis artifacts in **intensities of small waves, which are the least constrained by data**

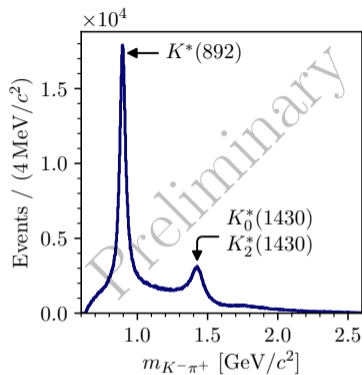
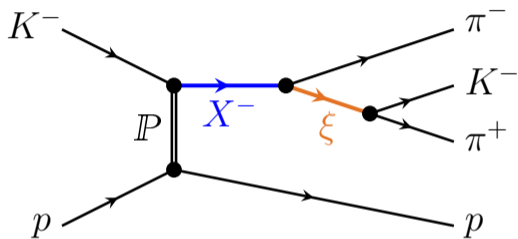
- ▶ Results validated by Monte Carlo input-output and systematic studies
- ▶ Imperfections considered in systematic uncertainties
- ▶ Results in agreement with previous experiments



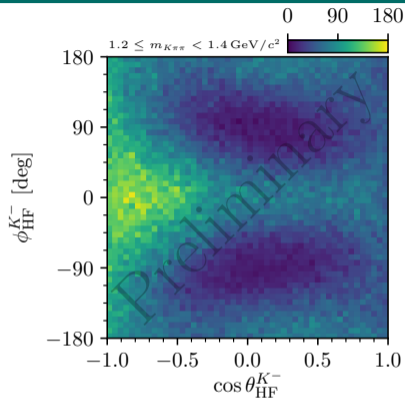
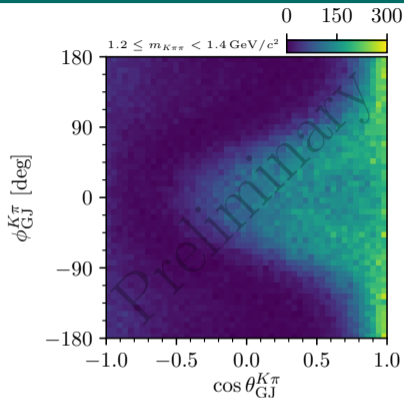
total resonance model, resonances, non-resonant, $\pi\pi\pi$ background, effective background



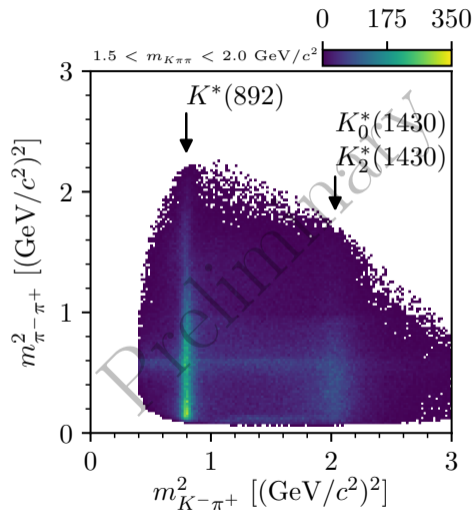
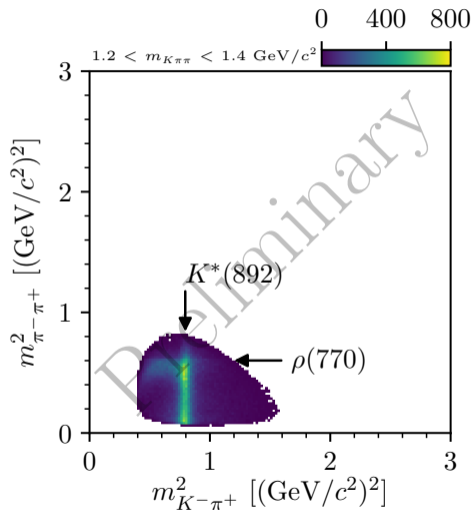
- ▶ Also structure in $\pi^-\pi^+$ and $K^-\pi^+$ subsystems
 - ↳ Successive 2-body decay via $\pi^-\pi^+$ / $K^-\pi^+$ resonance called **isobar**
- ▶ Also structure in angular distributions



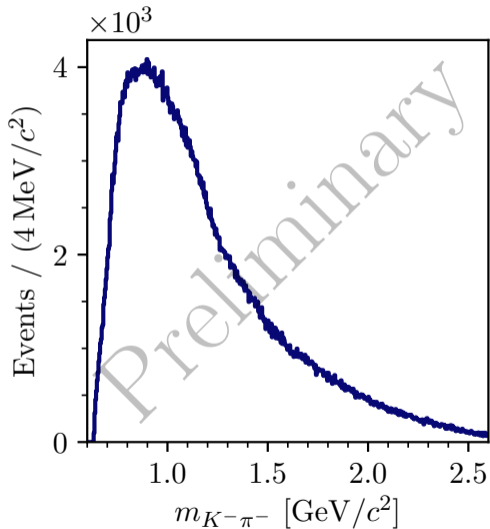
- ▶ Also structure in $\pi^-\pi^+$ and $K^-\pi^+$ subsystems
 - ↳ Successive 2-body decay via $\pi^-\pi^+$ / $K^-\pi^+$ resonance called **isobar**
- ▶ Also structure in angular distributions



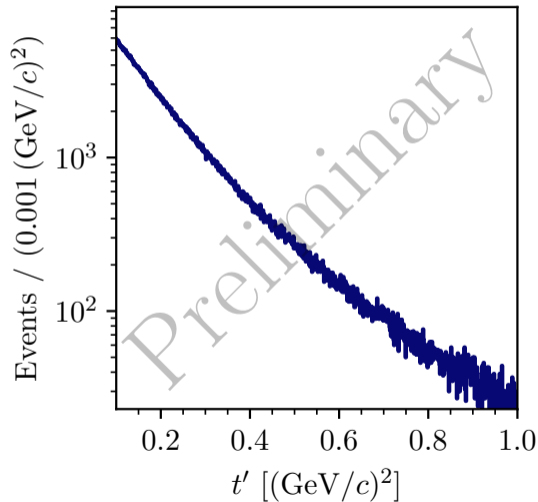
- ▶ Also structure in $\pi^-\pi^+$ and $K^-\pi^+$ subsystems
 - ↳ Successive 2-body decay via $\pi^-\pi^+$ / $K^-\pi^+$ resonance called **isobar**
- ▶ Also structure in angular distributions



- ▶ No dominant resonant structures

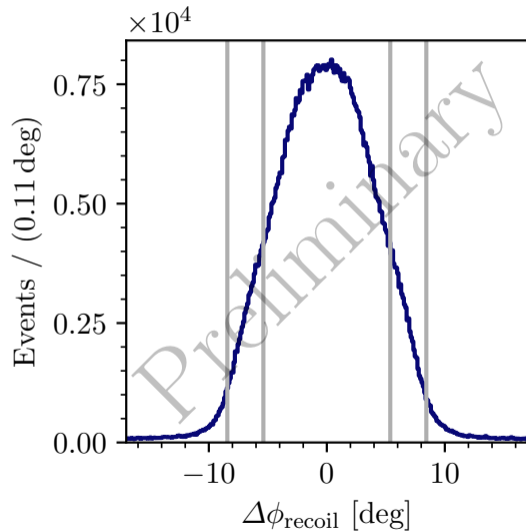
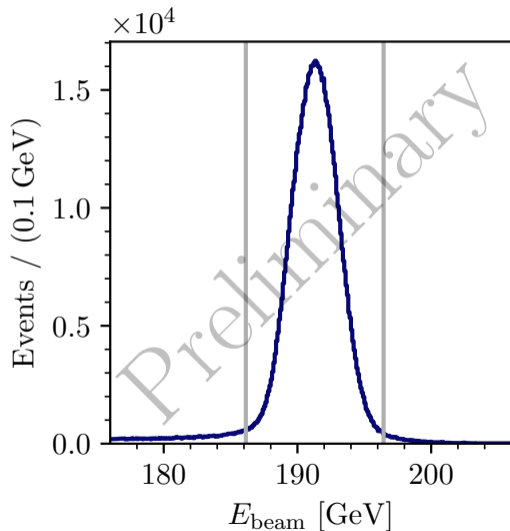


- ▶ Exponential shape
- ▶ Shallower for larger t'



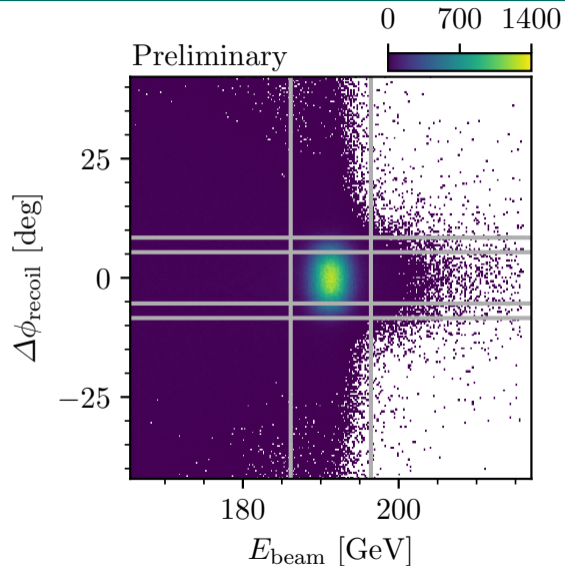
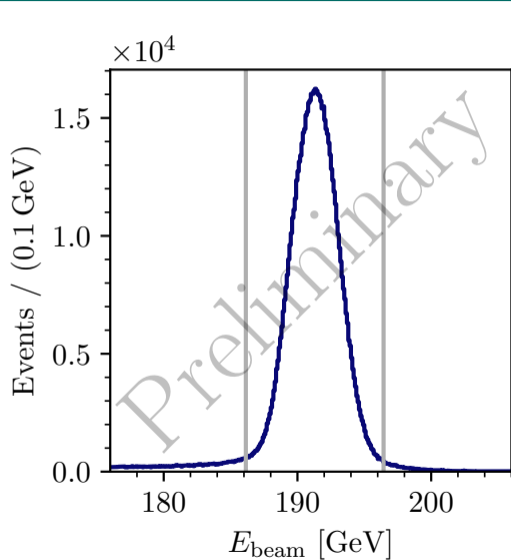
Kinematic Distribution of $K^-\pi^-\pi^+$ Events

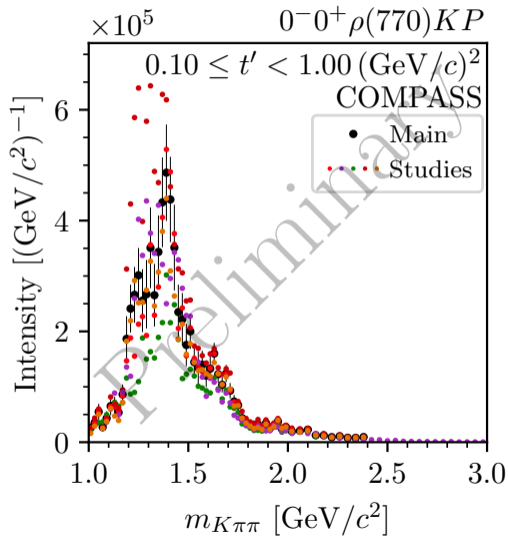
Exclusivity

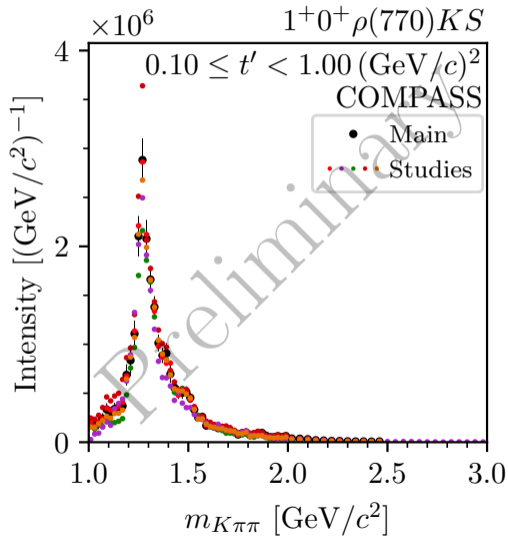


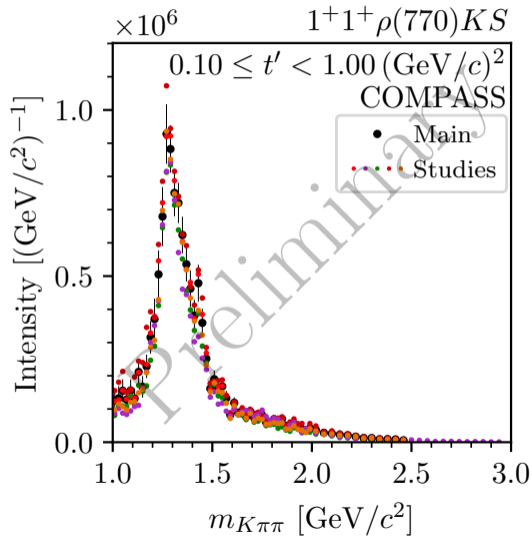
Kinematic Distribution of $K^-\pi^-\pi^+$ Events

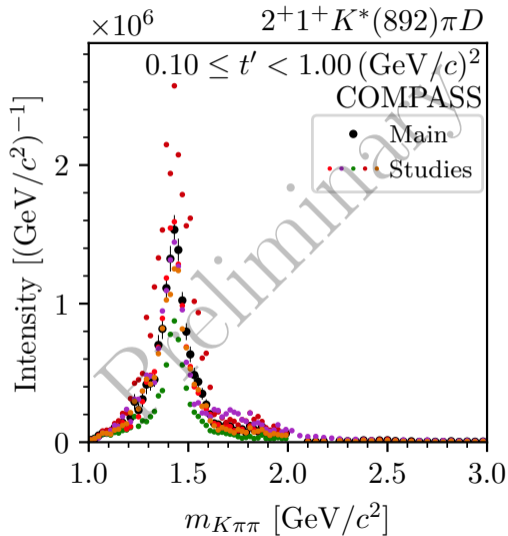
Exclusivity

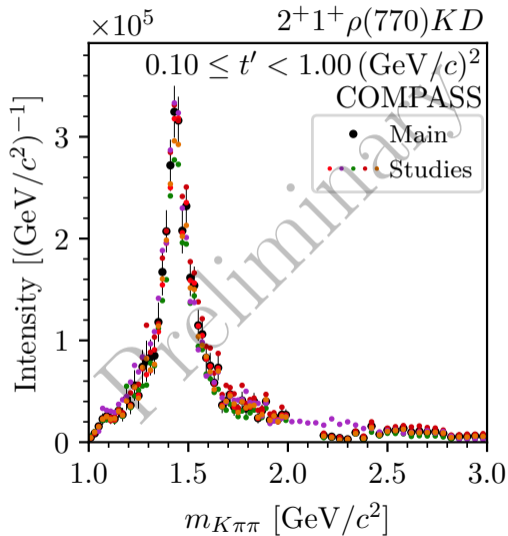


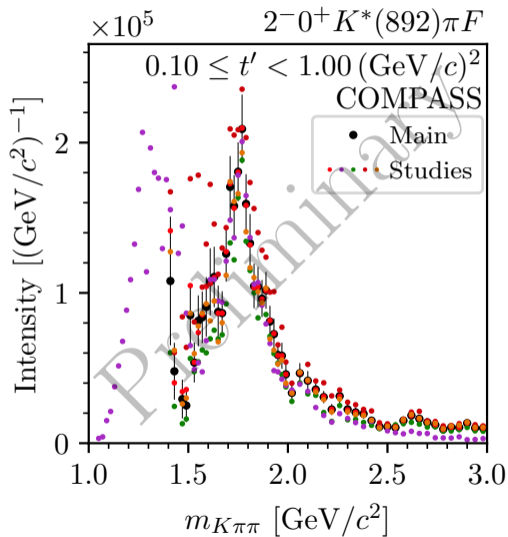


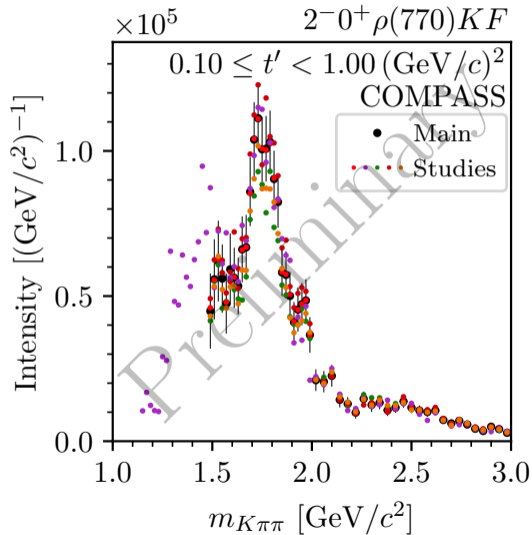


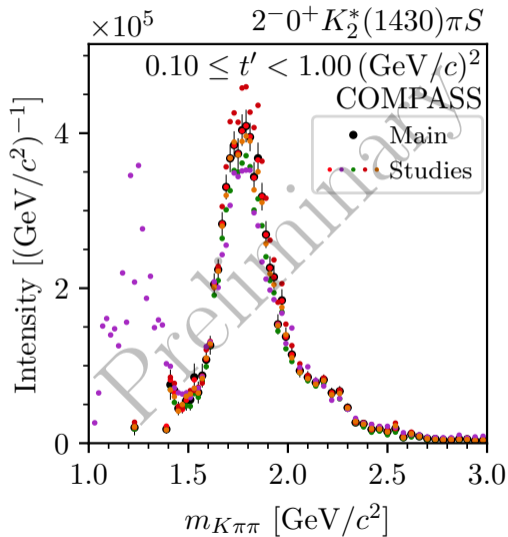


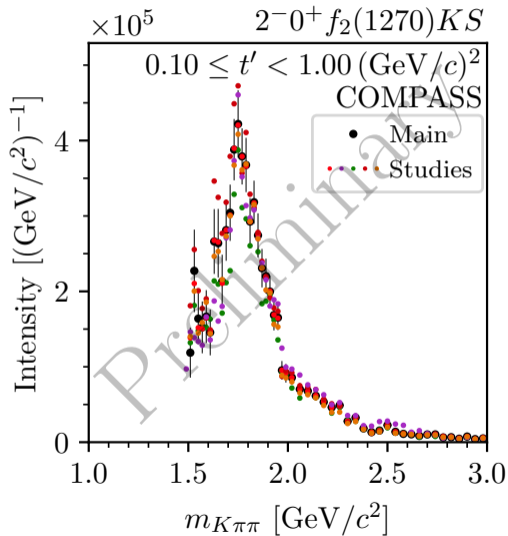


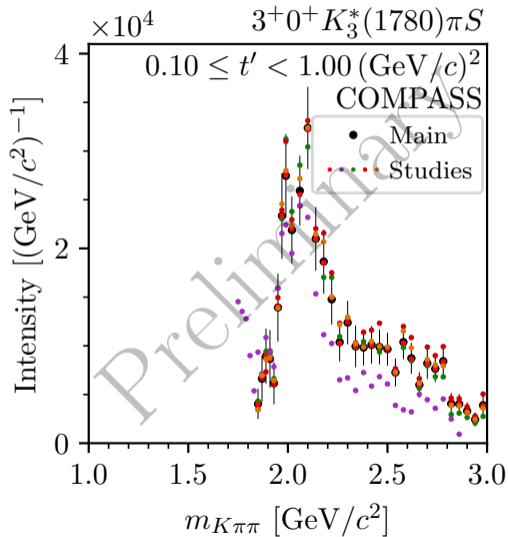


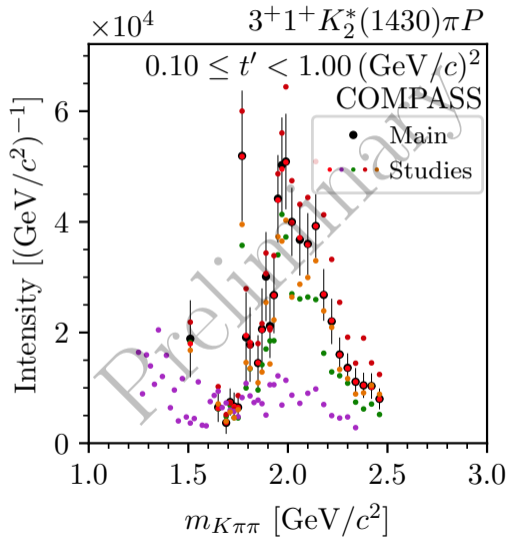


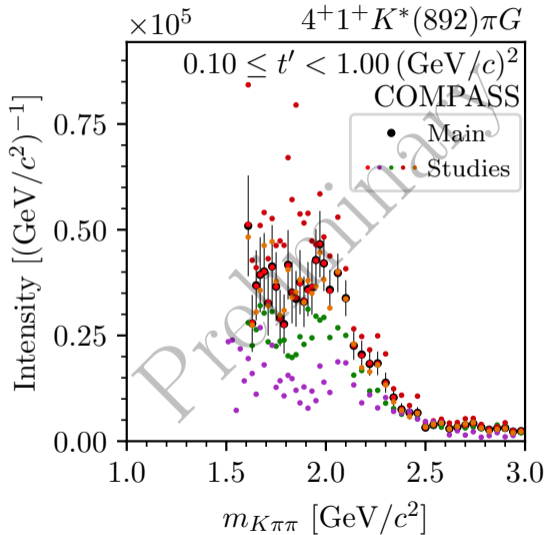


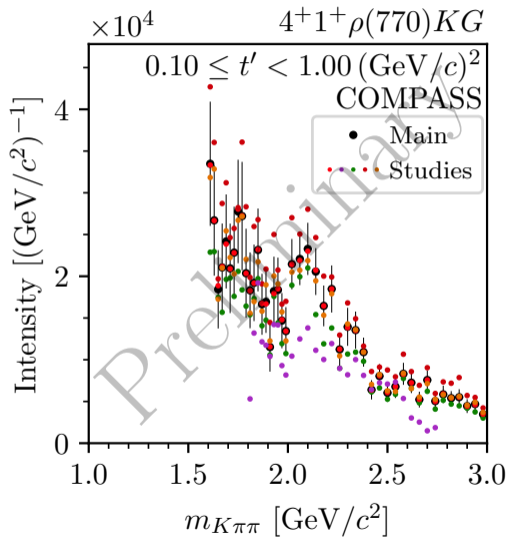


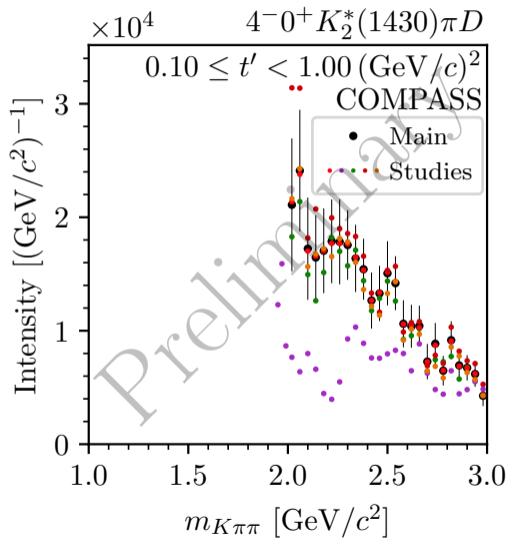


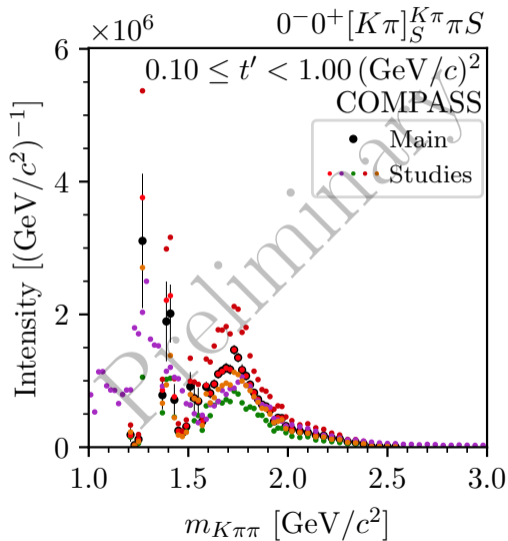


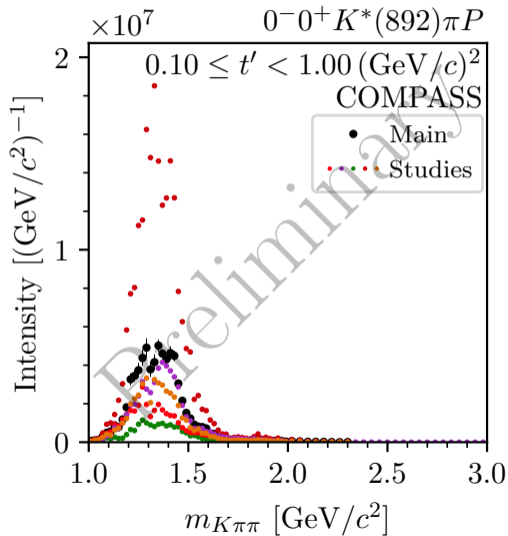


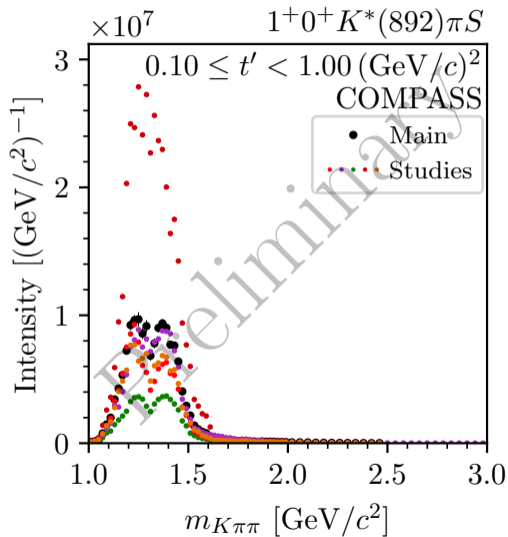


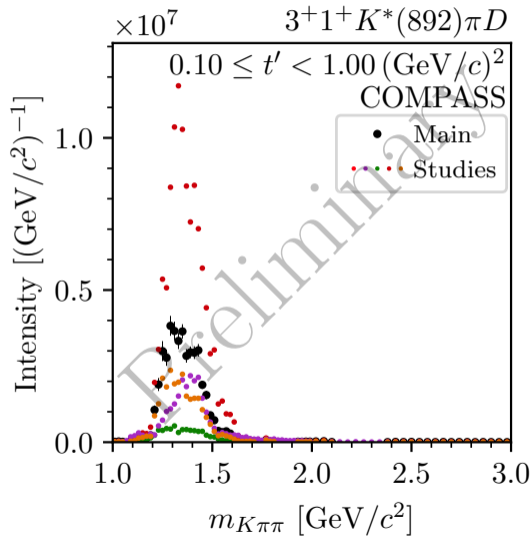




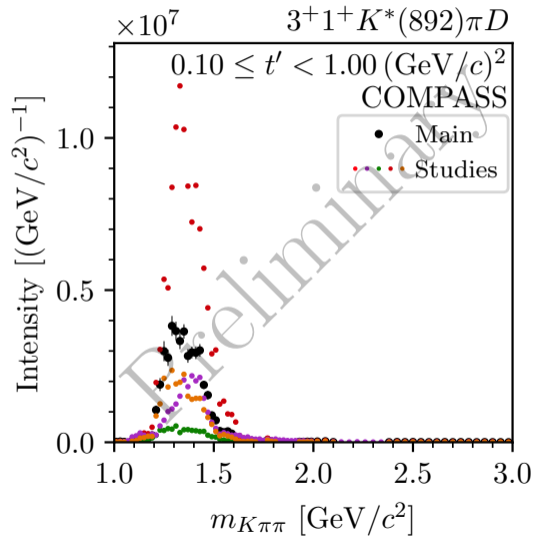




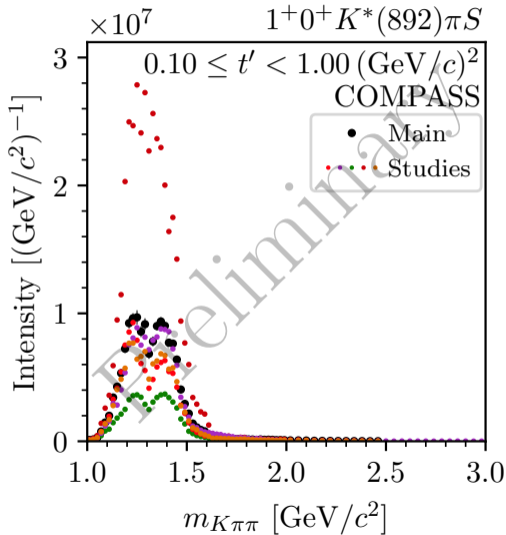




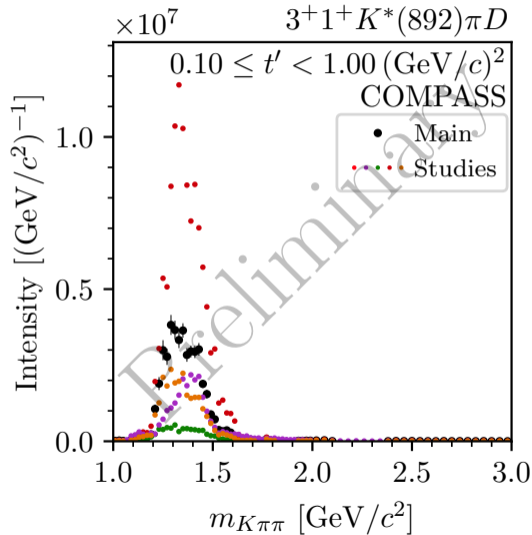
- ▶ Unexpected low-mass enhancement in $3^+ 1^+$ $K^*(892)\pi D$ wave
- ▶ Similar to dominant 1^+ wave
- ▶ Sensitive to systematic effects
- ▶ Decay amplitudes of different J^P are orthogonal
- ▶ Event selection requires to identify one of the two negative particles
 - ▶ Limited acceptance due to limited kinematic range of final-state PID
- ▶ Loss of orthogonality taking acceptance into account
 - ▶ Reduced differentiability of certain partial waves
- ▶ Only a sub-set of partial waves affected



- ▶ Unexpected low-mass enhancement in $3^+ 1^+$ $K^*(892)\pi D$ wave
- ▶ Similar to dominant 1^+ wave
- ▶ Sensitive to systematic effects
- ▶ Decay amplitudes of different J^P are orthogonal
- ▶ Event selection requires to identify one of the two negative particles
 - ▶ Limited acceptance due to limited kinematic range of final-state PID
- ▶ Loss of orthogonality taking acceptance into account
 - ▶ Reduced differentiability of certain partial waves
- ▶ Only a sub-set of partial waves affected

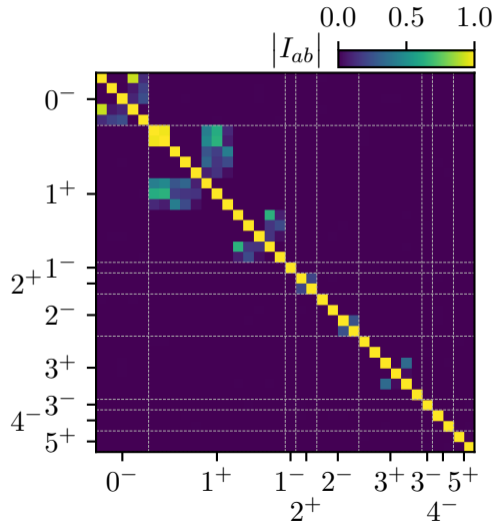


- ▶ Unexpected low-mass enhancement in $3^+ 1^+$ $K^*(892)\pi D$ wave
- ▶ Similar to dominant 1^+ wave
- ▶ Sensitive to systematic effects
- ▶ Decay amplitudes of different J^P are orthogonal
- ▶ Event selection requires to identify one of the two negative particles
 - ▶ Limited acceptance due to limited kinematic range of final-state PID
- ▶ Loss of orthogonality taking acceptance into account
 - ▶ Reduced differentiability of certain partial waves
- ▶ Only a sub-set of partial waves affected

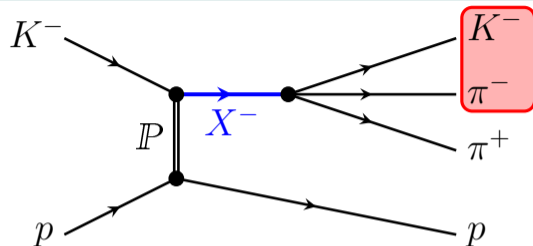


- ▶ Unexpected low-mass enhancement in $3^+ 1^+$ $K^*(892) \pi D$ wave
- ▶ Similar to dominant 1^+ wave
- ▶ Sensitive to systematic effects
- ▶ Decay amplitudes of different J^P are orthogonal
- ▶ Event selection requires to identify one of the two negative particles
 - ▶ Limited acceptance due to limited kinematic range of final-state PID
- ▶ Loss of orthogonality taking acceptance into account
 - ▶ Reduced differentiability of certain partial waves
- ▶ Only a sub-set of partial waves affected

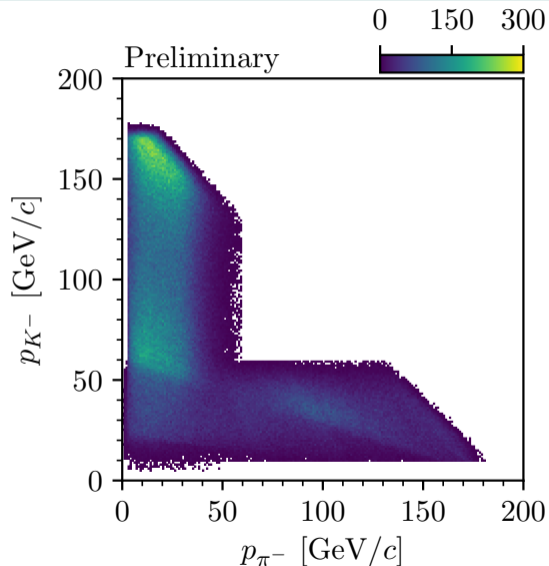
$$I_{a,b} = \int d\varphi_3(\tau) \Psi_a(\tau) \Psi_b^*(\tau)$$



- ▶ Unexpected low-mass enhancement in $3^+ 1^+$ $K^*(892) \pi D$ wave
- ▶ Similar to dominant 1^+ wave
- ▶ Sensitive to systematic effects
- ▶ Decay amplitudes of different J^P are orthogonal
- ▶ Event selection requires to identify one of the two negative particles
 - ▶ Limited acceptance due to limited kinematic range of final-state PID
- ▶ Loss of orthogonality taking acceptance into account
 - ↳ Reduced differentiability of certain partial waves
- ▶ Only a sub-set of partial waves affected

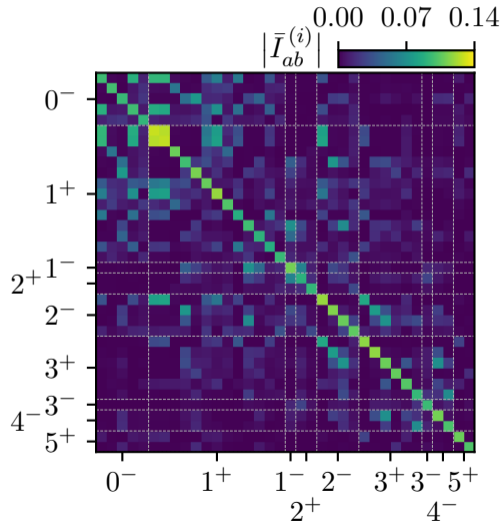


- ▶ Unexpected low-mass enhancement in $3^+ 1^+$ $K^*(892) \pi D$ wave
- ▶ Similar to dominant 1^+ wave
- ▶ Sensitive to systematic effects
- ▶ Decay amplitudes of different J^P are orthogonal
- ▶ Event selection requires to identify one of the two negative particles
 - ▶ Limited acceptance due to limited kinematic range of final-state PID
- ▶ Loss of orthogonality taking acceptance into account
 - ▶ Reduced differentiability of certain partial waves
- ▶ Only a sub-set of partial waves affected

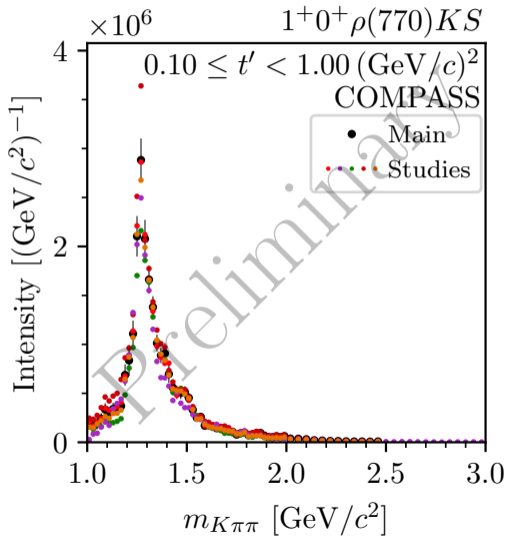


- ▶ Unexpected low-mass enhancement in $3^+ 1^+$ $K^*(892) \pi D$ wave
- ▶ Similar to dominant 1^+ wave
- ▶ Sensitive to systematic effects
- ▶ Decay amplitudes of different J^P are orthogonal
- ▶ Event selection requires to identify one of the two negative particles
 - ▶ Limited acceptance due to limited kinematic range of final-state PID
- ▶ Loss of orthogonality taking acceptance into account
 - ➡ Reduced differentiability of certain partial waves
- ▶ Only a sub-set of partial waves affected

$$\bar{I}_{a,b} = \int d\varphi_3(\tau) \eta(\tau) \Psi_a(\tau) \Psi_b^*(\tau)$$

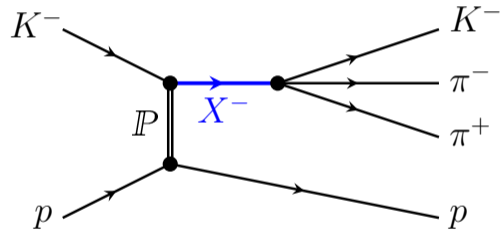


- ▶ Unexpected low-mass enhancement in $3^+ 1^+$ $K^*(892)\pi D$ wave
- ▶ Similar to dominant 1^+ wave
- ▶ Sensitive to systematic effects
- ▶ Decay amplitudes of different J^P are orthogonal
- ▶ Event selection requires to identify one of the two negative particles
 - ▶ Limited acceptance due to limited kinematic range of final-state PID
- ▶ Loss of orthogonality taking acceptance into account
 - ➡ Reduced differentiability of certain partial waves
- ▶ Only a sub-set of partial waves affected

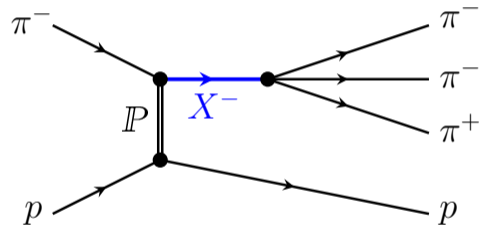


- ▶ Unexpected low-mass enhancement in $3^+ 1^+$ $K^*(892) \pi D$ wave
- ▶ Similar to dominant 1^+ wave
- ▶ Sensitive to systematic effects
- ▶ Decay amplitudes of different J^P are orthogonal
- ▶ Event selection requires to identify one of the two negative particles
 - ▶ Limited acceptance due to limited kinematic range of final-state PID
- ▶ Loss of orthogonality taking acceptance into account
 - ➡ Reduced differentiability of certain partial waves
- ▶ Only a sub-set of partial waves affected

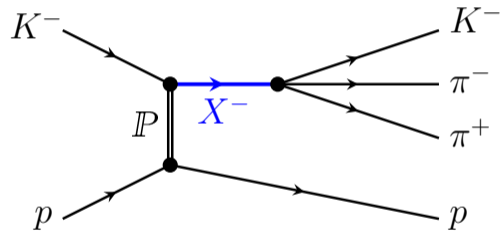
- ▶ $K^- \pi^- \pi^+$ and $\pi^- \pi^- \pi^+$ similar experimental footprint
- ▶ Distinguishable only by
 - ▶ Beam particle identification
 - ▶ Final-state particle identification
- ▶ Excellent beam PID:
 - ▶ Expect small contamination from beam π^-
- ▶ Final-state PID does not suppress $\pi^- \pi^- \pi^+$ background
 - ➔ Non-negligible $\pi^- \pi^- \pi^+$ background in $K^- \pi^- \pi^+$ sample of about 7%
 - ➔ Dominant background in $K^- \pi^- \pi^+$ sample



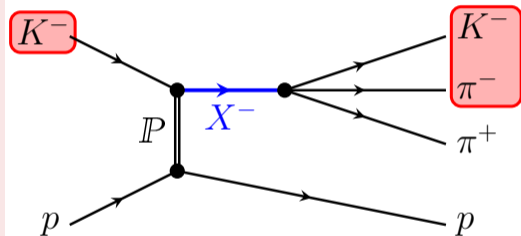
- ▶ $K^- \pi^- \pi^+$ and $\pi^- \pi^- \pi^+$ similar experimental footprint
- ▶ Distinguishable only by
 - ▶ Beam particle identification
 - ▶ Final-state particle identification
- ▶ Excellent beam PID:
 - ▶ Expect small contamination from beam π^-
- ▶ Final-state PID does not suppress $\pi^- \pi^- \pi^+$ background
 - ➡ Non-negligible $\pi^- \pi^- \pi^+$ background in $K^- \pi^- \pi^+$ sample of about 7%
 - ➡ Dominant background in $K^- \pi^- \pi^+$ sample



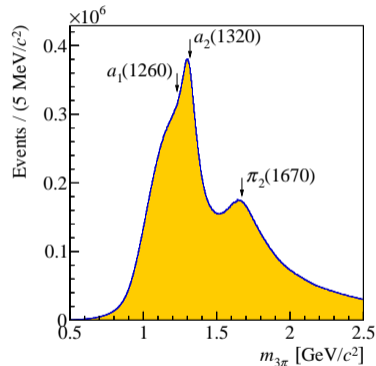
- ▶ $K^- \pi^- \pi^+$ and $\pi^- \pi^- \pi^+$ similar experimental footprint
- ▶ Distinguishable only by
 - ▶ Beam particle identification
 - ▶ Final-state particle identification
- ▶ Excellent beam PID:
 - ▶ Expect small contamination from beam π^-
- ▶ Final-state PID does not suppress $\pi^- \pi^- \pi^+$ background
 - ➔ Non-negligible $\pi^- \pi^- \pi^+$ background in $K^- \pi^- \pi^+$ sample of about 7%
 - ➔ Dominant background in $K^- \pi^- \pi^+$ sample



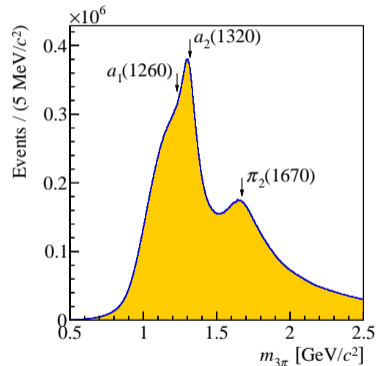
- ▶ $K^- \pi^- \pi^+$ and $\pi^- \pi^- \pi^+$ similar experimental footprint
- ▶ Distinguishable only by
 - ▶ Beam particle identification
 - ▶ Final-state particle identification
- ▶ Excellent beam PID:
 - ▶ Expect small contamination from beam π^-
- ▶ Final-state PID does not suppress $\pi^- \pi^- \pi^+$ background
 - ▶ Non-negligible $\pi^- \pi^- \pi^+$ background in $K^- \pi^- \pi^+$ sample of about 7%
 - ▶ Dominant background in $K^- \pi^- \pi^+$ sample



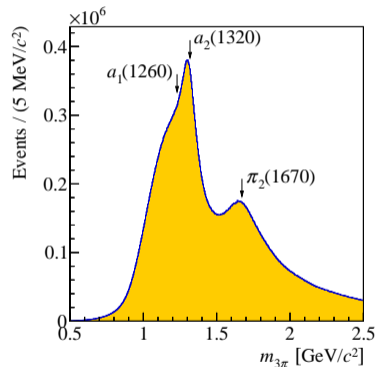
- ▶ Well established model for $\pi^- + p \rightarrow \pi^- \pi^- \pi^+ + p$
 - ▶ From very same data set
 - ▶ Measured with high precision
 - ▶ Acceptance corrected
- ▶ Generate $\pi^- \pi^- \pi^+$ Monte Carlo sample
- ▶ Mis-interpret $\pi^- \pi^- \pi^+$ Monte Carlo events as $K^- \pi^- \pi^+$
 - ▶ Apply wrong mass assumption
 - ▶ Same event reconstruction and selection as for $K^- \pi^- \pi^+$
- ▶ Perform partial-wave decomposition of mis-interpreted $\pi^- \pi^- \pi^+$ Monte Carlo sample
 - ▶ Using the same PWA model as for measured $K^- \pi^- \pi^+$ sample



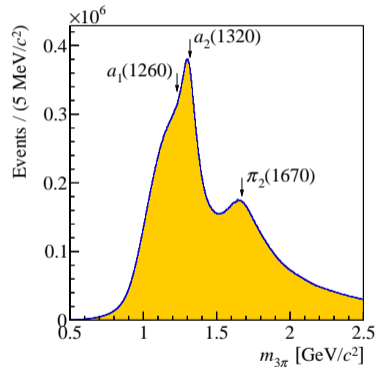
- ▶ Well established model for $\pi^- + p \rightarrow \pi^- \pi^- \pi^+ + p$
 - ▶ From very same data set
 - ▶ Measured with high precision
 - ▶ Acceptance corrected
- ▶ Generate $\pi^- \pi^- \pi^+$ Monte Carlo sample
- ▶ Mis-interpret $\pi^- \pi^- \pi^+$ Monte Carlo events as $K^- \pi^- \pi^+$
 - ▶ Apply wrong mass assumption
 - ▶ Same event reconstruction and selection as for $K^- \pi^- \pi^+$
- ▶ Perform partial-wave decomposition of mis-interpreted $\pi^- \pi^- \pi^+$ Monte Carlo sample
 - ▶ Using the same PWA model as for measured $K^- \pi^- \pi^+$ sample



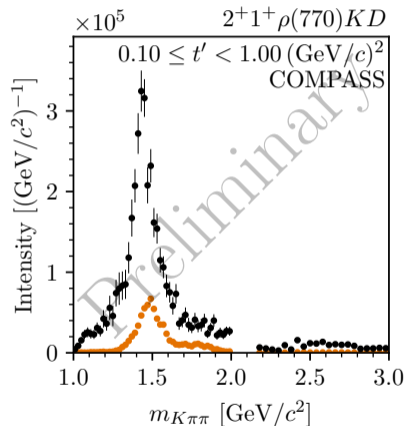
- ▶ Well established model for $\pi^- + p \rightarrow \pi^- \pi^- \pi^+ + p$
 - ▶ From very same data set
 - ▶ Measured with high precision
 - ▶ Acceptance corrected
- ▶ Generate $\pi^- \pi^- \pi^+$ Monte Carlo sample
- ▶ Mis-interpret $\pi^- \pi^- \pi^+$ Monte Carlo events as $K^- \pi^- \pi^+$
 - ▶ Apply wrong mass assumption
 - ▶ Same event reconstruction and selection as for $K^- \pi^- \pi^+$
- ▶ Perform partial-wave decomposition of mis-interpreted $\pi^- \pi^- \pi^+$ Monte Carlo sample
 - ▶ Using the same PWA model as for measured $K^- \pi^- \pi^+$ sample



- ▶ Well established model for $\pi^- + p \rightarrow \pi^- \pi^- \pi^+ + p$
 - ▶ From very same data set
 - ▶ Measured with high precision
 - ▶ Acceptance corrected
- ▶ Generate $\pi^- \pi^- \pi^+$ Monte Carlo sample
- ▶ Mis-interpret $\pi^- \pi^- \pi^+$ Monte Carlo events as $K^- \pi^- \pi^+$
 - ▶ Apply wrong mass assumption
 - ▶ Same event reconstruction and selection as for $K^- \pi^- \pi^+$
- ▶ Perform partial-wave decomposition of mis-interpreted $\pi^- \pi^- \pi^+$ Monte Carlo sample
 - ▶ Using the same PWA model as for measured $K^- \pi^- \pi^+$ sample
- ➔ Study $\pi^- \pi^- \pi^+$ background in individual $K^- \pi^- \pi^+$ partial waves

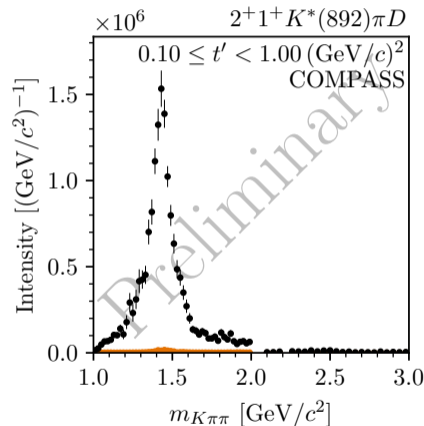


- ▶ Significant contribution to waves with $\rho(770)$ isobar
- ▶ $\pi^- \pi^- \pi^+$ produces peaking structures
- ▶ Largest relative contribution to $2^+ 1^+ \rho(770) K D$ wave
- ▶ Small contribution to waves with $K^*(892)$ isobar
- ▶ Also significant contribution to waves with $f_2(1270)$ and $K_2^*(1430)$ isobars
- ▶ No contribution to flat wave



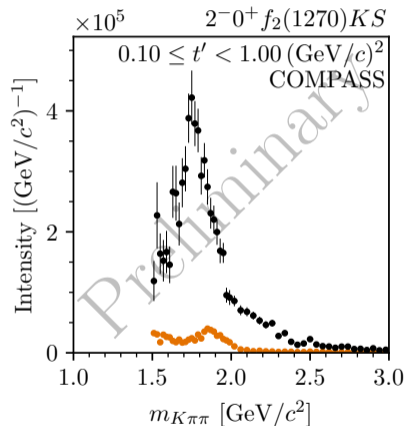
$K^- \pi^- \pi^+$ data, $\pi^- \pi^- \pi^+$ pseudo data

- ▶ Significant contribution to waves with $\rho(770)$ isobar
- ▶ $\pi^- \pi^- \pi^+$ produces peaking structures
- ▶ Largest relative contribution to $2^+ 1^+ \rho(770) K D$ wave
- ▶ Small contribution to waves with $K^*(892)$ isobar
- ▶ Also significant contribution to waves with $f_2(1270)$ and $K_2^*(1430)$ isobars
- ▶ No contribution to flat wave



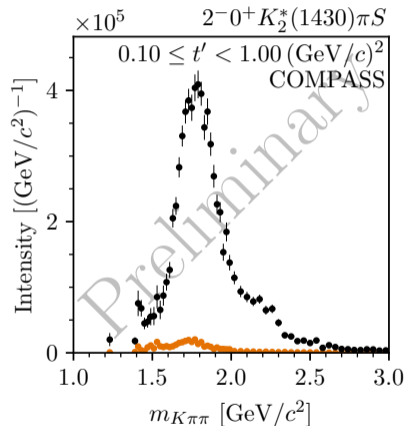
$K^- \pi^- \pi^+$ data, $\pi^- \pi^- \pi^+$ pseudo data

- ▶ Significant contribution to waves with $\rho(770)$ isobar
- ▶ $\pi^- \pi^- \pi^+$ produces peaking structures
- ▶ Largest relative contribution to $2^+ 1^+ \rho(770) K D$ wave
- ▶ Small contribution to waves with $K^*(892)$ isobar
- ▶ Also significant contribution to waves with $f_2(1270)$ and $K_2^*(1430)$ isobars
- ▶ No contribution to flat wave



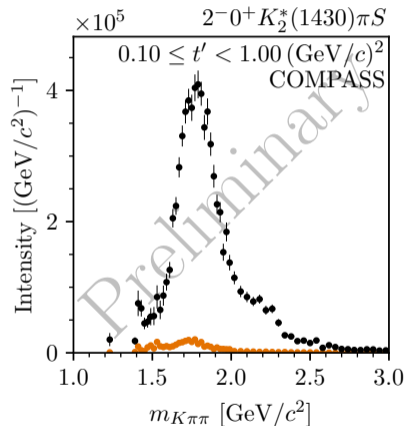
$K^- \pi^- \pi^+$ data, $\pi^- \pi^- \pi^+$ pseudo data

- ▶ Significant contribution to waves with $\rho(770)$ isobar
- ▶ $\pi^- \pi^- \pi^+$ produces peaking structures
- ▶ Largest relative contribution to $2^+ 1^+ \rho(770) K D$ wave
- ▶ Small contribution to waves with $K^*(892)$ isobar
- ▶ Also significant contribution to waves with $f_2(1270)$ and $K_2^*(1430)$ isobars
- ▶ No contribution to flat wave



$K^- \pi^- \pi^+$ data, $\pi^- \pi^- \pi^+$ pseudo data

- ▶ Significant contribution to waves with $\rho(770)$ isobar
- ▶ $\pi^- \pi^- \pi^+$ produces peaking structures
- ▶ Largest relative contribution to $2^+ 1^+ \rho(770) K D$ wave
- ▶ Small contribution to waves with $K^*(892)$ isobar
- ▶ Also significant contribution to waves with $f_2(1270)$ and $K_2^*(1430)$ isobars
- ▶ No contribution to flat wave



$K^- \pi^- \pi^+$ data, $\pi^- \pi^- \pi^+$ pseudo data

- ▶ 238-wave set can describe main features of $\pi^- \pi^- \pi^+$ pseudodata sufficiently well
- ▶ Largest deviation for $K^- \pi^+$ isobar system at thigh $m_{K\pi\pi}$

$\pi^- \pi^- \pi^+$ pseudo data,
prediction (weighted-MC) of $K^- \pi^- \pi^+$ PWD
to $\pi^- \pi^- \pi^+$ pseudo data

